2013

Effects of nitrite and oxygen on angiogenesis in vascular networks of the chicken embryo

Michael Connery
Virginia Commonwealth University

Effects of nitrite and oxygen on angiogenesis in vascular networks of the chicken embryo

A dissertation submitted in partial fulfillment of the requirements for the degree of Doctor of Philosophy at Virginia Commonwealth University.

by

Michael D. Connery

B.S., University of Virginia, 2005

Director: Dr. Roland N. Pittman

Professor, Department of Physiology and Biophysics

Acknowledgements

This work is the collaborative effort of an innumerable amount of people who have supported me and my education. While I have space here to recognize only a few individuals, I hope each person who has helped me in any small way knows they are a contributor in all the things I have been able to accomplish.

Dr. Pittman has been a constant source of guidance, support, and inspiration. We have worked through three projects and I'm always amazed at his vast scientific knowledge and his inexhaustible patience.

I credit Dr. Golub with the initial idea for my using chicken embryos as an animal model and his expertise and enthusiasm has been invaluable. He contributed significantly to nearly every piece of material developed for this research.

Sami Dodhi is responsible for pushing my limits, questioning my assumptions, helping me discuss scientific methodology, and being a best friend.

This would not have come together without the constant substantial, emotional, and spiritual help and support of Katarina Deshotel.

Table of Contents

List of Tables

List of Figures

List of Abbreviations

AV	Area Vasculosa
CAM	Chorioallantoic Membrane
cPTIO	2-(4-Carboxyphenyl)-4,4,5,5-tetramethylimidazoline-1-oxyl-3-oxide
cGMP	Cyclic Guanosine Monophosphate
ECM	Extracellular Matrix
EGF	Epidermal Growth Factor
ERC	“Empty” Reconstituted Cellulose
FGF	Fibroblast Growth Factor
Hb	Hemoglobin
HIF	Hypoxia Inducible Factor
HGF	Hepatocyte Growth Factor
IL-8	Interleukin-8
LDPE	Low-density Polyethylene
L-NAME	L-NG-Nitroarginine methyl ester
MAPK	Mitogen-activated Protein Kinase
MMP	Matrix Metalloprotease
NADPH	Nicotinamide adenine dinucleotide phosphate
NO	Nitric Oxide

NOS	Nitric Oxide Synthase
PKG	Protein Kinase G
PDGF	Platelet-derived Growth Factor
PO_2	Partial Pressure of Oxygen
PQM	Phosphorescence Quenching Microscopy
PVDC	Polyvinylidene Chloride
RBC	Red Blood Cell
RC	Reconstituted Cellulose
TGF	Transforming Growth Factor
VEGF	Vascular Endothelial Growth Factor

Abstract

EFFECTS OF NITRITE AND OXYGEN ON ANGIOGENESIS IN VASCULAR NETWORKS OF THE CHICKEN EMBRYO

By Michael D. Connery, PhD

A dissertation submitted in partial fulfillment of the requirements for the degree of Doctor of Philosophy at Virginia Commonwealth University.

Virginia Commonwealth University, 2013.

Director: Dr. Roland N. Pittman, Professor, Department of Physiology and Biophysics

Nitric oxide (NO) is an important mediator of angiogenesis and is primarily produced endogenously through the action of nitric oxide synthase (NOS). An alternate pathway for NO production is the conversion of nitrite to NO, which depends on the presence of hemoglobin (Hb) and hypoxic conditions. The angiogenic effects of topically applied sodium nitrite on two vascular beds in the ex ovo chicken embryonic model of angiogenesis were assessed. Gas barrier films were used to modulate local oxygen levels in the chorioallantoic membrane (CAM), a respiratory vascular network, and the area vasculosa (AV) on the yolk sac, a typical peripheral vascular network. The low-permeable film polyvinylidene chloride (PVDC) and highly permeable regenerated cellulose (RC) were applied to the surface of the vasculature to alter

oxygen diffusion and transport and produce a local environment of low or high oxygen, respectively. Phosphorescence Quenching Microscopy (PQM) was used to verify the oxygen levels in the vascular membranes underneath the films. Following 48 hours of continuous application of sodium nitrite (330 μg/kg/day), saline, or sodium nitrite + cPTIO (a NO scavenger) (1mg/kg/day), the angiogenic response was quantified by measuring vascular density and network complexity. The PVDC film reduced CAM PO_2 to 17.9±5.5 mmHg and AV PO_2 to 29.5±3.6 while the RC film maintained a PO_2 of 115 mmHg. At the edge of PVDC film, there was found to be a small area of transition between the nearby low and high PO_2 regions. After nitrite application, significant increases in vascularity were observed in the AV under hypoxic conditions, but not normoxic conditions ($p<0.03$). cPTIO inhibited nitrite-induced angiogenesis and returned vascularity to levels observed with saline application. No significant changes were observed in the CAM, but a trend of reduced angiogenesis after nitrite application was observed compared to saline and saline+cPTIO. These results indicate that two highly diffusible gases, NO and O_2, play important roles in the growth of new blood vessels, but in a way that appears to depend on the gas exchange function of the vascular network.

INTRODUCTION

Angiogenesis

Angiogenesis - the growth of blood vessels - is a normal biological process necessary for the growth and normal function of all vertebrates. Once multicellular organisms evolved to sizes large enough that diffusion was no longer a sufficient method of supplying adequate oxygen to maintain cellular respiration, circulatory systems became necessary for transport. The constant respiration of mammalian cells requires that they be no farther than 200 μm from a blood vessel. As organisms grow, the transport capacity necessary for homeostasis likewise increases and requires the growth and development of blood vessels to keep up with the demand. The process of angiogenesis through sprouting involves several steps including degradation of the ECM, invasion and proliferation by endothelial cells, lengthening of the new tube at its tip and introduction of blood flow. Formation of a new vessel sprout is preceded by increased vascular dilation and permeability. A secondary angiogenic process is intussusceptive microvascular growth in which a patent vessel is divided by tissue added to the lumen (Patan, 2004). This is a highly regulated process that is most activated during periods of new growth and healing.

After reaching adulthood, however, growth slows down and endothelial cells remain in a quiescent, non-proliferative state until an external stimulus induces them to “switch on” and reinitiate angiogenesis. Some natural initiators of angiogenesis include metabolic stress (including hypoxia), mechanical stress, inflammatory responses, and genetic changes (Carmeliet,

2000). Intercellular signaling molecules such as VEGF, angiopoetin, HIF, PDGF, FGF, HGF, EGF, IL-8, Proliferin, and TGF all interact to regulate concerted angiogenic efforts.

When the homeostasis of pro-angiogenic and anti-angiogenic factors is disturbed, serious medical conditions can result. A better understanding of the process and influences of angiogenesis can lead to the development of targeted pro-angiogenic and anti-angiogenic therapies with the potential to benefit as many as 500 million people worldwide (Carmeliet, 2005).

Angiogenic Pathology

1.6 million people are expected to be diagnosed with cancer in the United States in 2013 and the disease is the second highest cause of mortality among Americans (American Cancer Society, 2013). The morbidity and mortality of tumors are directly dependent on their ability to initiate angiogenesis. In order to grow, a tumor must provide its own blood supply or its central cells will undergo necrosis due to lack of oxygen. These hypoxic conditions trigger angiogenesis to restore blood flow and reverse the hypoxia. Likewise, metastasis to other organs requires angiogenesis, making anti-angiogenic drugs a highly desirable class for study of cancer therapy. However, insufficient blood supply to a tumor reduces the targeting and activity of blood-borne chemotherapy. The importance and visibility of cancer in society influences research focus and as a consequence, most angiogenesis research is done in the context of tumors and cancer.

Tumors influence their microenvironments in complex ways in order to ensure their own blood supply. Genetic mutations which up-regulate the expression of pro-angiogenic signaling

molecules are common and cancer cells often occupy a significant part of the lumen of tumor blood vessels, supplanting normal endothelial cells. Despite decades of concentrated research since the idea of anti-angiogenic tumor therapy (Folkman, 1971), there is still more to learn about the intricate balance of pro- and anti-angiogenic factors that influence the initiation of angiogenesis.

Worldwide, more than 7 million myocardial infarctions occur each year (White, 2008) and heart disease is the most prevalent cause of death in Western countries. In cases of slowly-developing coronary artery atherosclerosis, development of collateral circulation circumventing impeded vessels improves outcomes but is insufficient to restore blood flow to normal levels (Sasayama, 1992). Improved angiogenesis can bolster the effects of recruitments to restore blood flow to ischemic cardiac myocytes and prevent the necrosis and scarring that lead to eventual death by coronary syndrome (Ware, 1997).

Besides these examples, angiogenesis also plays a role in many other diseases that will only be mentioned in brief due to the relative insignificance to the disease progression or the low prevalence of the disease. On the one hand, some diseases are characterized by excessive angiogenesis and include obesity, multiple sclerosis, transplant arteriopathy, psoriasis, and retinopathy of prematurity, diabetic retinopathy, diabetic nephropathy, pulmonary hypertension, cystic fibrosis, ulcerative colitis, and liver cirrhosis. Diseases characterized by insufficient angiogenesis, on the other hand, include Alzheimer's disease, amyotrophic lateral sclerosis, hypertension, atherosclerosis, lymphedema, gastric ulcers, Crohn's disease, hair loss, lupus, pre-eclampsia, menorrhagia, respiratory distress syndrome, emphysema, and osteoporosis.

Role of Nitric Oxide in Modulating Angiogenesis

One major player in the modulation of angiogenesis appears to be NO. NO is a bioactive gas with a short lifespan and acts as a signaling molecule. It was initially identified as endothelium derived relaxing factor due to its vasodilatory properties (Furchgott, 1980; Palmer, 1987). NO has a wide range of physiological functions and mediates platelet aggregation, neurotransmission, and immune responses in addition to vascular effects. These are consistent with dysfunctions found in eNOS knockout mice, namely hypertension, impaired wound healing, and reduced angiogenesis (Lee, 1999). The primary vasoactive pathway for NO is through its reaction with soluble guanylate cyclase to increase cytoplasmic levels of cGMP. Higher cGMP levels activate PKG which phosphorylates different targets in the smooth muscle cell to reduce the calcium concentration and cause relaxation.

NO is primarily produced by NOS, of which there are three isoforms identified by the site of their initial location: endothelial (eNOS), neuronal (nNOS), and inducible (iNOS). These can be sub-categorized by their function: eNOS and nNOS are constitutive and calcium/calmodulin dependent, while iNOS is inducible and calcium/calmodulin independent. eNOS is a calcium/calmodulin dependent enzyme catalyzing the reaction of L-Arginine with NADPH to form NO and citrulline. eNOS activity is most closely related with angiogenesis, although iNOS activity as part of the immune response may be related to inflammation-induced angiogenesis.

Vasodilation seems to be a common precursor to angiogenesis and many pro-angiogenic compounds like NO, substance P, and bradykinin also have vasodilatory effects. Many angiogenic factors indirectly lead to NO production due to upregulation of eNOS. VEGF, TGF and FGF induce NO production in various vascular models (Papapetropoulos, 1997, Simão, 2005). L-NAME, a non-specific NOS inhibitor, reduces the pro-angiogenic effects of VEGF, FGF, TGF, and Substance P suggesting that NO is a necessary component of angiogenic signaling. NO acts to promote angiogenesis in many ways, including improving endothelial cell survival by inhibiting apoptosis and promoting proliferation and migration, possibly through stimulating podokinesis. NO also influences interactions with the ECM via inducing expression of alpha-v beta-3 and interacting with the b-FGF pathway. NO's vasodilatory effects may also promote angiogenesis indirectly by increasing local blood flow. Finally, NO can induce synthesis and release of VEGF, potentially creating a positive feedback loop which promotes angiogenesis (Polytarchou, 2004). Conversely, in cases with reduced NO, angiogenesis is also attenuated. Hypercholesterolemia models showed both reduced NO bioactivity and less ischemia-induced angiogenesis (Cooke, 2003).

NO signaling also appears to be an important part in other angiogenesis pathways. NO triggers the release of more VEGF and MMP, both potent angiogenesis activators (Zhang, 2003). VEGF-stimulated angiogenesis was attenuated by a NOS inhibitor and a guanylate cyclase inhibitor. Specifically, VEGF-induced expression of angiogenesis transcription factors is mediated by PKG, which is in turn regulated by cGMP. The following is a proposed cascade for the initiation of angiogenesis within endothelial cells: NO → cGMP → PKG → raf1 → MAPK.

NOS-independent NO

Besides the better-known NOS derived biological NO, there is recently increasing evidence of a secondary pathway. This is of particular importance to hypoxic conditions because oxygen is a necessary reactant and its depletion will reduce NOS activity. This may be a backup pathway during conditions of inactivated NOS and, while there are different theories about the specific mediator, the production of NO from inorganic nitrite has been reproduced even in the presence of a NOS inhibitor (Vitturi, 2011). Among the agents potentially responsible for reducing nitrite to NO are deoxyhemoglobin, deoxymyoglobin, electron transport chain proteins, xanthine oxidase, aldehyde oxidase, NO synthase, protons, vitamin C and polyphenols (Lundberg, 2010).

While sodium nitrite has long been known to be a vasodilator at super-physiological concentrations (Furchgott, 1953), its vasomotor function was more recently discovered to be mediated by NO production and enhanced by low pH (often present in hypoxic conditions) and in the presence of vitamin C. Nitrite has been found to be therapeutic in cases of ischemia-reperfusion injury in a number of organ models and this cytoprotection is lost with the application of the NO scavenger cPTIO (Webb, 2004).

In a study by Kumar et al (2008), a dose-response relationship was found between sodium nitrite concentrations and blood flow in rabbits with induced hindleg ischemia. At doses given twice a day in a range from 8.25 μg/kg to 3.3 mg/kg, all concentrations restored blood flow above control with the highest recovery coming at 165 μg/kg. cPTIO reversed the recovery back to baseline.

Hemoglobin Catalysis

Hb is an intriguing candidate as a possible catalyst for the reduction of nitrite into NO because the reaction seems to occur at near-physiological oxygen and pH levels (Patel, 2011). The ubiquitous nature of the vascular supply also makes RBCs attractive sensors of local hypoxia and mediators of the homeostatic response. This is supported by evidence that hypoxic blood flow in skeletal muscle is dependent on Hb saturation and not PO_2. In parallel, the reduction of nitrite into NO is also linked to Hb saturation and is maximized at 50%, within the physiological range experienced by arterioles where NO primarily acts (Patel, 2011).

Hb action is modulated by PO_2 because of the different reactions that can take place between a metalloprotein like Hb or myoglobin and nitrite. When the iron group in Hb is bound to oxygen (FeO_2), it reacts with nitrite to oxidize it into nitrate.

$$4NO_2^- + 4HbFe^{2+} - O_2 + 4H^+ \rightarrow 4HbFe^{3+} + 4NO_3^- + O_2 + 2H_2O. \text{ (Eq 1)}$$

Deoxygenated Hb, on the other hand, reduces nitrite to NO.

$$NO_2^- + HbFe^{2+} + H^+ \rightarrow NO + HbFe^{3+} + OH^- \text{ (Eq 2)}$$

Hb is also well known to be a sink for NO, rapidly reacting with NO and consuming it in either its oxygenated or deoxygenated forms. This suggests there may be a less-reactive intermediate

created in the RBC like N_2O_3 that can diffuse out of the cell without reacting before being broken down to produce NO (Patel, 2011).

Hypoxia

As stated in the context of angiogenesis, there are several severe and common diseases that are characterized by local hypoxia. An infarct refers to the necrosis secondary to uncorrected hypoxia, often caused by interruption in blood flow. The blood supply is most usually cut off by an obstruction within the feeding artery like a clot, embolus, or plaque. There are also other causes of impaired blood flow like vessel compression, reduced blood volume, or pathological vasoconstriction (Pinsky, 1995).

Homeostatic responses compensate for the reduction in oxygen transport to the respiring cells through both short term and long term mechanisms. Local hypoxemia immediately triggers vasodilation of the feed arterioles to reduce vascular resistance and increase blood flow (and therefore oxygen flow) to the affected area. As long as the interruption in blood flow is not too far upstream, compensation can occur by shunting more blood to patent blood vessels.

Over a longer time course, angiogenesis is initiated and new blood vessels grow to further reduce vascular resistance to the hypoxic area and increase blood flow. It seems natural that vasodilatory signaling molecules like NO that are released to mediate the vasodilation should also initiate angiogenesis.

Chicken CAM as an Angiogenesis Model

Despite being a very important biological process, angiogenesis is normally quiescent during adulthood necessitating special conditions to induce it before it can be studied (Carmeliet, 2005). Many adult mammalian models involve inducing hypoxia through arterial ligation and quantifying angiogenesis by the restoration of blood flow to the hypoxic area. These measurements, however, are secondary to actual vessel growth and the complex 3-D vascular patterns within cardiac or skeletal muscle are difficult to appreciate and quantify. The cornea is the primary model of vascular growth in adult mammals in which the vasculature can be appreciated in a single plane.

The chicken chorioallantoic membrane model has many advantages compared to adult models (Ribatti, 2008). The chorioallantoic membrane is a vascular organ derived by a fusion of the allantois and chorion (Figure 1). It develops in direct contact with the egg shell and its primary purpose is as a respiratory organ. It is a dense vascular bed that grows rapidly over the course of several days allowing for quick responses to environmental changes. The blood vessels and their architecture are very easy to access and appreciate because they grow in a single layer, are surrounded by clear connective tissue, and are situated directly under the shell. The CAM also accepts and engrafts implants and tumors from other species (Deryugina, 2008, Ribatti, 1995).

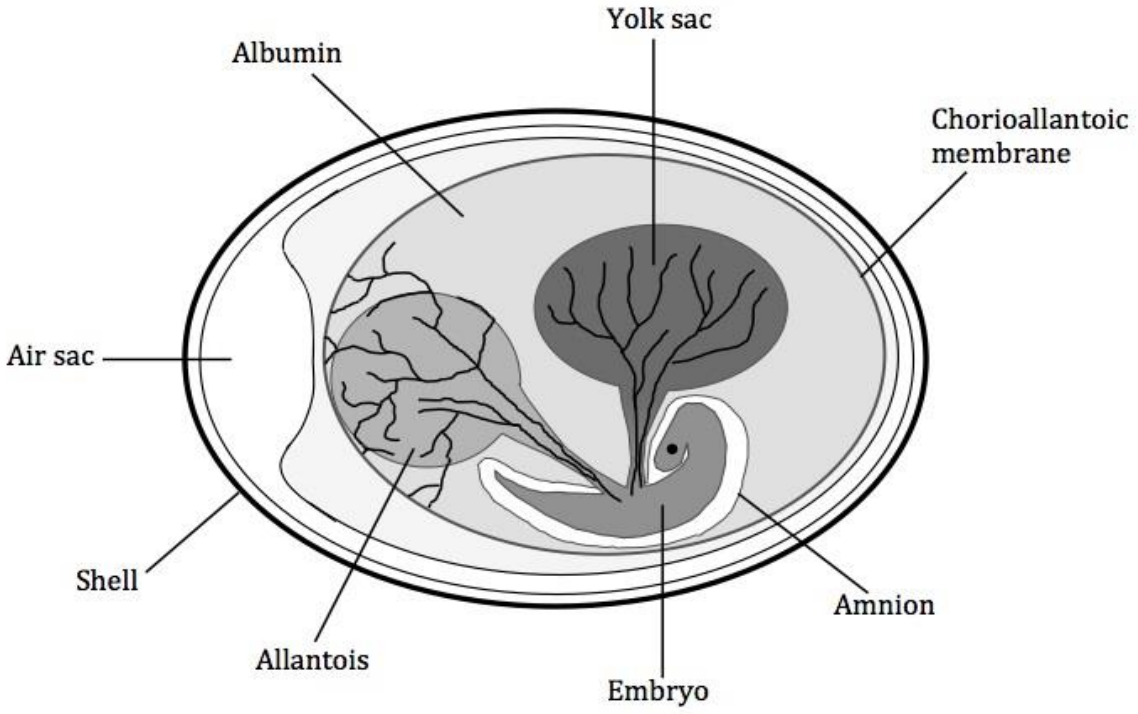

Figure 1
Diagram of Chick Egg and Embryonic Structures
The major extra-embryonic structures of the chicken embryo as they appear in the egg shell. The two vascular beds shown are chorioallantoic membrane (CAM) vasculature which spreads from the allantois, and the area vasculosa (AV) associated with the yolk sac. These blood vessels were observed for their angiogenic responses.

Once incubated, chicken embryos begin developing inside the egg and quickly reach certain growth milestones (Figure 2). The CAM typically begins development between Day 4 and 5 after incubation when the outer layer of the allantois fuses with the chorion and vessels form between the layers. The high level of angiogenic activity between Day 8 and 10 makes the CAM especially sensitive to changes made by pro-angiogenic or anti-angiogenic factors.

The first embryonic blood vessels develop through vasculogenesis in the area vasculosa of the yolk sac by mesodermal cells (Mayer, 1978). Blood islands composed of hematopoetic cells (blood cell precursors) and angioblasts (endothelial cell precursors) form in the splanchnopleuric mesoderm. FGF and its receptor are important in this development but are not expressed in older embryonic or adult tissues and probably do not play a role in angiogenesis. Separate blood islands grow together initially to form a primary capillary plexus. After this capillary plexus is formed by vasculogenesis, for the rest of the organism's life, blood vessels will be grown primarily through angiogenesis. The expanding mesoderm is ringed by its outmost vessel, the marginal sinus. By early Day 2 of incubation, the heart is already pumping blood (Risau, 1995).

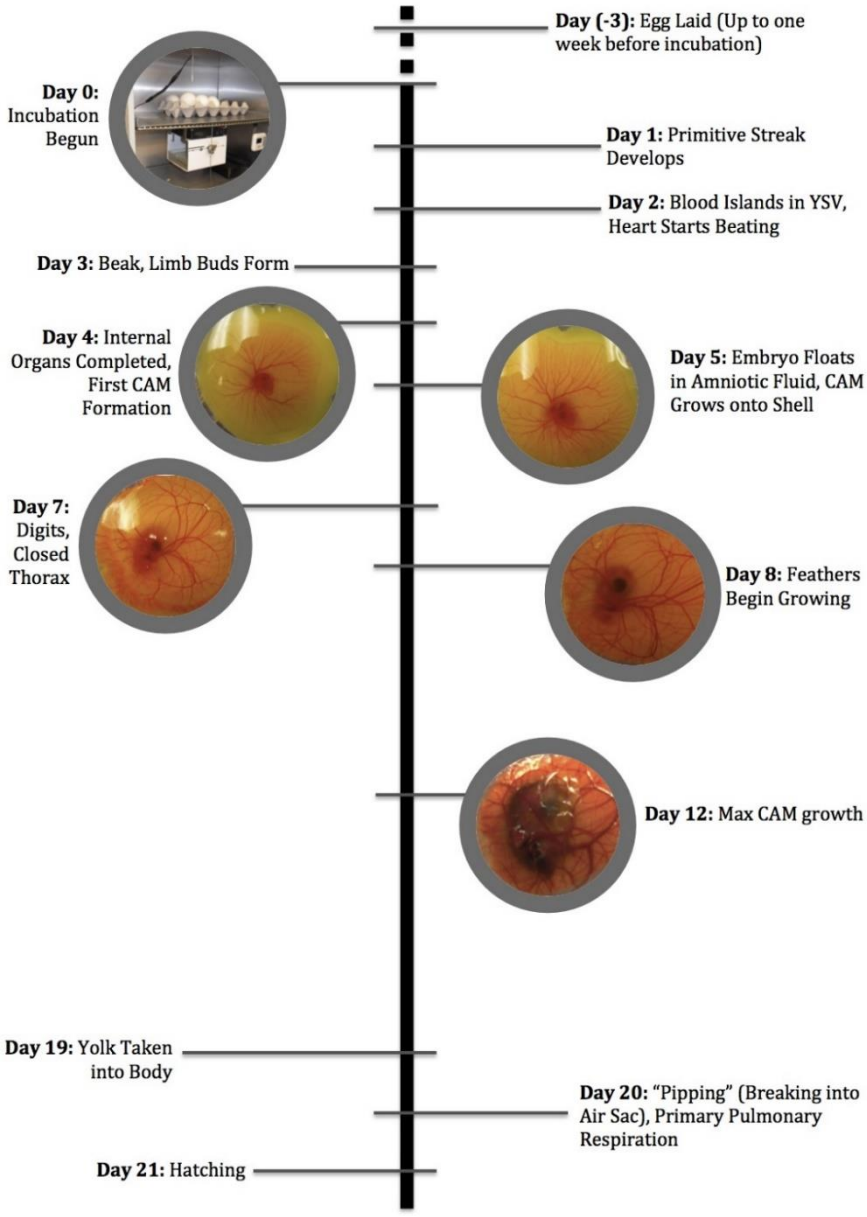

Figure 2
Timeline of Chick Development
This timeline lays out the major milestones during development from laying (which takes place anywhere from 1 to 7 days before incubation) and hatching at D21. The accompanying images are representative of the appearance in the ex ovo model. The AV is first visible invading the yolk sac D2 and the CAM later grows over top of it.

Ex ovo Model

The ability of chicken embryos to grow and develop outside the shell allows for certain advantages over models of CAM growth within the egg shell when examining the vasculature (Dohle, 2009). The entire contents of the egg shell (embryo, yolk, and albumin) can be emptied into a container and will survive as long as 16 days (out of the 21 day total time necessary for hatching). This is ample time for examination of the CAM which finishes its maximum development by Day 12 post-incubation.

There are several possible containers suitable for holding the embryo while incubating. A petri dish is the simplest, but can be upgraded to a curved-bottom glass dish. Another option is a sack of hanging polyethylene (Auerbach, 1974).

The removal of the embryo from the shell reveals a complete viewing area and more liberal possibilities for intervention when compared to observation of a small area of CAM viewed through a window of removed shell. The *ex ovo* preparation also makes the AV visible and available for intervention and quantification in addition to the CAM (Jakobson, 2009). The AV is a vascular network that grows into the vitelline membrane surrounding the yolk and develops earlier (D3) than the CAM. It is supplied by a pair of lateral vitelline arteries and veins and two unpaired anterior and posterior veins. The terminal sinus is the outermost circumference of the vascular network and serves to funnel blood back to the veins. Before the CAM becomes functional, the embryo's metabolic oxygen needs can be provided by diffusion so the primary purpose of the AV during development is to deliver nutrients from the yolk to the developing embryo. The bare-bones cellular contents of AV endothelial cells also show some similarities to

cancer vasculature and bear some similar structural and growth characteristics (Allen, 1993). This has led to some interest in using the AV as an angiogenic model for testing angiogenic therapeutic agents like the CAM (Ribatti, 1996). Having two available vascular beds increases the flexibility of the chicken embryo model of angiogenesis, particularly because they can be tested individually due to their differing developmental rates and because one has a primarily respiratory function while the other is somatic.

The egg shell poses a significant barrier to oxygen diffusion and its removal exposes the embryo more directly to oxygen than *in ovo*. The shell is about 300 um thick and gasses are exchanged through gas filled pores (10,000 in number with a diameter of about 16 um). There is an air space within the shell that expands throughout development as the embryo loses mass due to water vapor diffusion. As the oxygen consumption of the embryo increases with its mass, the PO_2 of the air within the sac lowers (Romijn, 1938). However, during the early embryonic development the air sac PO_2 is very close to atmospheric PO_2 and remains above 135 mmHg until D12, the last day of observations. This is higher than the PO_2 of the blood leaving the CAM (96 mmHg at D12 according to Tazawa, 1971). This suggests the binding kinetics of oxygen to blood may be the limiting factor instead of the shell during this period of development (Piiper, 1980) or that a shunt is mixing deoxygenated blood with oxygenated blood leaving the CAM.

Induction of Hypoxia

Typically, testing physiological responses to hypoxia involves either reducing available oxygen to the respiratory system or reducing blood flow to a target area. The more significant physiological conditions that produce hypoxia are localized (tumors, infarcts) and are not

associated with hypoxemia. Applying a hypoxic gaseous environment reduces oxygen tension throughout the entire specimen instead of a localized area and does not allow for very low oxygen environments without a high death rate. When testing the activity of sodium nitrite, RBC's are an activator and reduce it into NO, but ischemic conditions would limit the availability of Hb catalyst.

The use of chicken embryonic vascular structures offers a unique opportunity to finely regulate oxygen exposure. Both the AV (before CAM development) and the CAM primarily derive oxygen not from flow of oxygenated blood, but from direct diffusion with the air. Under normal conditions, this diffusive capacity would be only slightly impeded by the shell because of the air pores in it, but the *ex ovo* model allows for direct gaseous equilibration. Each vascular bed is actively respiring in the process of angiogenesis, but the oxygen supply is normally abundant enough to maintain high tissue and blood oxygen levels. This allows for localized impediment of oxygen transport through interruption of the tissue-atmospheric interface.

A clear barrier film can impede the exchange of oxygen and reduce the PO_2 of the tissue it covers while still allowing it to be properly appreciated and quantified. Polyvinylidene chloride (PVDC) has very strong gas barrier properties (oxygen permeability of 0.053 P x 10^{10} cm^3 cm^{-2} mm^{-1} sec^{-1} $cmHg^{-1}$) (Chandra, 1987, Schmitz, 2000) and effectively stops free gas exchange across its surface. Because the tissue underneath consumes oxygen faster than it is supplied by the flow through the vasculature or by diffusion from adjacent tissue outside the boundaries of the film, the diffused oxygen within the tissue is quickly depleted, producing local hypoxia without interrupting blood flow or producing widespread hypoxemia. Regenerated cellulose

(RC) can act as a negative control because while still being clear and maintaining its structural properties, it is highly permeable to oxygen. Untreated cellulose has much higher oxygen permeability (7.8 P x 10^{10} cm^3 cm^{-2} mm^{-1} sec^{-1} $cmHg^{-1}$) and after treatment has pores introduced through the film to allow the passage of large molecules. The specific RC film used was designed to impede the diffusion across its surface of molecules greater than 12kDa with the diffusion rate inversely proportional to the molecular weight. Oxygen, at 32Da is much smaller than the cutoff value and should not have any impediment for diffusion across the barrier.

Phosphorescence Quenching Microscopy

PQM is a non-invasive method for determining the PO_2 of blood or tissue in-vivo. The decay of phosphorescent emmittance by a Pd-porphyrin probe is influenced by the availability of oxygen for binding (Zheng, 1996). This method can be used to verify hypoxic or normoxic conditions under barrier films dependent on their oxygen permeability.

cPTIO

cPTIO is a member of the Imidazolineoxyl N-Oxides and a NO scavenger. cPTIO has a radical-radical reaction with NO and one of its oxygen groups.

$\cdot NO + cPTIO \rightarrow \cdot NO_2 + cPTI$ (Eq 3)

This is followed by a further reaction of $\cdot NO_2$ to nitrite and nitrate by the following reaction:

$2\cdot NO_2 \rightleftharpoons N_2O_4 + H_2O \text{ -> } NO_3^- + NO_2\text{-} + 2H^+$ (Eq 4)

This reaction takes place in a completely stoichiometric manner and its reaction rate of NO scavenging is a third that of Hb, but three times that of albumin and ten times that of molecular oxygen (Akaike, 1993).

Endpoints

There are a number of ways to measure the angiogenic response of the CAM, including semi-quantitative methods and quantitative methods. Among the semi-quantitative methods are the application of a score based on subjective observed changes in vascular density (0 for no change, +1 for small increase, +2 for large increase) (Knighton, 1977). Another involves image analysis and counting the number of vessels within a radius of the area of interest that converge toward the center (Dusseau, 1988). The lengths of vessels can be used to calculate index density (Strick, 1991).

A quantitative method of determining vascular density is observing the CAM through an eyepiece with a cross-hatch reticule and counting the number of reticule intersections occupied by vessels and dividing by the total number of intersections (Elias, 1983). There is also a molecular method which involves measuring ^{3}H-thymidine incorporated into the CAM as a percentage of total thymidine (Splawinsli, 1988).

Once images are taken of vasculature, there are several options for quantifying the vascularity. In this study three methods were chosen as endpoints: total vascular length (length), number of bifurcations (bifurcations), and fractal dimension (complexity). Length, bifurcations (Doukas, 2008), and complexity (Vargas, 2007, Demir, 2009) can all be calculated simply from a

skeletonized tracing of a vascular bed and reflect different aspects of vascular density, the ultimate measure of gross angiogenic activity.

Purpose of Present Study

The purpose of this study is to test the hypothesis that nitrite, applied topically to the developing vascular networks of the chick embryo, produces angiogenic changes through the release of NO. The *ex ovo* angiogenesis model was chosen because it provides two easily accessible vascular beds that, because of their oxygen delivery functions, we anticipate may have different responses to hypoxia. The CAM is a well-studied angiogenesis model and is primarily an organ for oxygen uptake from the atmosphere. The AV is a non-respiratory vascular network that is not as well understood and provides exciting opportunities for novel experimentation. Previous studies suggest that conversion of nitrite to NO takes place primarily under hypoxic conditions and requires the Hb in RBCs. To induce local hypoxia, sections of the low-permeability gas barrier film PVDC was applied to the surface of the vascular beds to impede the oxygen flux across the film and produce a region of localized hypoxia. If nitrite influences angiogenesis through NO release, we predict that hypoxic conditions are necessary for nitrite-induced changes in vascularity. Also, any NO-mediated effects of nitrite application should be reversed in the presence of a NO scavenger.

The objectives of this study were to:

1. Validate the AV as an alternative angiogenesis model in the *ex ovo* chicken embryo with different physiological reactions to oxygen.

2. Produce reproducible regions of low, steady PO_2 using barrier films.

3. Determine the conditions necessary for nitrite-induced pro-angiogenic or anti-angiogenic effects.
    a. Determine the necessity of hypoxia on nitrite-induced NO activity.
    b. Determine the nitrite-induced angiogenic effects in hypoxia.
4. Compare the physiological responses of the AV and CAM vascular networks to hypoxia.

MATERIALS AND METHODS

Materials

Egg Sources and Transport

Fertilized chicken eggs were purchased from local farmers (Lynn Matthews, Kenny, Furbelow Farms, Tuckahoe Lamb & Cattle, Tomten Farms) with roosters in their flock on a weekly or bi-weekly basis. The eggs were transported to the laboratory either by car or bus. During periods of extreme weather, the eggs were carried in a Styrofoam box to maintain temperature and carried in a 10-gallon trash bag to prevent jostling during transport.

When arriving at the laboratory, the preincubator's water reservoirs were refilled and the heating and rocking units plugged in to bring the interior volume up to 99.5 ^{o}F. The eggs were wiped down with a paper towel to remove any dirt and debris from the surface before being placed in the pre-incubator rocking mechanism with the large end of each egg facing up.

Preincubation Chamber

A professional circulated air incubator with egg turner (#4200, Farm Innovators Inc., Plymouth IN) was used to incubate eggs for the first three days until plating (Figure 3, B). The device was calibrated (the temperature knob was increased successively until an alcohol thermometer,

resting on the turner platform, remained steady) at 99.5 ºF. The water reservoirs were regularly filled to maintain humidity.

Overflow Incubation Chamber

Another circulated air incubator (#2200, Farm Innovators Inc., Plymouth IN) served to store *ex ovo* embryos when the primary incubator was at full capacity or when it needed to be emptied for sanitization (Figure 3, C). When measuring and calibrating temperature, the interior alcohol thermometer rested on a stacked petri dish and lid to match the height of the incubating embryos. The water reservoirs were regularly filled to maintain humidity.

Incubator

An incubator (Model 12-140, Quincy Lab, Inc., Chicago IL) was modified to suit the needs of *ex ovo* chicken embryos (Figure 3, D). The lower metal plate separating the heating coils from the main central incubator area had holes drilled into the center and a downward facing fan was installed to circulate warmed air. A dish of water was kept on the lower shelf to maintain humidity. A motor was suspended under the upper shelf and its crankshaft used to slowly raise and lower a perforated metal plate resting on the upper shelf and holding the incubating embryos. The motor power was controlled by an oscillator that completed the circuit for 80 seconds once every 65 minutes. Due to warping of the incubator door, the top and bottom of the door were held in place with duct tape to keep it from popping open. A digital thermometer was placed on top of the incubator housing and the probe hung down through a hole in the top of the incubator to the level of the embryos. The dial was regularly adjusted to maintain the temperature within 1 degree of 99.5 ºF.

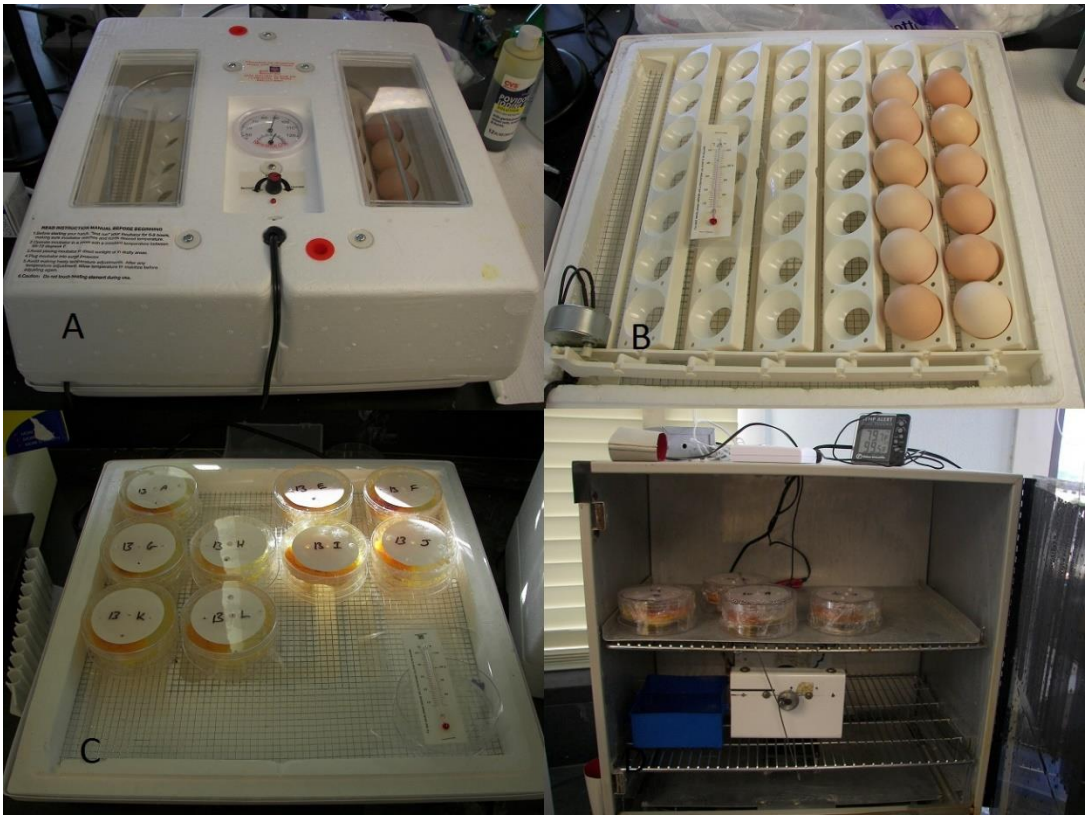

Figure 3
Incubation Chambers
Views of the different incubation chambers used. The preincubator (B) with eggs in an automated rocker and the overflow incubator (C) with Poultry Dishes look similar from the outside (A) and each have an internal thermometer. The incubator (D) Contains Poultry Dishes, a motor (1), water reservoir (2), probe for a digital thermometer (3), and fan (4).

Poultry Dish

The “poultry dish” is a container for incubating a shell-less chicken egg while maximizing survivability and CAM visibility. It was composed of two petri dishes with accompanying lids; one 90 mm (diameter) x 15 mm (height) and one 90 mm x 20 mm (Figure 4). Holes were drilled into both dishes with a 40 mm (diameter) circular bit. Soapy water was added while drilling to prevent warping due to friction-generated heat. After drilling, the hole was dried and any debris or protrusions removed from the hole using a sharp blade. The lid of the 15 mm high dish had five holes drilled into it with a 3/16” bit in a cross pattern. The lid used when applying fluid intervention had four holes drilled in a T-shape. An adhesive (General Purpose Spray Adhesive, Loctite, Westlake OH) was sprayed onto one side of a 70 mm circle of filter paper (Quantitative, Whatman, Bound Brook NJ) and blotted with a paper towel to remove excess adhesive before being pressed onto the interior of the lid with holes. The tubing lid had a semi-circle of filter paper applied to expose one half of the lid. Once the adhesive dried, the filter paper was punctured by pushing a pair of tweezers through the holes. All components were rinsed with water, sprayed with 70% isopropyl alcohol and dried before use.

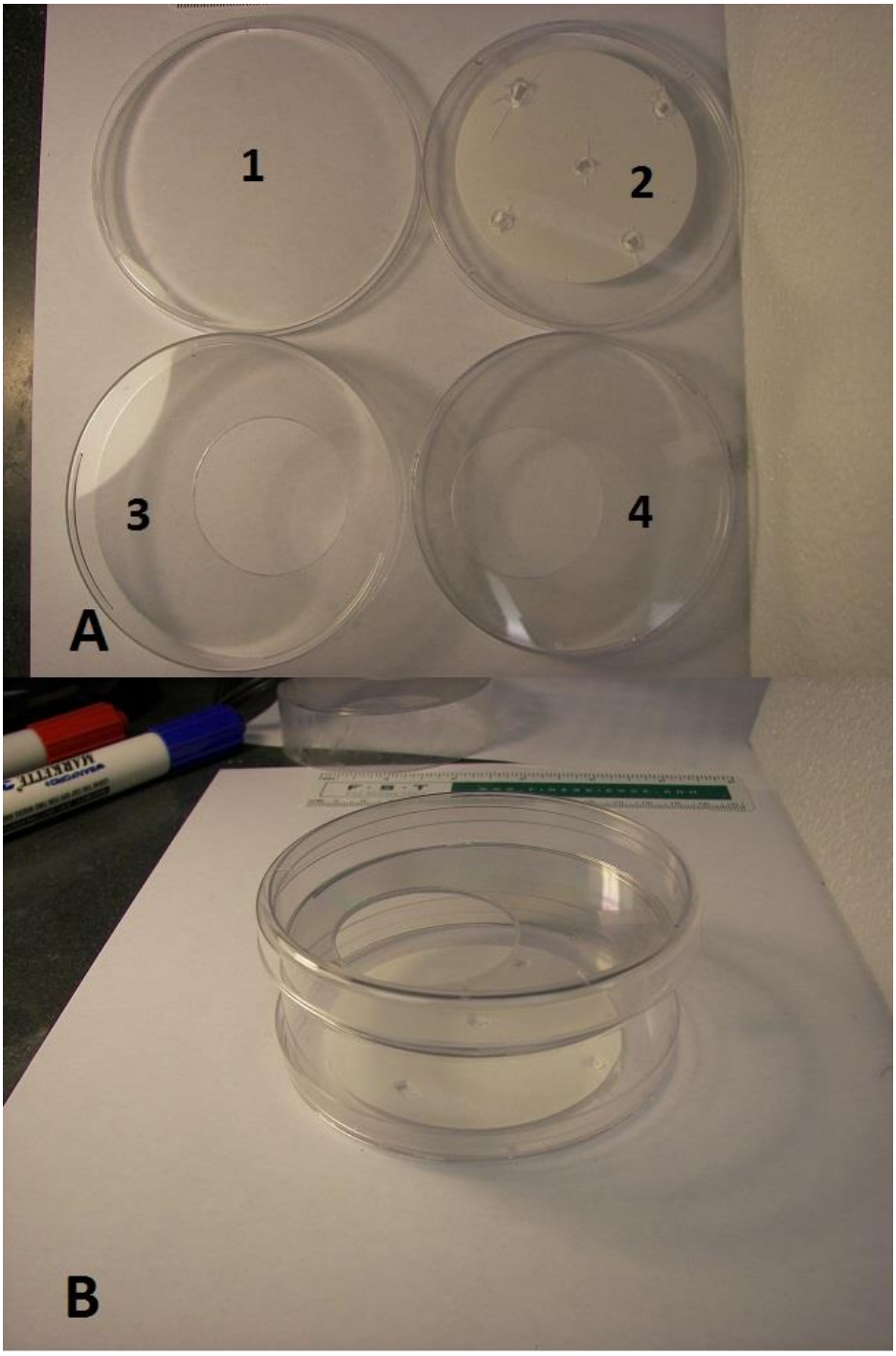

Figure 4
Poultry Dish
The Poultry Dish was composed of the base (A1), the lid (A2), the large dish (A3) and the small dish (A4). They were assembled (B) so that the base fits on the small dish, the holes of the two dishes align, and the lid fit on the large dish. The image shown is a Poultry Dish upside down to allow for appreciation of the internal structure.

The poultry dish was assembled by placing the 15 mm dish upside down with the 20 mm dish placed right side up with the two 40 mm holes aligned. The 20 mm high lid acted as the base and prevents any egg white that leaks over the side from contaminating the incubation chamber. The larger capacity dish allowed more space for gas and prevents egg white overflow. The holes in the 15 mm dish lid on top allowed for increased air flow while the filter paper prevented water condensation from the high humidity from dropping onto the embryo. The semi-circular filter paper on the tubing lid allowed visualization when placing the tubing used for topical application of fluids.

When quantifying angiogenesis in the observation chamber, it was necessary to prepare a fog-free lid because the humidity in the poultry dish caused condensation on the lid which blurred the images. Anti-Fog (C-Clear, Las Vegas NV) was sprayed onto the interior surface of the lid of a 15mm lid, wiped off with a paper wipe (Kim-Wipe, Kimberly-Clark, Dallas TX), then the gel was spread onto the surface and wiped off with a cotton cloth.

Solution Application

Needles (22G1½", Becton Dickinson, Franklin Lakes, NJ) were cut to ½" in length with the edge of a Dremel (Dremel, Racine WI). The flat surface of the Dremel was then used to flatten the tip and round the edges to remove any impediment to flow and ease the placement of the tubing. PE50 tubing (Intramedic Clay Adams Brand, Becton Dickinson, Franklin Lakes NJ) was fitted over the entire length of the needle and measured and cut to a length of three feet. A 1 ml syringe (Monoject, Kendall, Mansfield MA) filled with the appropriate experimental solution was secured onto the needle and all air bubbles flushed from the syringe and tubing.

Up to nine syringes at a time were applied using a multi-syringe pump (PHD2000, Harvard Apparatus, Holliston MA). It was set to pump 1ml syringes with an interior diameter of 4.55 mm, at a rate of 0.0002 ml/min and stop after pumping 0.6 ml. The pump was placed on a platform elevated to the height of the embryos in the incubator next to the door of the incubator to reduce the length of tubing from the pump to the poultry dishes.

Plating Materials

A piece of PE-240 tubing was cut to a length of 12-15 cm, a plastic ring (110 mm diameter, 40 mm height), and a triangular stirring rod were sprayed with a 70% isopropyl alcohol solution and allowed to air dry (Figure 5). Plastic wrap (Kirkland brand low-density polyethylene, Polyvinyl Films, Sutton MA) was also used.

Solutions

A solution of Howard's Ringer solution was made by mixing 7.2 g sodium chloride, 230 mg calcium chloride dihydrate, and 370 mg potassium chloride in 1 liter of deionized water (Celebra-Thomas, 2005). An antibiotic solution was made by mixing 384 mg penicillin G potassium salt (Sigma-Aldrich, St. Louis MO) and 288 mg streptomycin sulfate salt (Sigma-Aldrich, St. Louis MO) with 60 ml Howard's Ringer solution. A sodium nitrite solution was made by dissolving 327 mg sodium nitrite in 100 ml deionized water and diluting it 1:10 in Howard's Ringer solution.

Camera for Developmental and Film Placement Images

A camera (Kodak EasyShare P850, Rochester, NY) was used to take still gross images of the embryos during development and concurrent with angiogenesis measurements. The camera was attached to a weighted standing base and leveled with a bubble level. Once secured, the height from the table would remain constant throughout the pictures. A scale bar was included in all pictures by placing the metric scale within the edge of the image. The scale was elevated to the height of the CAM by placing it on two stacked petri dish bottoms. The pictures were taken by first centering the scale in the middle of the frame and focusing before moving it and bringing in the poultry dish to the center of the frame while maintaining focus.

Figure 5
Plating Materials
The materials needed for plating, including a triangular stirring rod (A), plastic ring (B), and polyethylene plastic wrap (C).

PQM Hardware

Phosphorescence excitation was provided by a Xenon flash lamp (Model FX-249, EG&G Optoelectronics, Salem, MA), with an output of 0.5 J, flash duration of 3 μs, and a flash rate of 1Hz or 10Hz and through a 40 μm diameter circular diaphragm. A number of filters were used between emission by the flash lamp and detection by the photomultiplier tube. The light first passed through a 430 nm bandpass excitation filter (430BP100, Omega Optical Inc, Brattleboro, VT), then split with a dichroic longpass beamsplitter with a cut-on wavelength of 510 nm (FT510, Zeiss, Oberkochen Germany), and the emission passed through an emission filter with a cut-on wavelength of 650 nm (Oriel Corp. Stratford, CT). The emitted light was sent to a photomultiplier tube (model R1617, Hamamatsu, Middlesex, NJ) which then output to a low-noise current-to-voltage converter (model OP27EP, Analog Devices, Norwood, MA). The signal was sent both to an analog-to-digital converter (At MIO/6F5, National Instruments, Austin, TX) for PC acquisition and to an oscilloscope (model 72-3060, Tenma Test Equipment, Springboro, OH) for visual monitoring.

PQM Software

The ASGARD program (SOURCE) was used to process the signal from the PC analog-to-digital converter at a sampling rate of 200 kHz, 400 points per decay curve, and a cutoff value of 3 V. The number of sequential decay curves depended on the type of data collected and the rate of acquisition. Static measurements (no moving stage) were typically for 20 s (20 points at 1 Hz or 200 points at 10 Hz). Scans with stage movement at constant speed provided by the stage motor needed to be long enough to collect data throughout the midline of a 2 cm wide film patch and

the uncovered tissue on each side. This time period was typically 80 s (80 points at 1 Hz and 800 points at 10 Hz).

Microscopic Stage Chamber

This chamber maintains the embryonic environment while under microscopic examination. The chamber is functionally identical to the stereomicroscopic chamber, but with some adaptations for the shorter focal distance and smaller available space. The base, housing, and lid are all composed of cut fiberglass, with the lid having a hole for the microscope objective to fit into (Figure 6). A foam ring is placed around the objective flush to the lid to prevent excess air circulation with the exterior environment. An incandescent light bulb (painted black to prevent interference with PQM measurements) provided a heat source and a small fan circulated air in the interior of the chamber. The chamber was screwed to the lateral adjustment strip to provide for fine adjustments in position under the objective.

Automated Microscope Stage

The microscope stage was augmented to move at a slow constant rate so that successive PQM measurements could be taken at known distances apart. A motor powering a slowly rotating drive shaft was attached to the microscope platform adjustment knob by a heavy-duty rubber band with a textured interior surface (Figure 7). The motor arrangement is attached to the microscope's base stage by a spring to provide balancing tension when the rubber band is attached. The band is removed after use to prevent warping the band or spring. The motor moved the stage at a constant rate of 0.19 mm/s.

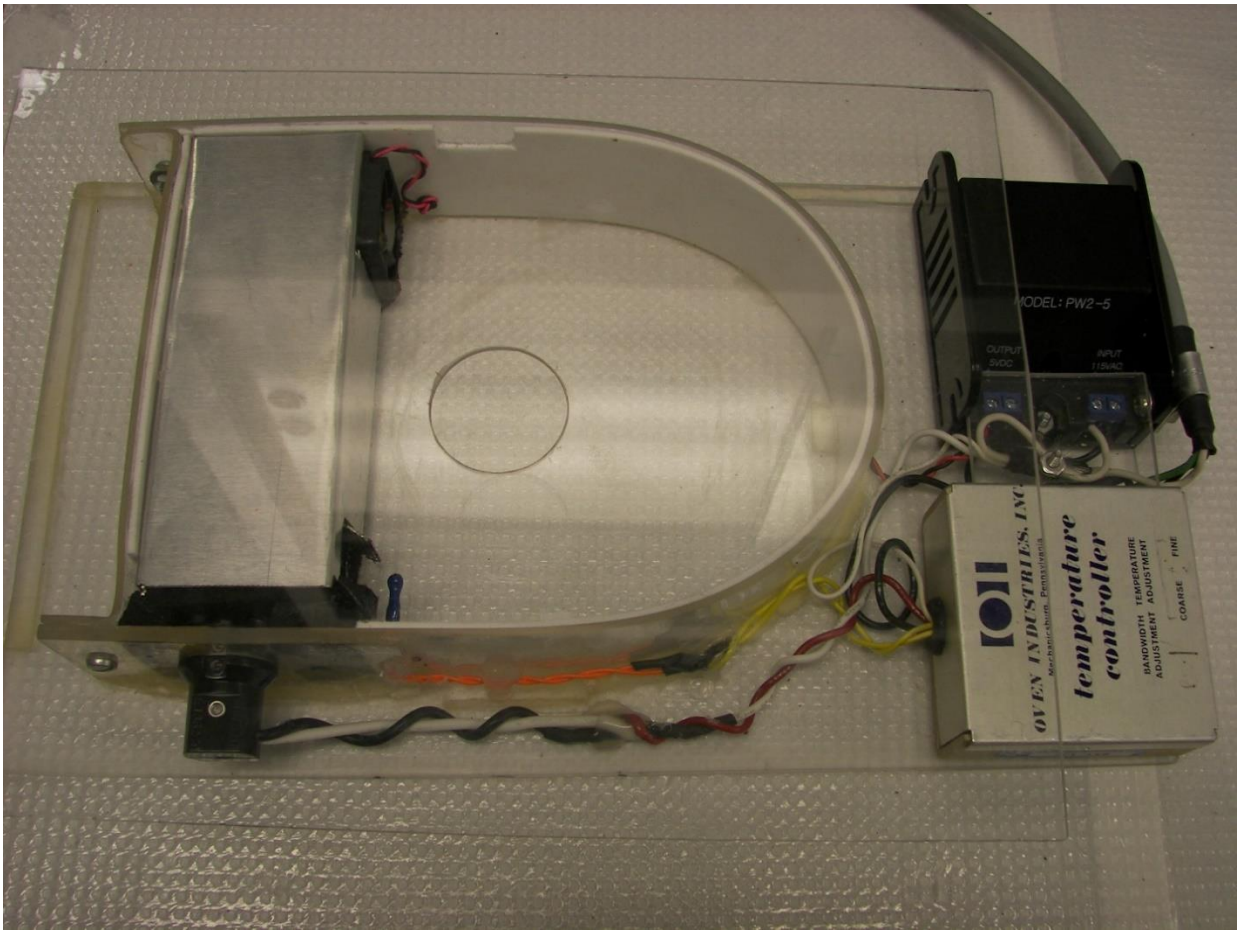

Figure 6
Microscopic Stage Chamber
A chamber that can be mounted onto the microscope to maintain embryo temperature during PQM data acquisition.

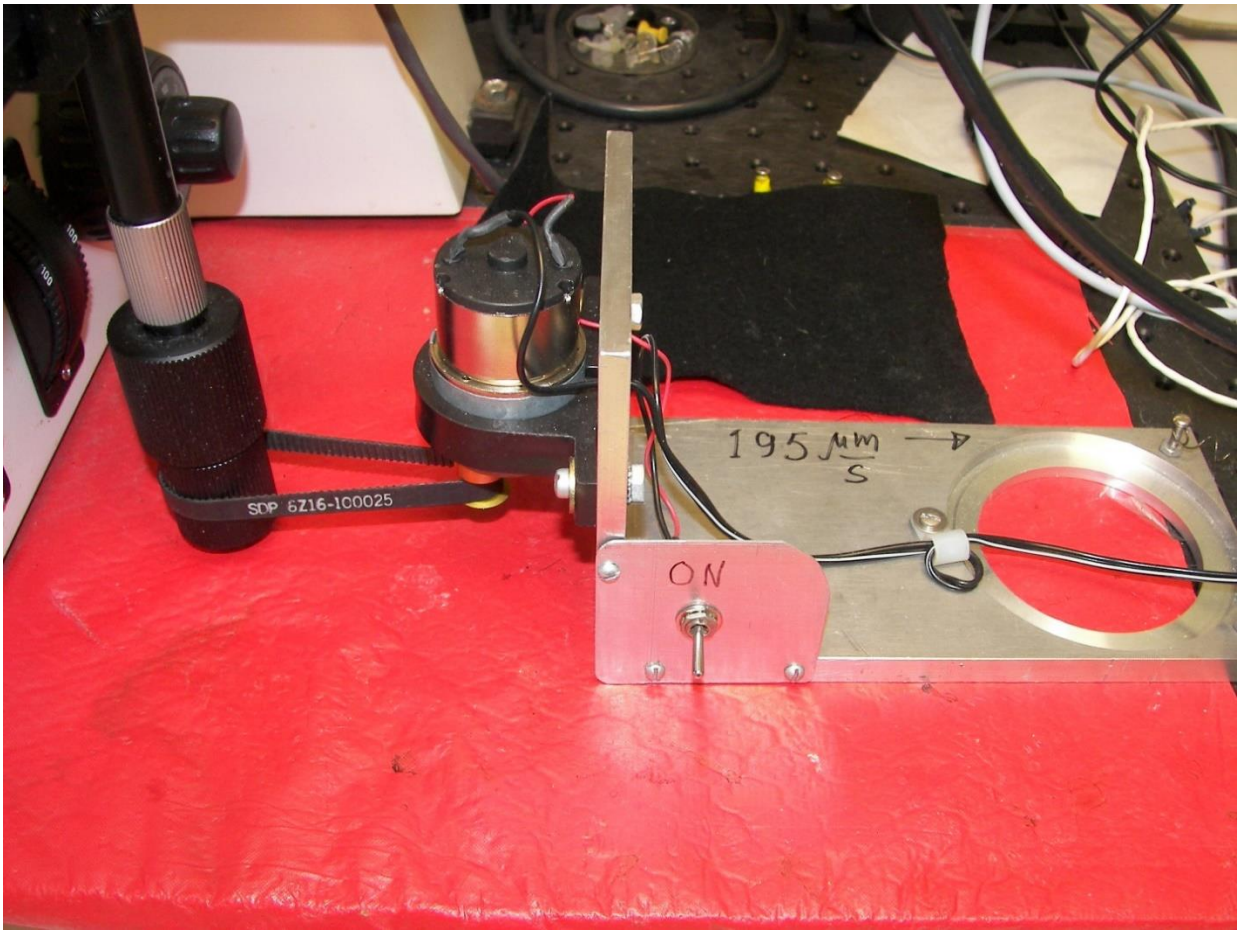

Figure 7
Automated Microscope Stage
The motor is attached to the horizontal fine adjustment knob by a textured rubber band. When activated, it moves the stage at a velocity of 0.195 mm/s.

Stereomicroscope

A stereomicroscope (SMZ645, Nikon Instruments, Melville NY) was used for taking low-magnification images, image sequences, and movies for angiogenesis quantification. An LED ring attachment provided illumination and a sheet of foam with a hole cut out of it was placed between the lights and the sample to reduce glare. Images were captured by a miniVue camera (Aven, Inc., Ann Arbor MI) replacing one eyepiece of the stereomicroscope. Images used for quantification of angiogenesis were taken at 1X magnification. The camera was connected to a PC by a USB port and images and videos were saved using the MicroCapLink program (Spectrum Software, Sunnyvale CA).

Stereomicroscopic Visualization Chamber

A microscopic visualization chamber was assembled within a 8”x6.5”x4”(WxLxH) Styrofoam box (Figure 8). A heating element was placed along the bottom and shorter sides and calibrated to maintain a temperature of 99.5 ^{o}F. A small hole allows the placement of a temperature probe used for calibration and to confirm interior temperature maintenance. A small fan circulates air within the chamber. The Styrofoam lid was replaced with a clear plastic lid to allow visualization into the chamber without exposing the contents to the outside environment. The lid surface in contact with the box was padded with glued foam to create a seal. Rubber bands around the shorter dimension of the box keep the lid in place. Push pins on the bottom corners allow the rubber bands to be placed around the box without lifting or tilting it and must be leveled to keep the box stable.

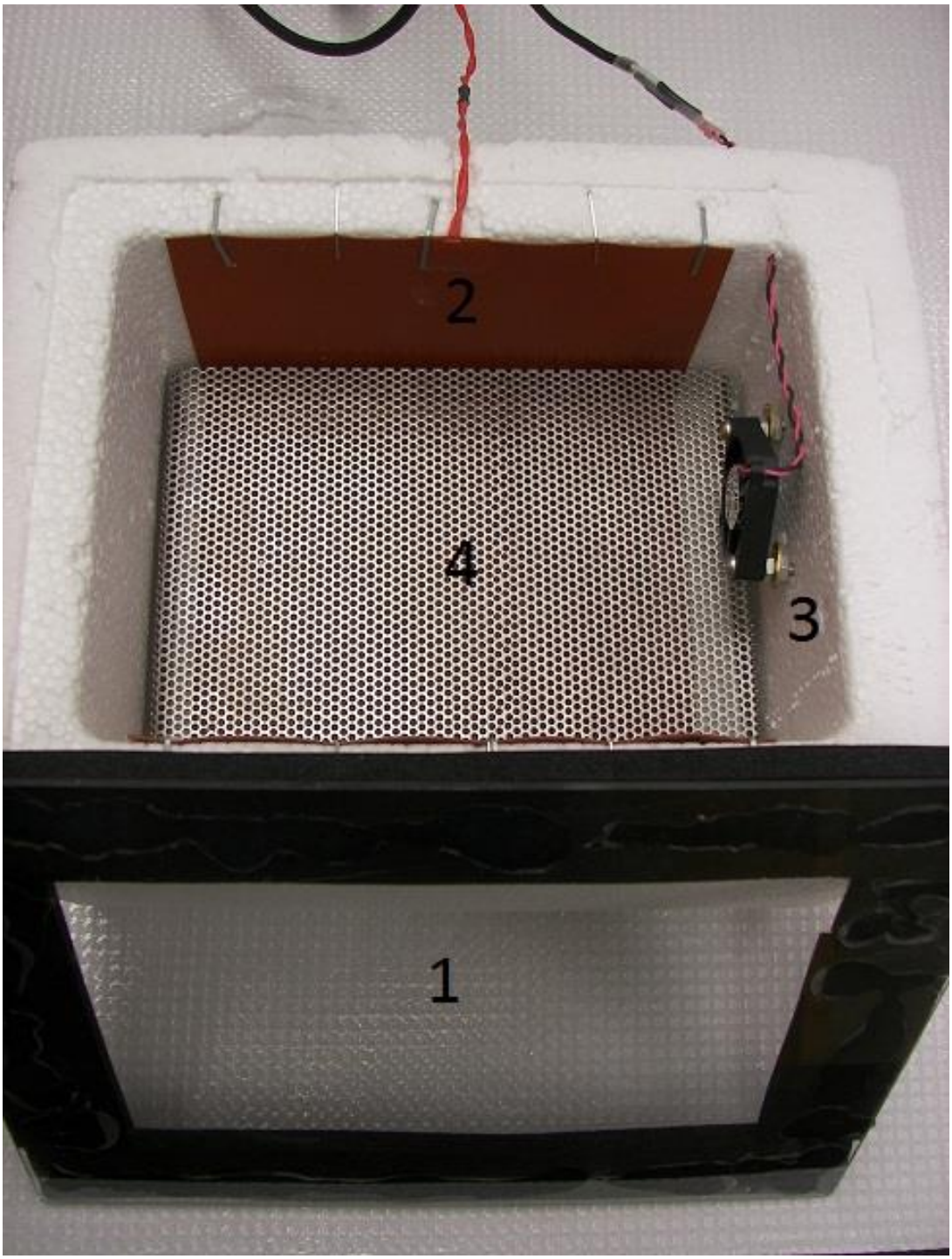

Figure 8
Stereomicroscopic Visualization Chamber
The chamber used to maintain embryo temperature during angiogenesis measurements. The components include a Styrofoam housing, the lid (1), the heating element (2), fan (3), and base (4).

Films

A low-density polyethylene film (Kirkland food wrap, Polyvinyl Films, Sutton MA) was used to provide a hanging support structure that would conform to a rounded shape when holding the egg yolk. This film was also used in preliminary studies as a high-permeability film. To maintain aseptic conditions, the first 200 cm of film in the roll (that was exposed to air) was discarded before the film was cut to length for use.

Polyvinylidene chloride film (Krehalon, Deventer, Netherlands) was used as an oxygen-impermeable film. Dialysis tubing was used as a highly oxygen-permeable film. Before being placed on the embryo, films were cut by placing a sheet between two pieces of printer paper and cutting out 10 mm diameter circular sections by pressing an appropriately sized hole-punch through the paper and into a piece of balsa wood. A central hole 2 mm in diameter was punched out similarly using a needle. “Empty” film patches (ERC) were made by cutting squares of film with 10 mm circles cut out in their centers (Figure 9).

PQM probe

Pd-Porphyrin probe was produced according to the methods laid out by Golub, et al (2007).

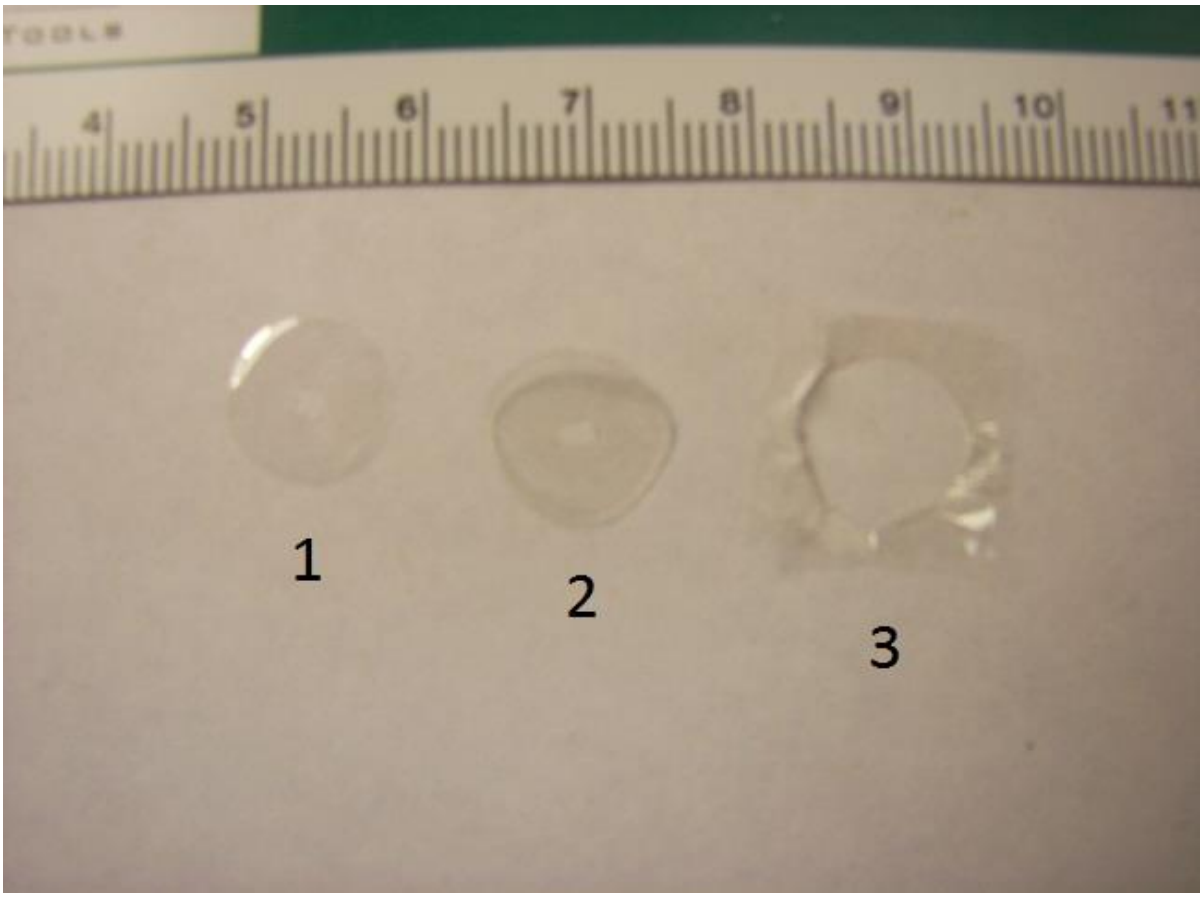

Figure 9
Film Patches
Patches of clear barrier film placed on vascular beds to impede oxygen flow. The three types of film used were PVDC (1), RC (2), and ERC (3).

Methods

Preincubation Conditions

During the first three days of incubation, the eggs were monitored to confirm correct temperature (99.5 ^{o}F), humidity (>70%), and activity of the rocker. The water reservoirs were refilled with deionized water when necessary.

Plating Technique

Plating refers to the transfer of the egg contents (embryo, yolk, and white) from the shell to the poultry dish. After 72 hours of incubation, the eggs were mature enough to survive the plating process and continued to grow long enough for the CAM to be appreciated and observed. Longer pre-incubation periods produced a weakening of the yolk sac membrane and its adhesion to the eggshell and greatly complicated a successful plating procedure.

All materials needed for plating were assembled and all components in contact with multiple eggs (the stirring rod, the piece of tubing, the worn gloves, the film-holding ring, and the film-resting surface) were sterilized by spraying with alcohol and air drying. The table top was covered with several paper towels and materials placed on top of them for ease of clean up in the case of a spilled egg. The eggs were prepared by wiping with a betadine solution (CVS, Woonsocket, RI), applied using a cotton ball before being replaced in the preincubator. The antibiotic solution was acquired either by preparing a new batch or retrieving and thawing a previously made solution.

During plating, as during preparation of all materials and all contact with embryos, nitrile examination gloves were worn and sterilized by spraying with alcohol and air drying and a mask was worn to prevent contamination by oral contaminants. A sealable freezer bag for the disposal of any discarded eggs was placed inside a beaker to keep it upright. A spare piece of paper towel was kept nearby to wipe down gloves and tubing after contact with egg white.

To plate an egg, first a square of film was cut from the roll. The first cut was measured to be 2/3 (but at least ½) of the width of the roll before a second cut was made to square it off. The square was placed on the plastic ring and pressed down slightly in the center to create an indentation for the egg to fall into without being so deep as to make contact with the table top.

A single egg was removed from the preincubator. The stirring rod was arranged on the table top perpendicular to the long axis of the shell as it was being held. The shell was cracked by striking it against the cutting edge halfway down its length. The embryo and was usually protected from the impact by being rotated into the large end of the egg. The thumb of the right hand was used to probe the crack and ensure that both the shell and the tough membrane directly beneath it were breached; this was confirmed by the observation of liquid inside or dripping from the crack. The left hand firmly held the egg around the middle while the thumb of the right hand applied pressure towards the small end of the egg against the crack to slowly expand the tear in the membrane and shell. When the opening was smoothly widened without excess pressure, the egg was turned so the crack faced downward while the two halves of the shell were pulled apart in one fluid motion. The contents of the egg (yolk, white, and embryo) fell into the hanging film sack.

If the shell membrane was not punctured when cracking the egg, application of force to the shell could have caused it to be crushed by the force before the membrane tore. Therefore, if a tear in the membrane was not observed from visible egg white, the egg would be struck again or if the shell was already heavily crushed, the membrane may have to have been manually opened by carefully puncturing it with a gloved thumb or a detached piece of eggshell. If, alternatively, the force of the egg onto the cutting edge was too great, the shell around the impact area had a tendency to crumble, making the application of necessary separating force difficult without driving the broken shell pieces into the egg, assuming the yolk sac membrane had not already been ruptured.

If, after removing the egg contents from the shell, the yolk membrane was ruptured, the yolk could be seen spilling into the white. This was not compatible with embryonic survival for more than another 48 hours and the egg was discarded in the freezer bag and a note made on the record sheet that the egg was spilled. If the yolk was intact, the embryo was located. After 72 hours of incubation, the embryo had a visibly beating single chambered heart and the beginnings of a circular AV around it. There was also often a discoloration of the yolk on the hemisphere on which the embryo lies. Unfertilized eggs or embryos that failed to thrive did not have these features but had a distinct white spot. These attributes were be noted before discarding the egg contents in the freezer bag and the shell as well as any film that came in contact with the egg thrown away. The record noted whether the egg was discarded due to failure to thrive (“D”), yolk spillage due to technical error (“S”) or both. The protocol sheet used to record data is included in appendix 1.

The embryo often fell into the hammock facing downward and if allowed to incubate in this orientation soon expired. The length of tubing was used by holding it by its ends and passing its length under the yolk. The tubing would catch thick egg white attached to the yolk and cause it to rotate in the direction the tubing was passed underneath it. If the motion was too vigorous, the yolk ruptured, wasting the egg. If the yolk would be over-rotated by one pass of the tubing underneath it, the progress of the tubing should be stopped and can be pulled out from one side without rotating the yolk further. After use, the tubing was wiped clean on the paper towel.

With the embryo centered on the top of the yolk, it could then be transferred by lifting the plastic ring complex and placing it on top of a new poultry dish. The dish was prepared by removing both the top and bottom lids and aligning the holes of the bottoms with the smaller dish half upright and the larger dish half upside down. The interior surface of the upper dish was lubricated with water or a lubricant to allow for easier movement of the film within the dish. The yolk settled in the hole through the dish but only lightly. The edges of the film were lifted from the plastic ring and held in a point above the dish at this point and the plastic ring lifted completely away. The poultry dish was then lifted with one hand and more film pulled through the hole from the bottom with the other hand until the entire yolk was sitting within the hammock and spherical with only the embryo on the surface. The direction the film was pulled in maintained the embryo's upward position and care was taken not to cause it to rotate to the side of the yolk. The pulling of the film caused it to be taut from the central hole to the upper rim of the dish. If necessary, the tubing was used again to press the film down until it was flush with the base of the upper dish around its edge. After use, the tubing was wiped clean on the paper towel. The excess film overlapping the edge of the dish was pulled flat against the outer

circumference and the edges tucked underneath the edge of the lower dish half. Placing the lower lid secured the film and prevented the weight of the egg from pulling the film down into the lower half of the dish.

Before being placed in the incubator, the embryo is given its first dose (1.2 ml) of antibiotic solution and the top (filter paper) lid was placed on top. The eggs were identified by the date of plating and a letter (usually A-L for a dozen eggs) which was written on the top of each poultry dish lid in permanent marker.

Incubation Conditions

The eggs were checked twice a day (morning and afternoon) to confirm survival, correct temperature (99.5 ^{o}F), and humidity (>80%). Because the on-board humidity gauge of the Farm Innovators incubators do not recognize values above 80%, the presence of condensation on the inside of the glass viewing areas was a better indicator of proper incubation humidity. The water reservoirs were checked daily and refilled with deionized water when necessary. Embryonic death could usually be detected by a collapse and regression of the AV and imperceptible heartbeat during early incubation (before 10 days) and by a reduction in the vividness of the red blood in the vessels and a cessation of fetal movement during late incubation (after 10 days). An image of the embryo was taken using the unmagnified camera and if the cause of death could be determined (fungal or bacterial contamination, spilled egg yolk, etc.) it was recorded. The remains were placed in a sealed freezer bag (Ziplock) and frozen until disposal. Embryos surviving experimental procedures were euthanized by freezing in bags before reaching hatching age. Frozen egg contents were disposed of in the same manner as frozen animal carcasses.

Egg Maintenance after Plating

1.2 ml of antibiotic solution (7.68mg Penicillin G/5.76mg Streptomycin) were applied directly after plating and every three days afterwards. These times corresponded to simultaneous activity that required embryonic exposure. D3 (three days after initial incubation) marked the time of plating, while AV angiogenesis measurements were taken on D6 and CAM angiogenesis measurements were taken on D9.

Film Placement

The embryos were examined for suitability for experimentation before placement of a film patch. Evidence of spilled yolk or contamination failed exclusion criteria and resulted in immediate euthanization of the embryo. When placing a film patch on the AV, a larger exposed area (often overflowing the hanging hammock) was preferentially selected. In CAM studies, embryos with CAM that had developed enough to grow beyond the yolk borders were preferable due to their optical properties and increased contrast. A piece of film from one of the film groups – PVDC, RC, or ERC (an "empty" patch of RC film) – was prepared by separating it from its paper covering, picking it up using sterilized forceps, and spraying it on both sides with isopropyl alcohol. The film was air dried for thirty seconds before the excess alcohol was rinsed off by repeated submersion in a dish filled with deionized water. In cases where the film showed a preference for bending in one direction, effort was made to reverse the direction of preferential folding with two pairs of forceps. The film was then placed on either the AV or the CAM (Figure 10) and the poultry dish lid was replaced.

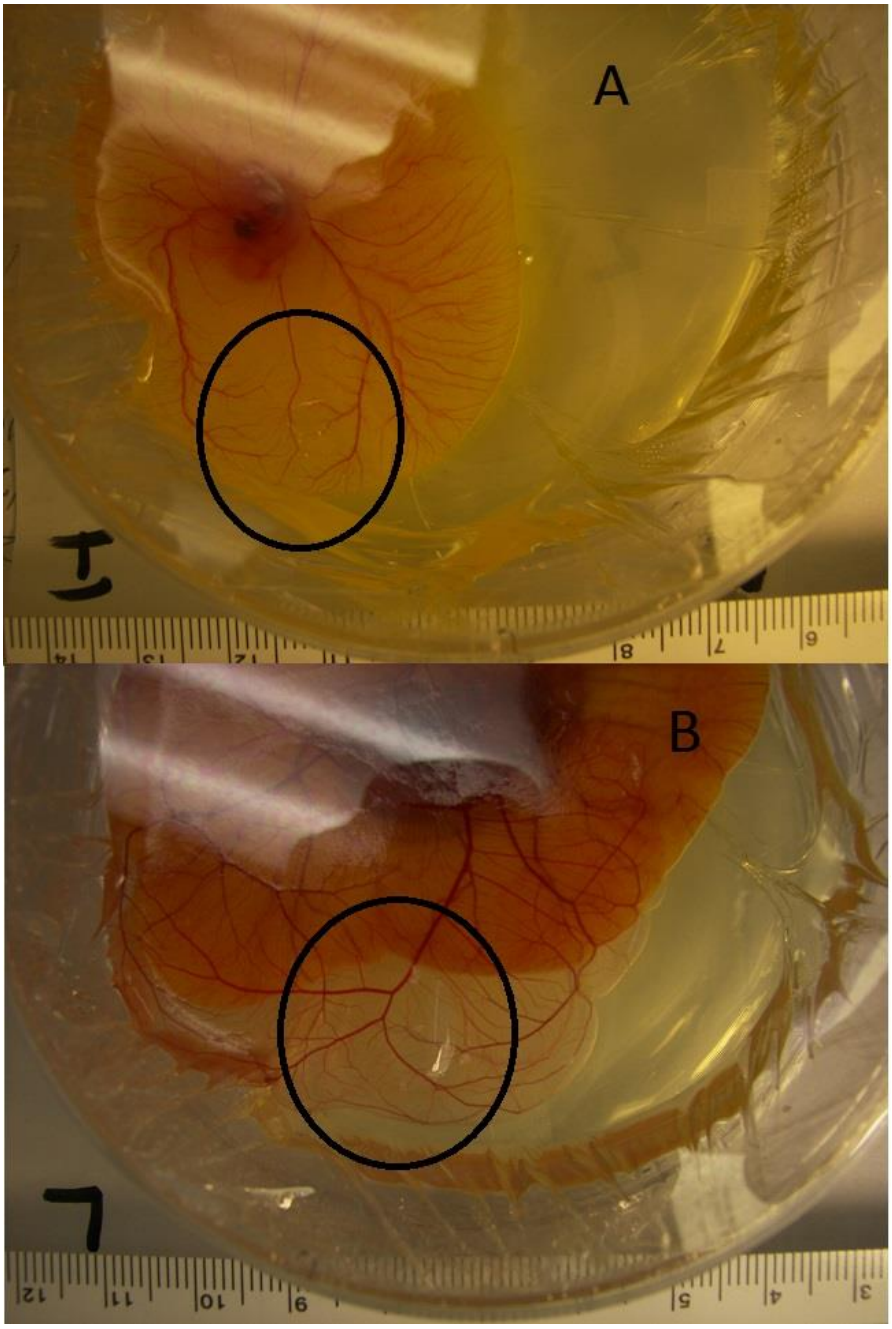

Figure 10
Film Patches on Vasculature
Film patches as they appear on the AV (A) and CAM (B). The film is designed to be clear so as not to obscure any vasculature underneath, but is circled in black and identifiable by the glare around the edges.

Phosphorescence Quenching Microscopy (PQM)

In order to make oxygenation measurements, Pd-porphyrin probe was applied to the CAM and AV under the film, as well as being applied to the edges of the film. Excitation decay curves were converted to oxygen measurements using a rectangular distribution model fitting program.

PQM Methodology and Scanning

A sequence of regularly spaced PQM measurements taken with a constantly moving microscope stage (a "scan") produces a series of data that correspond to the changing availability of oxygen throughout the range observed. To test the oxygen barrier properties of PVDC when placed on respiring vascular beds of the chick embryo, circular sections of film were used to maintain radial symmetry for reliable variations in atmospheric oxygen exchange and diffusion. Topical application of nitrite or control solution necessitated a central hole in the film, which maintains radial symmetry but exposes the central film area to atmospheric oxygen. Scans through the center of the film allowed determination of the observable area under the film which was maintained at low stable PO_2.

PQM produces a series of decay curves that can be processed to determine PO_2 at that point and time. The sequence gives a series of PO_2 values at known times apart depending on the rate of excitation illumination. Flash rates of 1 Hz and 10 Hz were used, resulting in sequences of data with points 1 s and 0.1 s apart, respectively. The translational velocity of the motorized automated microscope stage was measured by measuring the distance traveled (using a mounted ruler) by the elapsed time. The stage was calculated to move at a rate of 0.195 mm/s. Using an acquisition rate of 1 Hz produced points separated by a distance of 0.195 mm while an

acquisition rate of 10 Hz produced points separated by 19.5 um. PQM method results in the consumption of oxygen and therefore, with a 40 um circular excitation area, sequential recordings at 10 Hz will have overlap between successive measurements and produce slightly lower PO_2 readings. For this reason, when determining PO_2 values for the three groups (Air, PVDC and RC), averages were taken of recordings at a 1 Hz flash rate. When determining the size of areas with different oxygenation levels, fine spatial resolution was more important than accuracy of PO_2 measurements so 10 Hz recordings were used.

A typical scan (Figure 11) of a PVDC film shows several distinct areas with corresponding PO_2 levels: the uncovered sections (outside the edges on each side and over the central hole) with high PO_2 and the covered sections with low PO_2. There are small transitional areas at the film boundaries where the PO_2 is at an intermediate level between the stable high or low PO_2 areas. Multiple scans were taken of each film and values from each scan were averaged to produce a single mean value for each film.

Determination of Film Oxygen Barrier Properties

Steady state PO_2 values were determined by selecting the section of 1 Hz scan data corresponding to the desired film state and averaging those PO_2 data points to get an average PO_2 for that section of that scan. All the section averages were compiled and averaged to get a single PO_2 for that condition of the embryo (n=1).

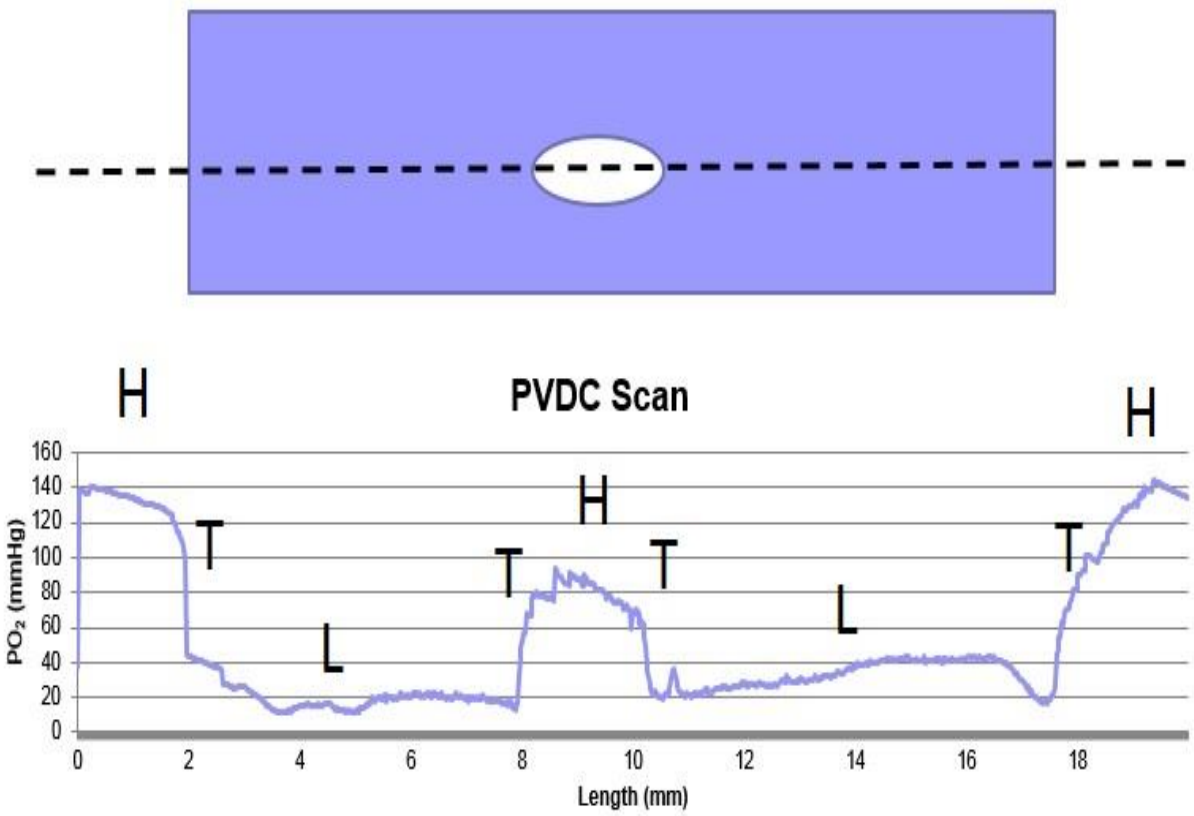

Figure 11
PO_2 Scan
A diagram with a schematic of the (circular) film patch (above) distorted to match the scan. The dotted line indicates the path the microscope objective takes while taking continuous PQM measurements. A plot of the measurements (below) shows regions of PO_2 that correspond to regions on the film. Regions under the film have low PO_2 (L), while regions exposed to air have high PO_2 (H). There are small transitional regions (T) between the two regions where the PO_2 changes quickly as a function of distance traveled.

Transitional data were compiled by examining the periods in 10 Hz scan data between the high and low steady states where the PO_2 changed in a linear fashion (Figure 12). The data for each transition region were modeled using linear regression and the slope was recorded, as well as the distance over which the PO_2 change was linear. These data points for each transition section were averaged to get a single slope and distance mean for each embryo (n=1).

For PQM measurements, embryos and films were prepared and applied as described for angiogenesis quantification. AV measurements were taken on D6 and CAM on D9 or D10.

Description of Chemicals and Control Groups

Embryos ready for angiogenesis quantification were assigned randomly to a film group (PVDC, RC or ERC) and an intervention (Saline, Nitrite or Nitrite+cPTIO). (Table 1) shows the n-value distribution for the angiogenesis experiments conducted.

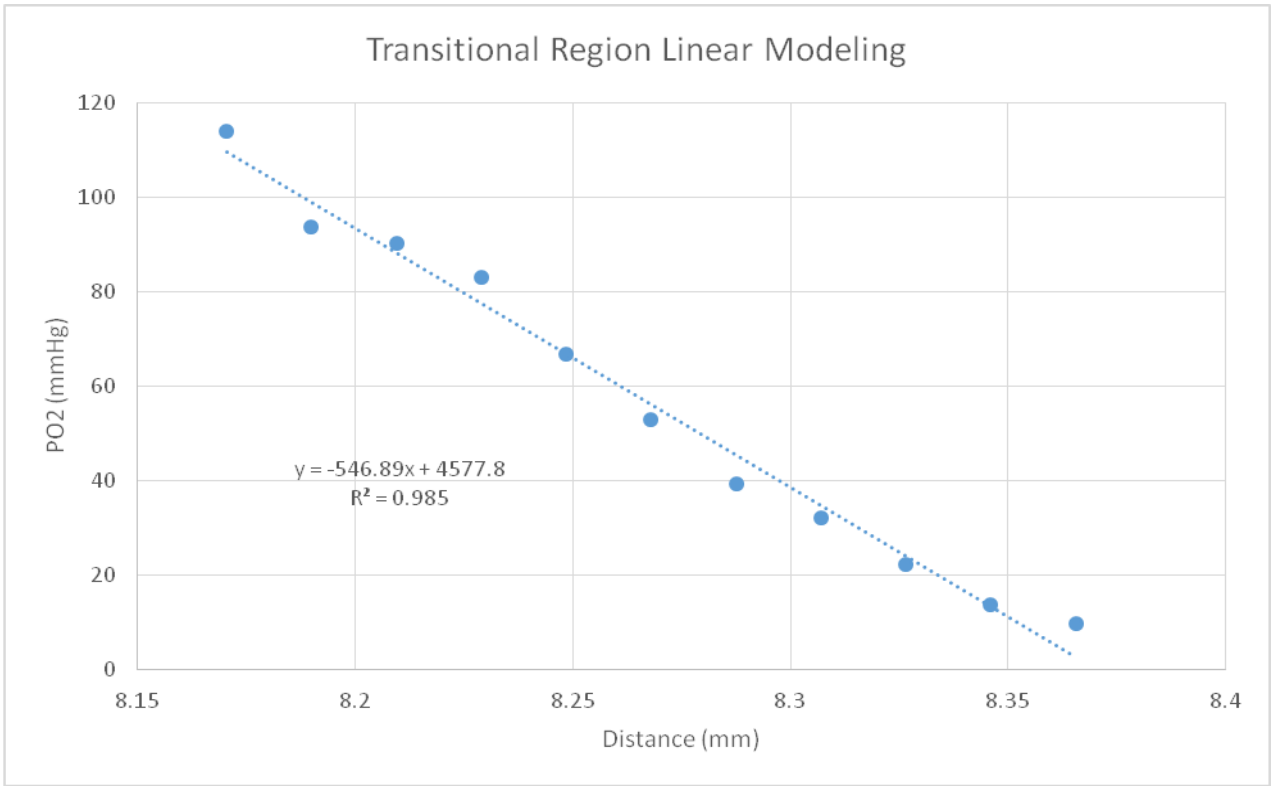

Figure 12

Transition Region Modeling

The points from each transitional region were isolated to those that fit a linear pattern. Linear regression determined the slope of the best fit line (546 mmHg/mm in this example) and the x-value (distance) difference between the first and last points of the area was recorded as the length of the transitional region.

Angiogenic Image Acquisition

In order to access an unimpeded viewing area, the incubation lid (with filter paper) was replaced temporarily with a lid treated with anti-fog spray. After film patch placement, unmagnified images were made using the Nikon camera to display gross structures and the placement of the film patch in relation to other structures. The poultry dish was transferred to the stereomicroscopic visualization chamber and aligned so that the center of the film was aligned with the eye of the embryo (easily identifiable by its solid black color). The film was then divided into four quadrants- top, bottom, left and right. An image at 1X magnification was taken in each of these quadrants in addition to one middle image of the central hole in the case of non-empty films. These film images were considered part of the Experimental group. Control group images (unassociated with film patches) were taken to the left and right of the film and 5 mm away from the nearest edge. (Figure 13) shows the orientation of angiogenesis quantification sites. The embryo then had its incubation lid replaced and was returned to the incubator.

Table 1

AV				CAM			
	ERC	PVDC	RC		ERC	PVDC	RC
Saline	4	3	3	Saline	2	2	3
Nitrite	6	6	6	Nitrite	5	5	5
Nitrite+cPTIO	5	5	4	Nitrite+cPTIO	2	2	1

A list of the number of trials performed for a given vascular bed (AV or CAM), a given film type (ERC, PVDC, or RC), and a given fluid intervention (saline, nitrite or nitrite and cPTIO).

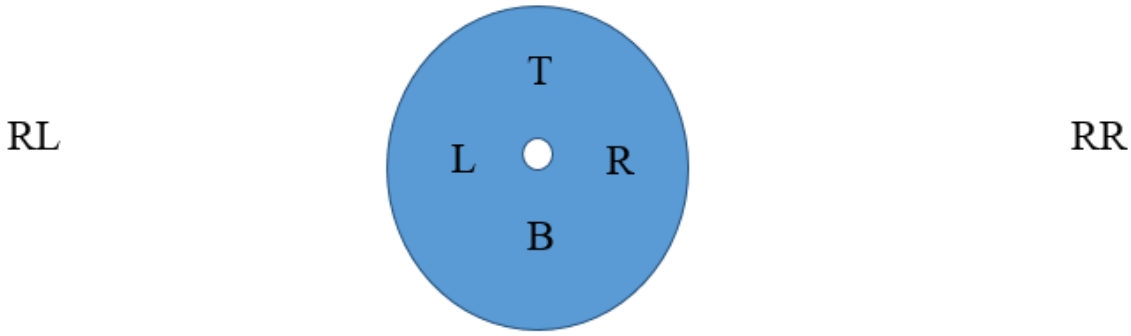

Figure 13
Orientation of Angiogenesis Quantification Sites
The circular film area has four experimental sites that are recorded for angiogenesis quantification. They lie to the left (L), right (R), top (T), and bottom (B) of the central film hole. Two additional control images are taken to the remote left (RL) and remote right (RR) of the film.

Solution Application

To continuously apply solution, a tubing lid (with semi-circular filter paper and three holes) was placed onto the poultry dish so that the paper side concealed the embryo while the film remained under the transparent half of the preparation. A marker was used to approximate the point on the lid directly above the center of the film and the tubing lid was replaced by the original lid. A hole was drilled through the marked spot using a 1/16" drill bit. The tubing from a syringe loaded in the syringe pump was fed through the hole and positioned so that the tubing tip lay just above the center of the film (Figure 14). Hot glue was used to secure the tubing in place (twirling the tubing when the glue is still hot, then letting it settle downwards as it cooled was an effective strategy). The poultry dish was then placed back in the incubator and, after the process was repeated for each embryo, the tubing for each dish was secured to the incubator frame with electrical tape. The pump was then turned on and allowed to continuously pump the solution in the syringes onto the embryos inside the incubator for the next 48 hours.

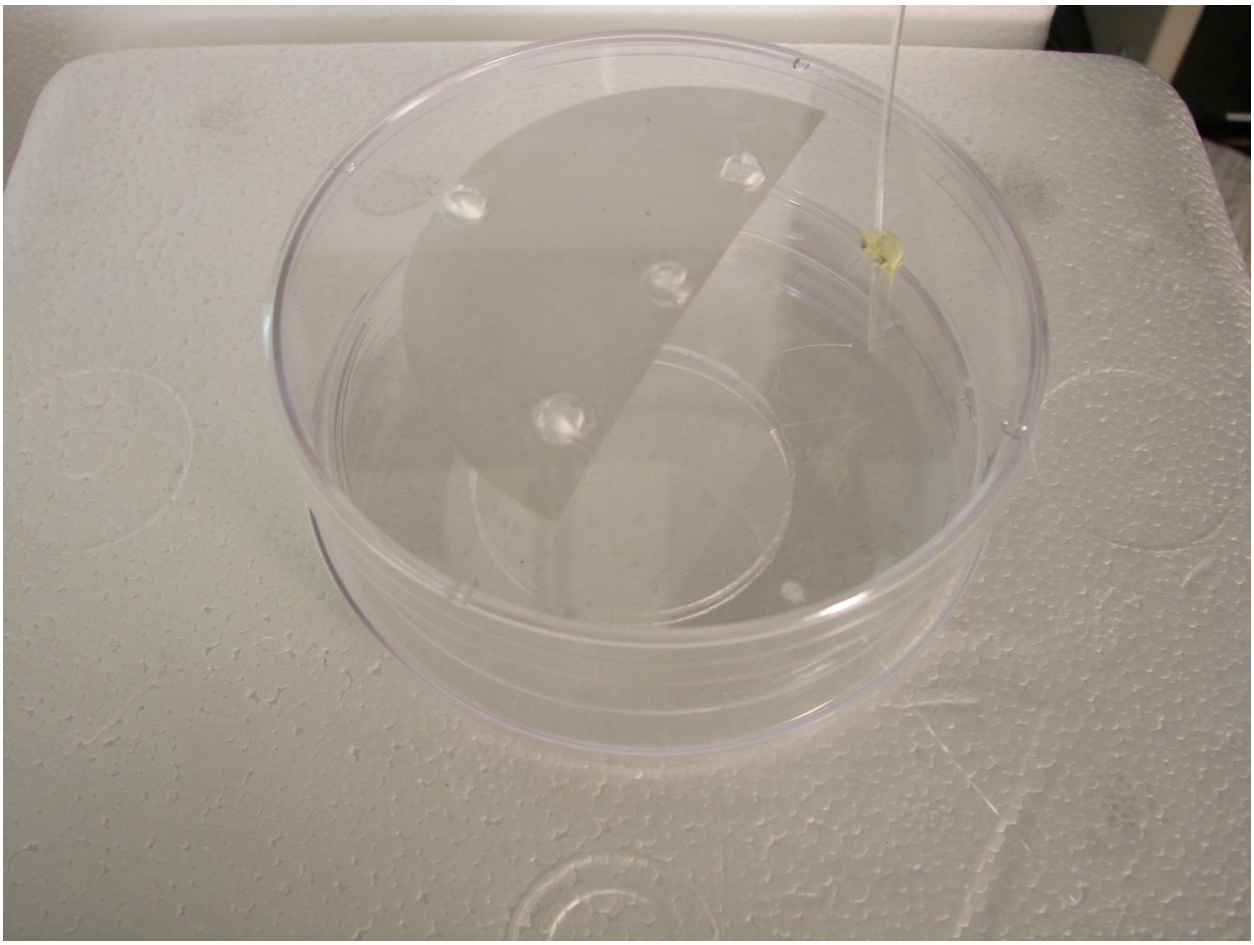

Figure 14
Solution Pump Setup
The Poultry dish uses a lid with a semi-circular piece of filter paper to allow for better visualization during tubing placement. The tubing is fed through a hole drilled in the lid and secured with hot glue. A syringe pump delivers the desired solution at a constant flow rate.

Experimental Design for Angiogenesis Measurements

Baseline measurements for the AV were taken on D6 when the vessels had stopped spreading farther along the yolk sac, but continued to increase in vascular density. The experimental solutions were applied via tubing to the center of the placed films for a period of 48 hours before another set of angiogenesis measurements were taken on D8. CAM angiogenesis measurements were taken once the CAM spread beyond the edge of the yolk far enough (~10 mm) to fit the entirety of the applied film. This usually occurred on D9 or D10. There is some variation between batches of eggs or even eggs within a single batch. Some reasons for this include genetic differences between breeds, the season, differences in development when incubation is started, the time delay between hatching and incubation, and incubator conditions (Hamburger, 1951). Again, an experimental solution was applied and measurements taken after 48 hours had passed.

Image Processing for Angiogenic Variables

Low-magnification images were processed to determine the number of vessel bifurcations, total vascular distance, and complexity (i.e., fractal dimension of network). Initially, a 3mmx3mm section of the image was isolated for examination, based on previous findings that at least 3mm of vasculature under PVDC film is hypoxic. A vascular map was first made by manipulating the contrast between the vessels and background, then manually tracing the vasculature with a 10-pixel wide line. Only arterioles and venules – identifiable by their larger size, regular pattern, and thicker walls – were mapped, while capillaries and sinuses were not. The points where one vessel split into two or where a vessel took more than a 45 degree turn were counted to determine the number of bifurcations. The number of dark pixels was necessarily proportional to the total

length traced and can be converted by multiplying by the length conversion factor (distance/pixel) and dividing by the width of the lines (10 pixels). The FracLac plugin (NIH) was used to calculate complexity. (Figure 15) gives a graphical representation of this process. See Appendix 2 for a full description of the procedure.

Statistical Analysis

Unless explicitly stated, all aggregate data are presented as the mean of a population with error bars representing the standard error. JMP (JMP 10.0.2 SAS Institute, Inc. Cary, NC) was used to perform significance tests (analysis of variance in cases of multiple factors and t-test on two independent means). Significance was concluded at a level of $p < 0.05$.

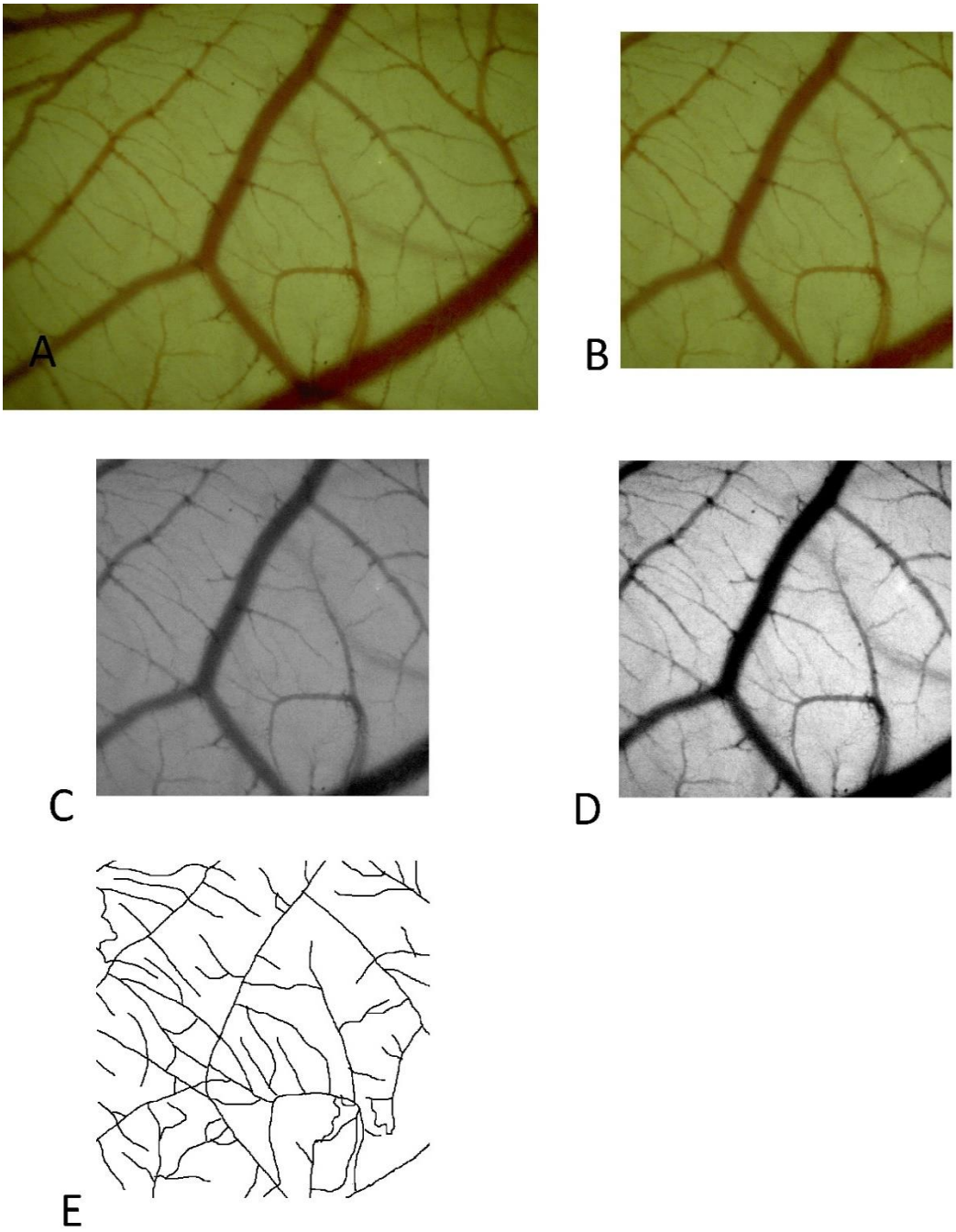

Figure 15
Angiogenesis Processing Example
These are the steps taken to quantify angiogenesis from the images taken by the stereomicroscope. The initial image (A) is cropped to a 3 mm x 3 mm square (B), as this is an area under the PVDC film we can be confident is at low steady-state PO_2. The green data from the color image is isolated (C) and the contrast enhanced (D) before the vasculature is manually traced (E).

RESULTS

PO_2 under Films

As anticipated, the low-permeability PVDC film produced a low PO_2 environment in the CAM it covers (Figure 16). The PVDC film reduced CAM PO_2 to 17.9±5.5 mmHg and AV PO_2 to 29.5±3.6 while the RC film maintained a PO_2 of 121±9.7 mmHg. Uncovered areas of vascular bed exposed to room air maintained a PO_2 of 112.5±3.7 mmHg in the CAM and 117.4±5.5 mmHg in the AV. There was no significant difference in PO_2 between CAM covered by Air and RC film, while PO_2 for the CAM under PVDC film was significantly lower than uncovered areas of the same vascular bed.

PO_2 Transition Regions

The average length for a section of the CAM under PVDC film to be at a steady-state low PO_2, when measured through the midline of a film circle, was 3.81±0.19 mm. A t-test showed that this length was larger than the 3 mm visible area used to analyze the angiogenesis data ($p<0.006$). The slope of the linear portion of the transition region between low and high PO_2 at the edge of a film piece was 332.11±20.58 mmHg/mm. This linear transition region occupied an average distance of 0.26±0.02 mm.

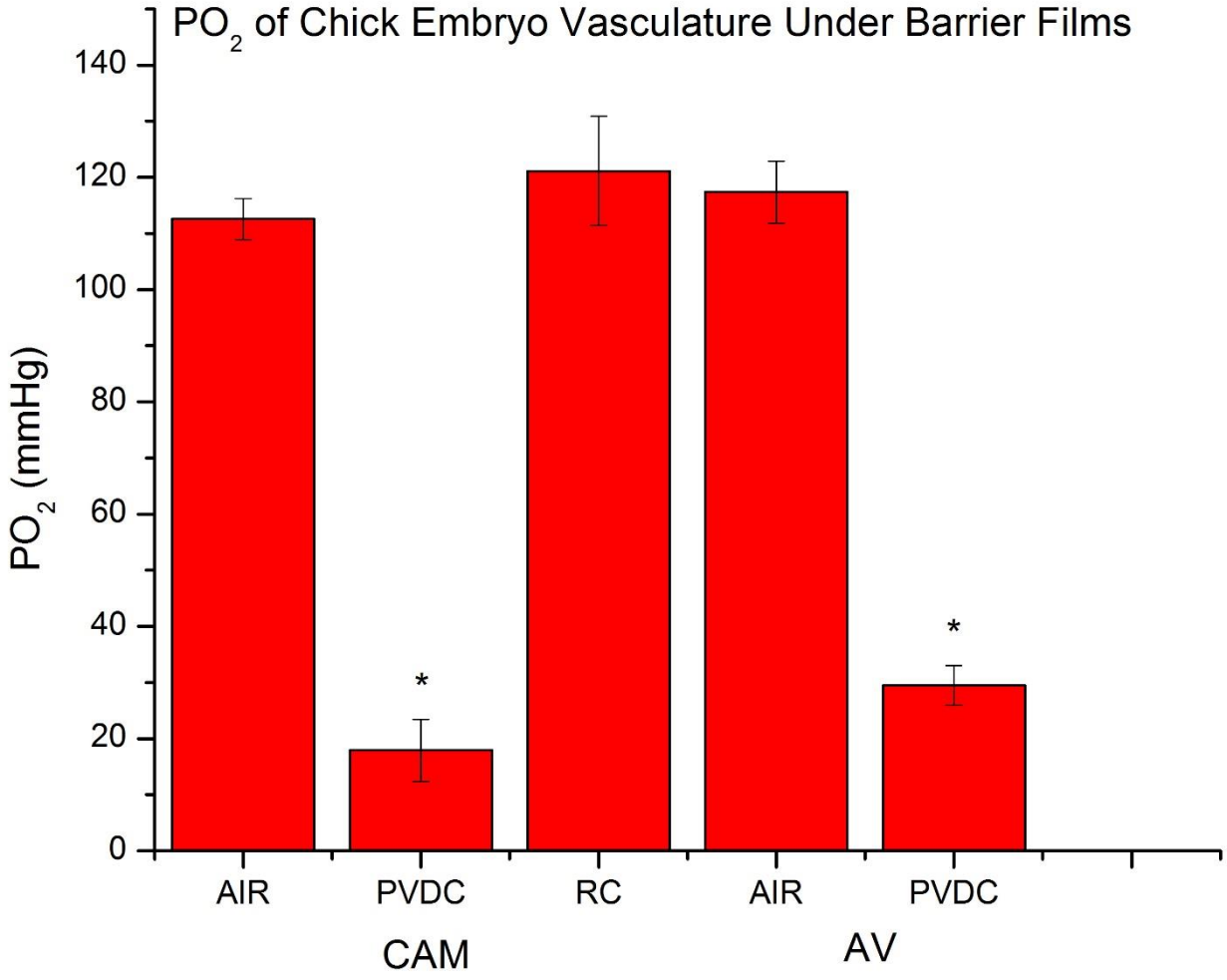

Figure 16
Steady State PO_2 by Film
A comparison of the steady-state values between different film regions. In the CAM, regions under PVDC film (n=6) was less than either those areas exposed to air (n=9) or those under RC film (n=4). In the AV, the PVDC regions (n=3) were likewise less than the uncovered regions (n=3). In each case, the PVDC group had a statistically lower PO_2 ($p<0.001$).

Vascular Bed Comparison

It was evident that the organization of the vasculature differed markedly between the CAM and AV vascular beds. As shown in (Figure 17) the AV has a structure more closely resembling a capillary plexus with irregular growth of the arterioles and venules. The AV microvessels were also more difficult to distinguish from capillaries because, while the capillaries were more prominent and visible, their diameter spanned a continuum up towards that of arterioles and venules. The CAM has a regular structure of alternating branching arterioles and venules. There was a highly significant ($p<0.0001$) difference between the baseline vascularity in the two vascular beds according to all three measures of vascularity (Figure 18).

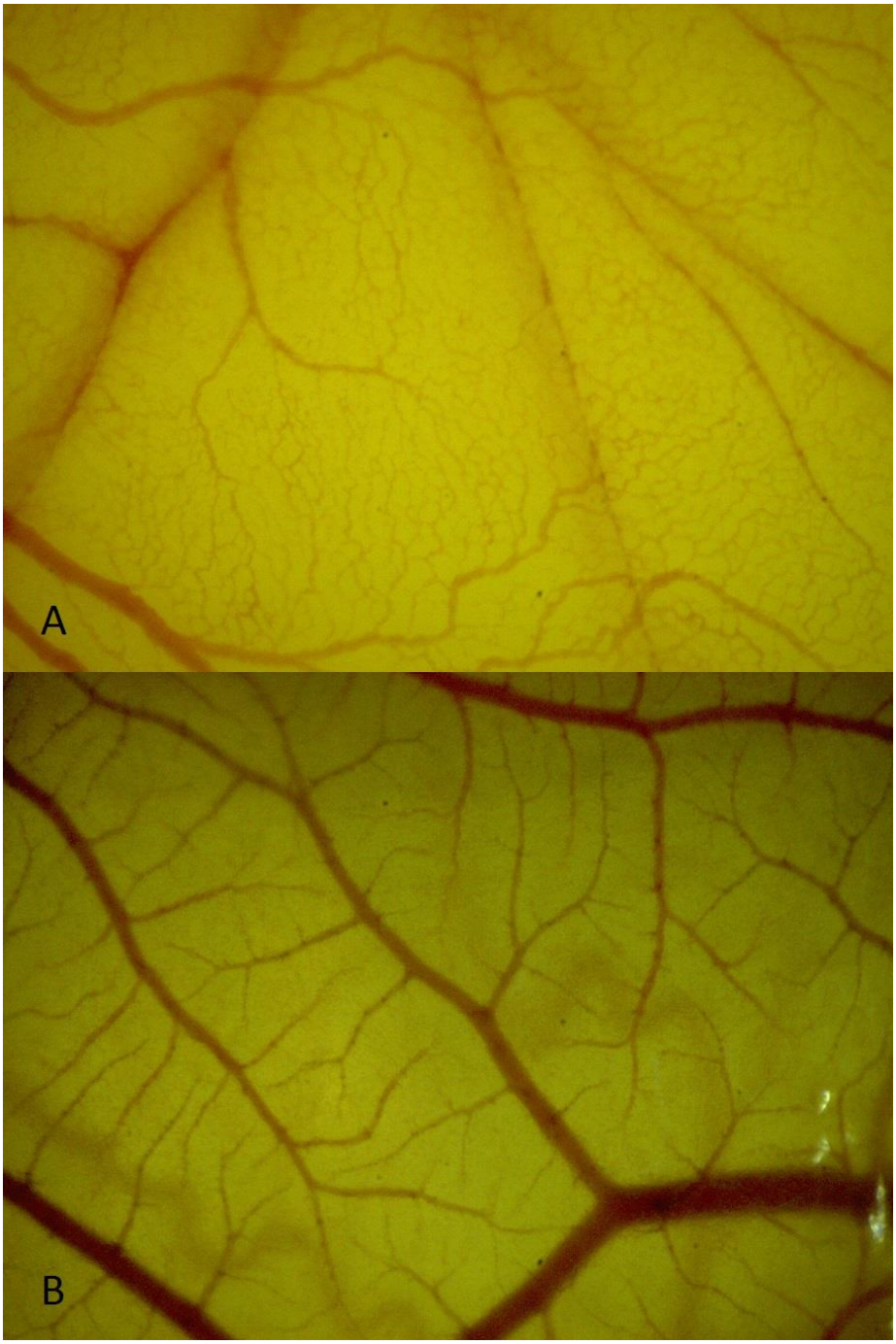

Figure 17
Vascular Bed Gross Comparison
A gross comparison between the vasculature visible in the AV (A) and in the CAM (B) networks. The capillaries are less differentiated in the AV and there is a spectrum of vessel sizes which form a disorganized branching pattern of capillaries resembling a sinus. The CAM vasculature exhibits a more conventional network regularity with regularly spaced bifurcations and a hierarchy of vessels getting smaller the farther away they are from the feed vessel.

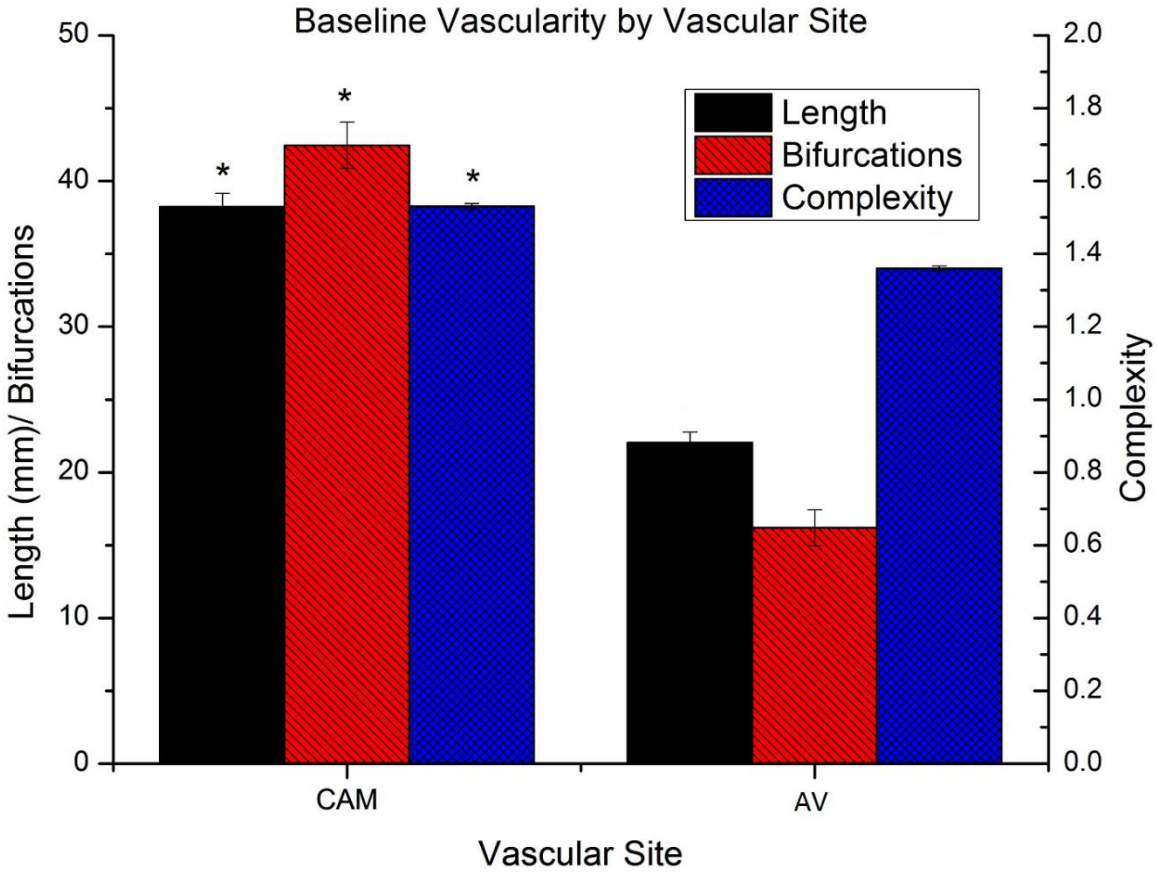

Figure 18
Baseline Vascularity Differences Between Vascular Beds
By the three measures of vascularity used, the vascularity of the CAM (*) was found to be significantly different from the matching value for the AV ($p < 0.0001$). The total vascular length and number of bifurcations is plotted on the same scale on the left axis of the plot, while the axis for the complexity measurement is on the right axis.

Baseline Comparisons

To confirm there were no significant differences between the different selected populations, the baseline values for each set of groups were compared. In both the AV (Figure 19) and CAM (Figure 20), there were no significant differences that could be attributed to film treatments (PVDC, RC, or ERC) or the intervention groups (Saline, Nitrite, or cPTIO). In the CAM there was no difference between the experimental (under film) or control (away from film) sites. There was found to be a significant difference between the baseline experimental and control sites in the AV ($p=0.043$). This may be attributable to a slight distortion or obscuration of the vasculature by the presence of the film, but also may be a consequence of normal variability. The other angiogenic measures (length and complexity) were not significantly different. The observed difference may be attributable to a slight distortion or obscuration of the vasculature by the presence of the film, but also may be a consequence of normal variability. Some slight obscuration was observed, but due to the curvature of the film used, not their optical properties. The RC film pieces, particularly, were cut from a strip of film dispensed from its storage state in a roll. Therefore even when excised, the film piece maintained its curvature and because it is stiffer than PVDC, its downward curvature would impart a slight deformation to the tissue it was placed onto. This deformation would put some parts of the vascular bed in the viewing field out of focus and may have led to the reduction in observed bifurcations attributable to small, easily missed shoots.

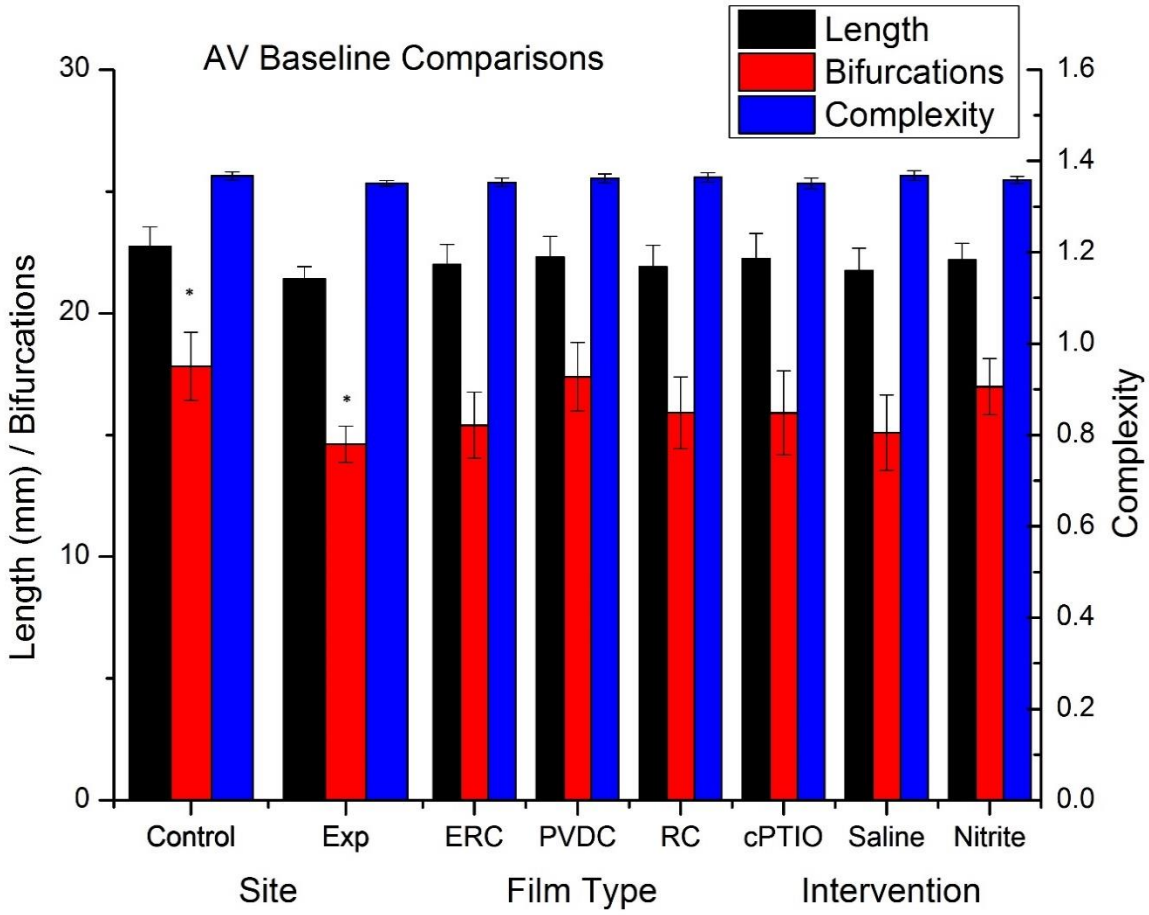

Figure 19
AV Baseline Vascularity Comparisons
These data represent the vascularity observed in the AV before incubation with film and application of the fluid intervention. There was a significant difference in the average number of bifurcations (*) between the vasculature under film (Exp) and that outside the film (Control) ($p=0.043$). The other groups and vascular endpoints had no significant differences.

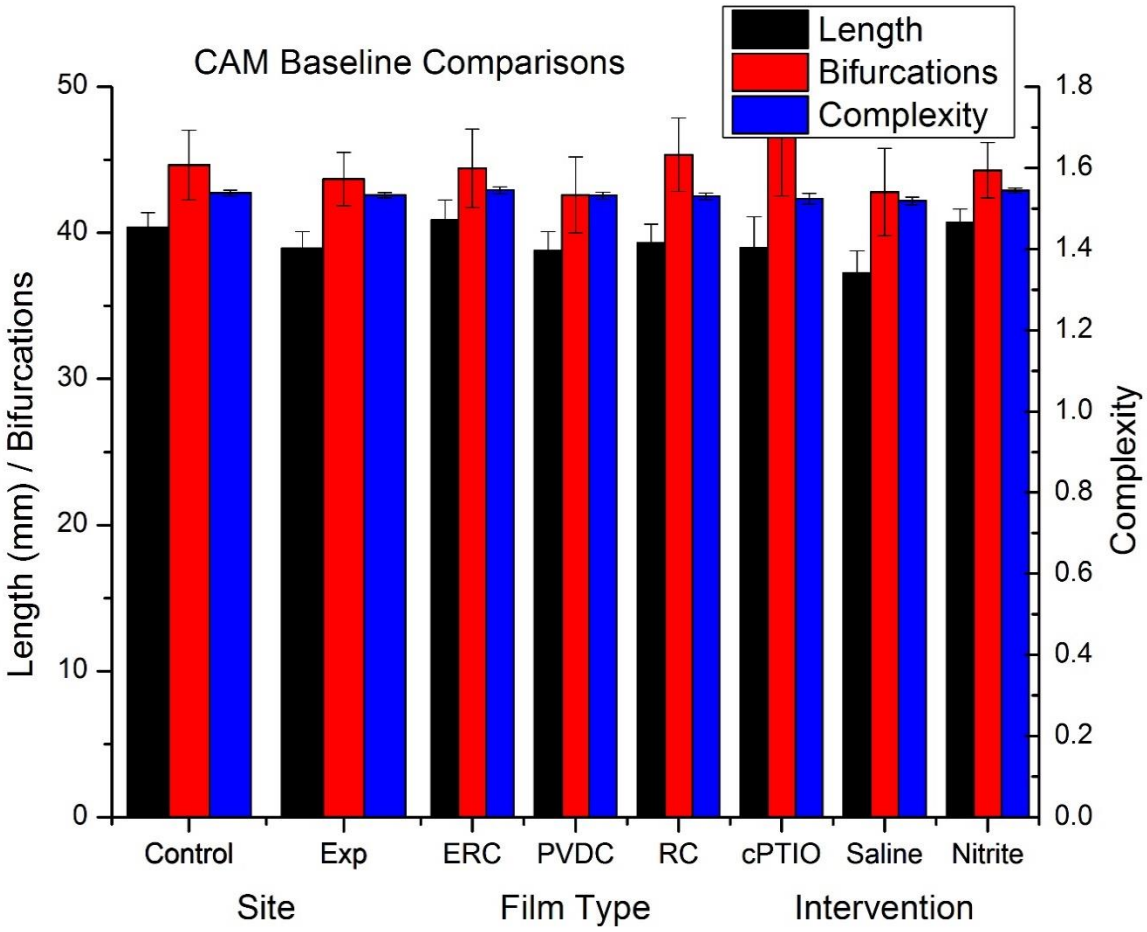

Figure 20
CAM Baseline Vascularity Comparisons
These data represent the vascularity observed in the CAM before incubation with film and application of the fluid intervention. There were no significant differences found between any of the groups.

Changes in Angiogenesis at Control Sites

Angiogenesis data collected from control sites at least 5 mm from the edge of the film were examined to determine if local changes in oxygen availability or fluid intervention could produce angiogenic effects distant from the site of intervention.

In the AV, no significant differences were observed among either the film groups (Figure 21) or the fluid interventions (Figure 22). In the CAM as well, no significant differences were observed for either the film groups (Figure 23) or the fluid interventions (Figure 24).

In the AV there was a trend for an increased number of bifurcations as a consequence of naturally driven angiogenesis, but no significant differences (Figure 25).

In the CAM, there was a clear and statistically significant ($p < 0.005$) increase in vascularity between baseline measurements and follow-up measurements conducted 48 hours later (Figure 26). The average vascular length increased by 8.7 mm (6%), the average number of bifurcations increased by 17.9 (15%) and the average complexity increased by 0.04 (0.4%).

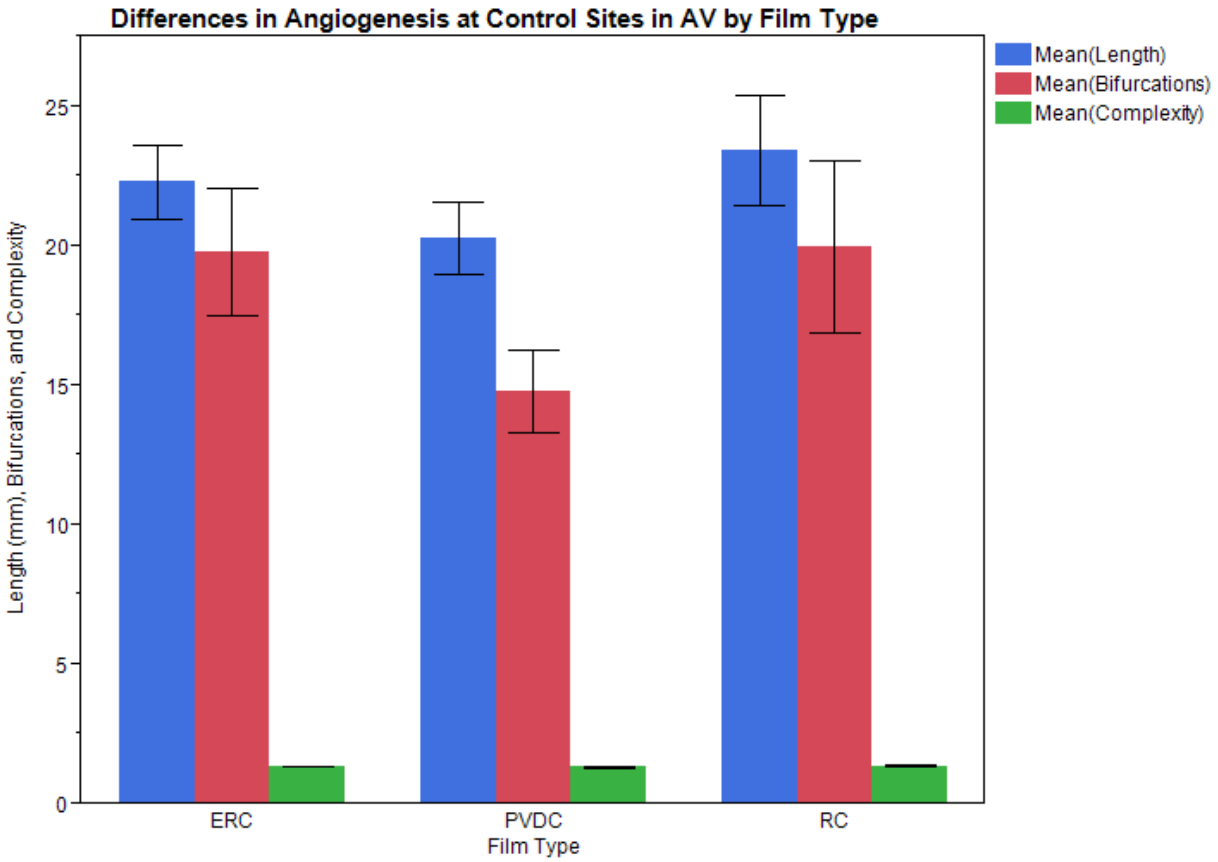

Figure 21

AV Angiogenesis at Control Sites by Film Type

When comparing sites outside the film area, no significant differences were observed attributable to the film type placed on the AV.

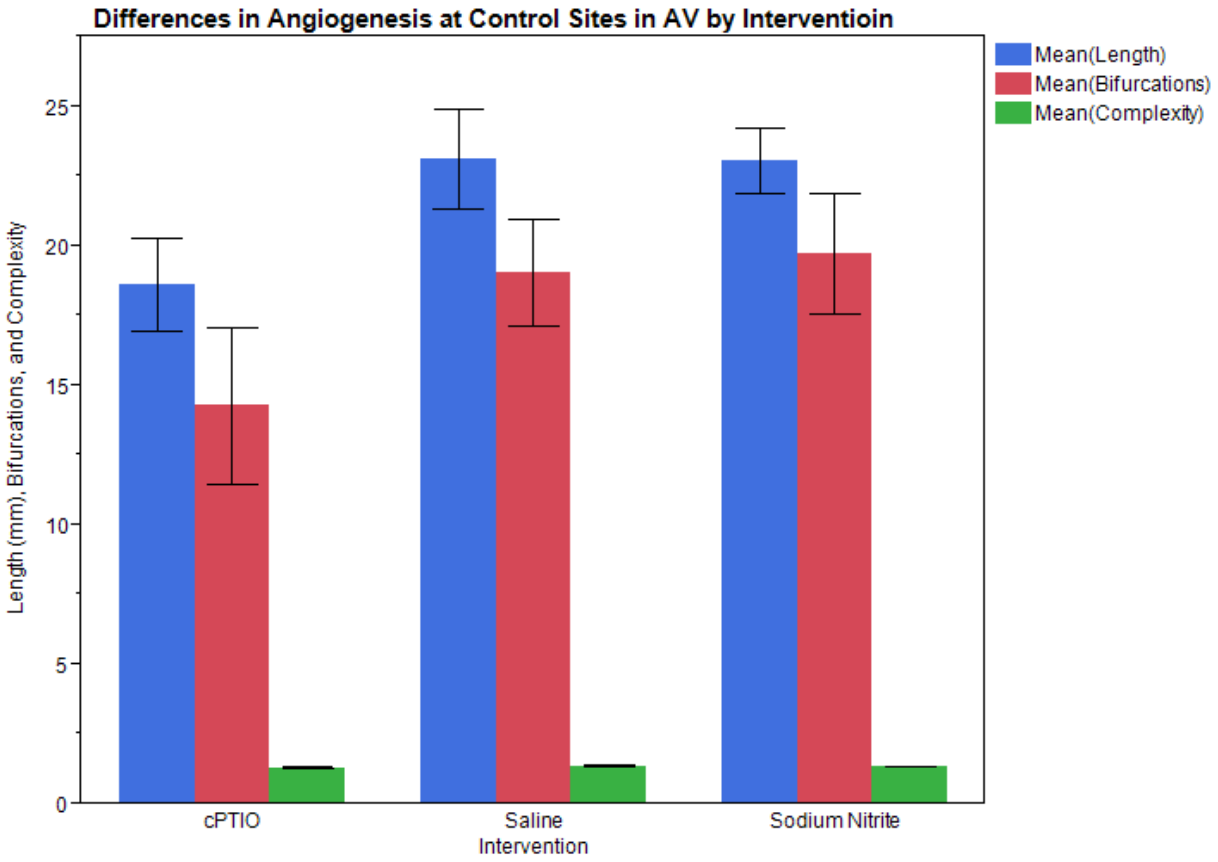

Figure 22
AV Angiogenesis at Control Sites by Intervention
When comparing sites outside the film area, no significant differences were observed attributable to the type of chemical in the fluid applied to the AV.

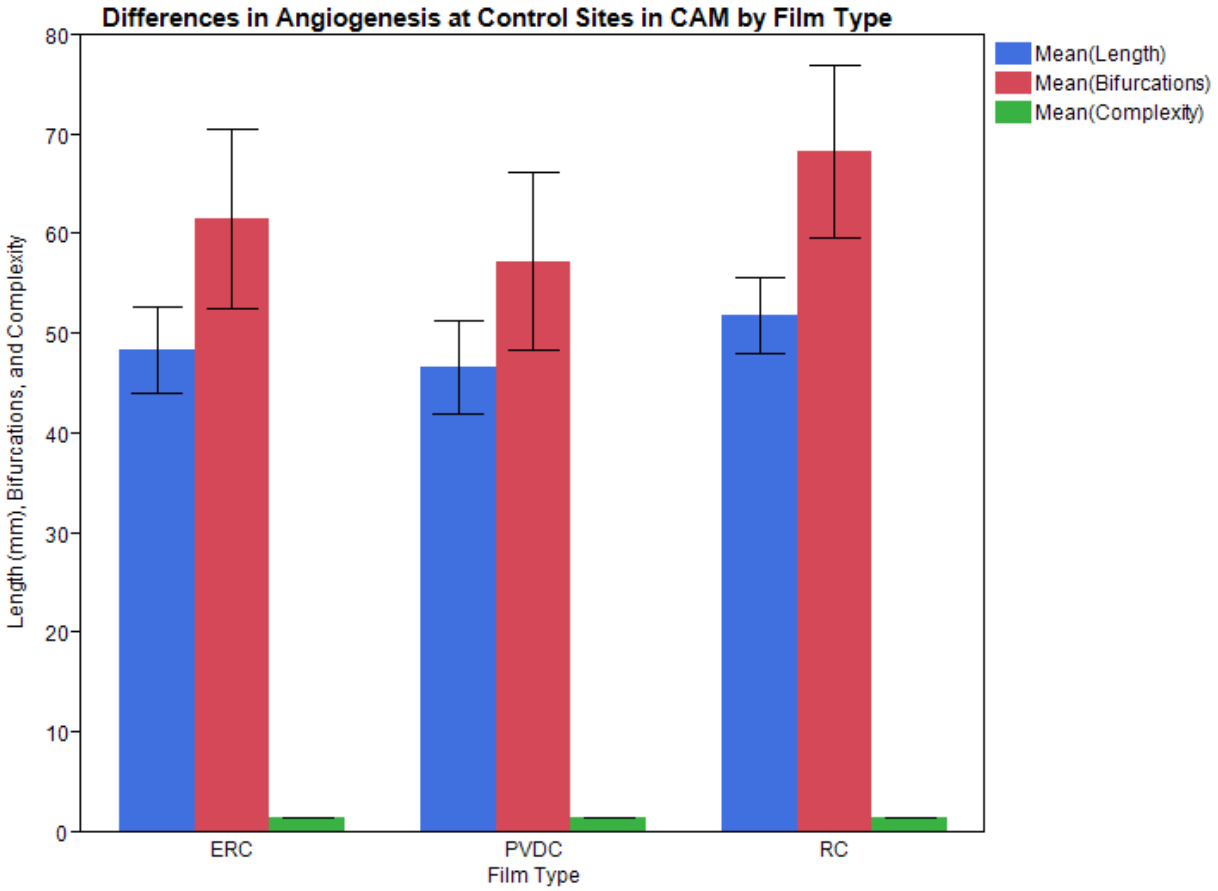

Figure 23

CAM Angiogenesis at Control Sites by Film Type

When comparing sites outside the film area, no significant differences were observed attributable to the film type placed on the CAM.

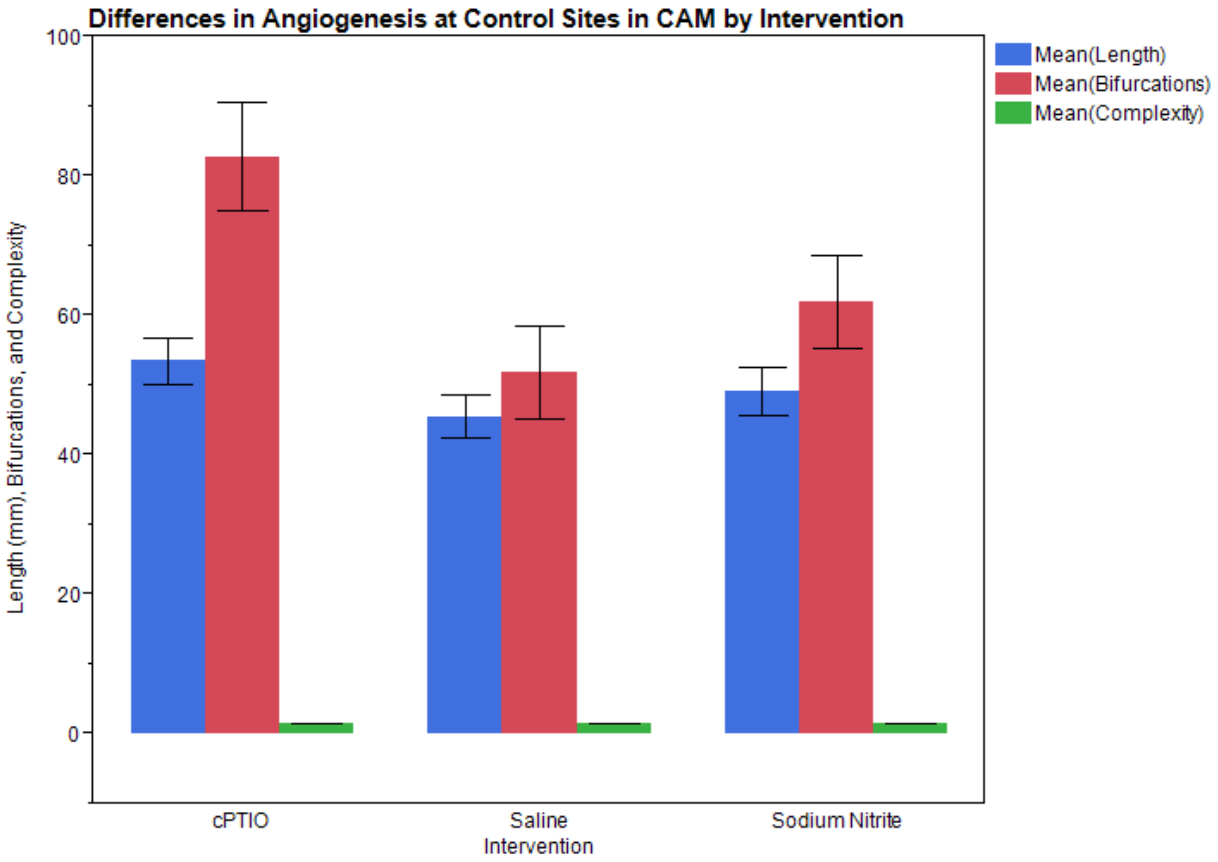

Figure 24

CAM Angiogenesis at Control Sites by Intervention

When comparing sites outside the film area, no significant differences were observed attributable to the type of chemical in the fluid applied to the CAM.

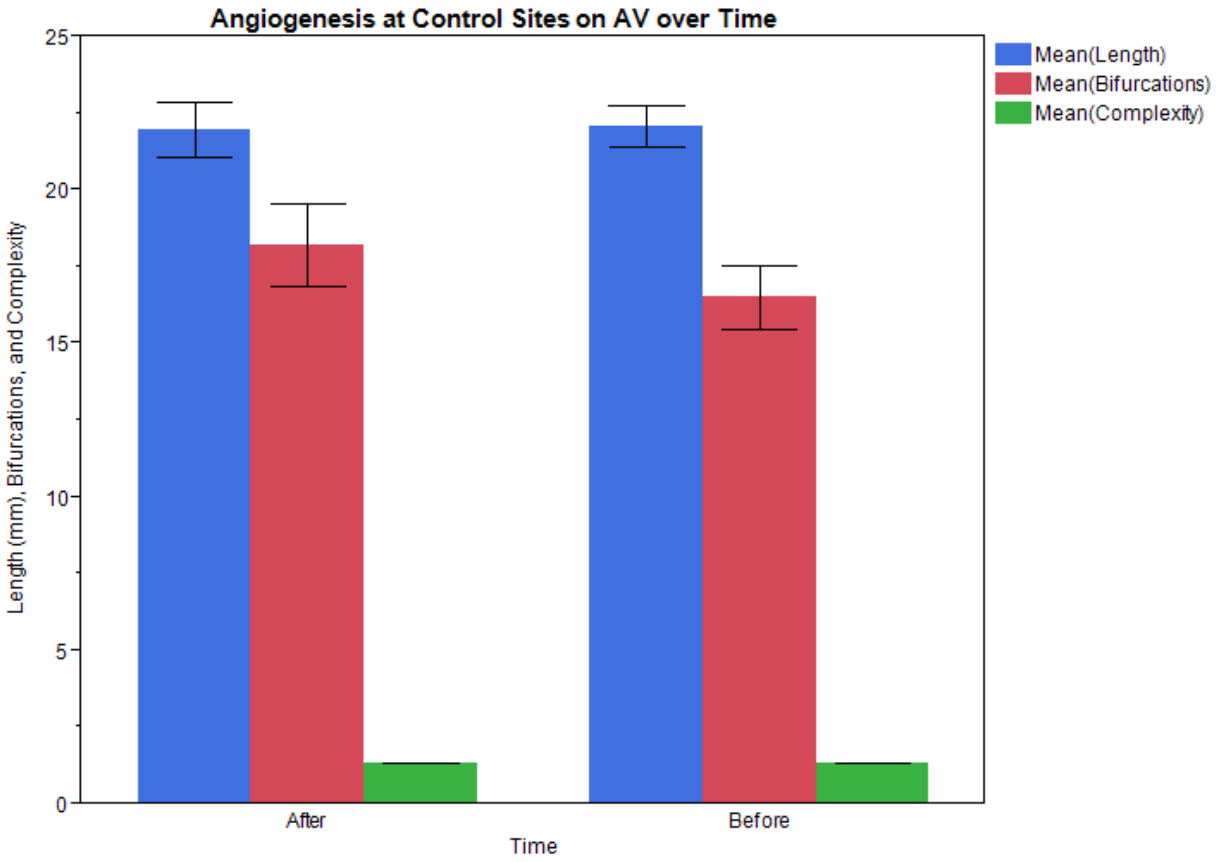

Figure 25
Control Angiogenesis in AV
There were no indications of angiogenesis through observation of AV vascularity after a 48 hour period in control sites.

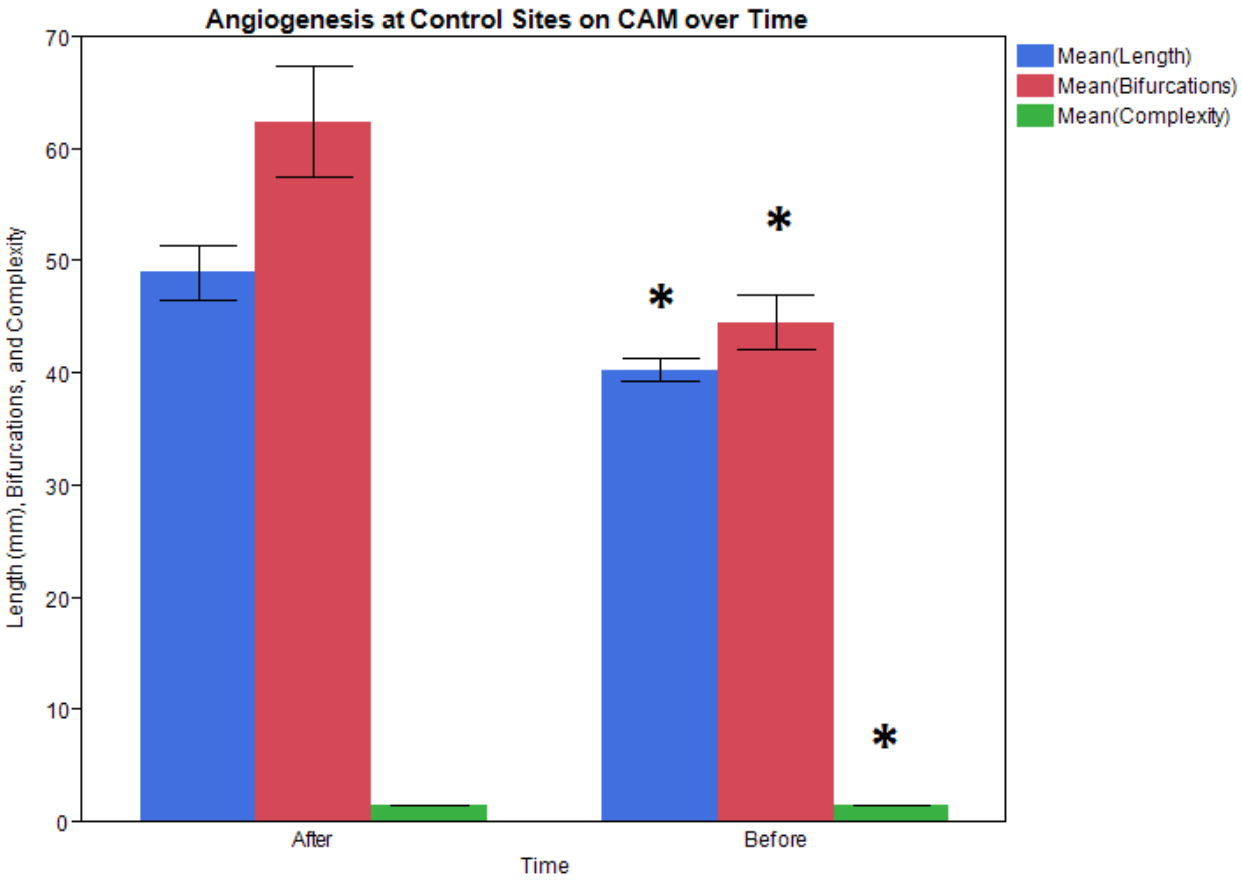

Figure 26
Control Angiogenesis in CAM
There was a significant increase in vascularity attributable to angiogenesis in control sites of the CAM between D10 and D12 (* $p < 0.005$).

Effects of Saline on Local Hypoxia-Induced Angiogenesis

The angiogenic effects of different levels of local oxygen were examined in embryos treated with 48 hours of a control solution of saline. With a control intervention (saline), there were no significant differences between the three film groups in either the AV (Figure 27) or CAM (Figure 28). There was a slight trend of reduced angiogenesis in the CAM, but it was not significant.

Effect of Nitrite on Angiogenesis

The angiogenic effects of different chemical interventions were compared after 48 hours of application to an uncovered vascular area. In the AV the only significant finding was that of a difference in length attributable to a reduction in length in the Nitrite+cPTIO group (Figure 29). This finding was not accompanied by corresponding reductions in the complexity or number of bifurcations.

In the CAM, while there was a large amount of variability in the readings, there were trends that suggest that nitrite inhibited angiogenesis. Although not statistically significant, nitrite application to the CAM resulted in a reduction in all three measures of angiogenesis (Figure 30). This trend was reversed when cPTIO was added to the nitrite.

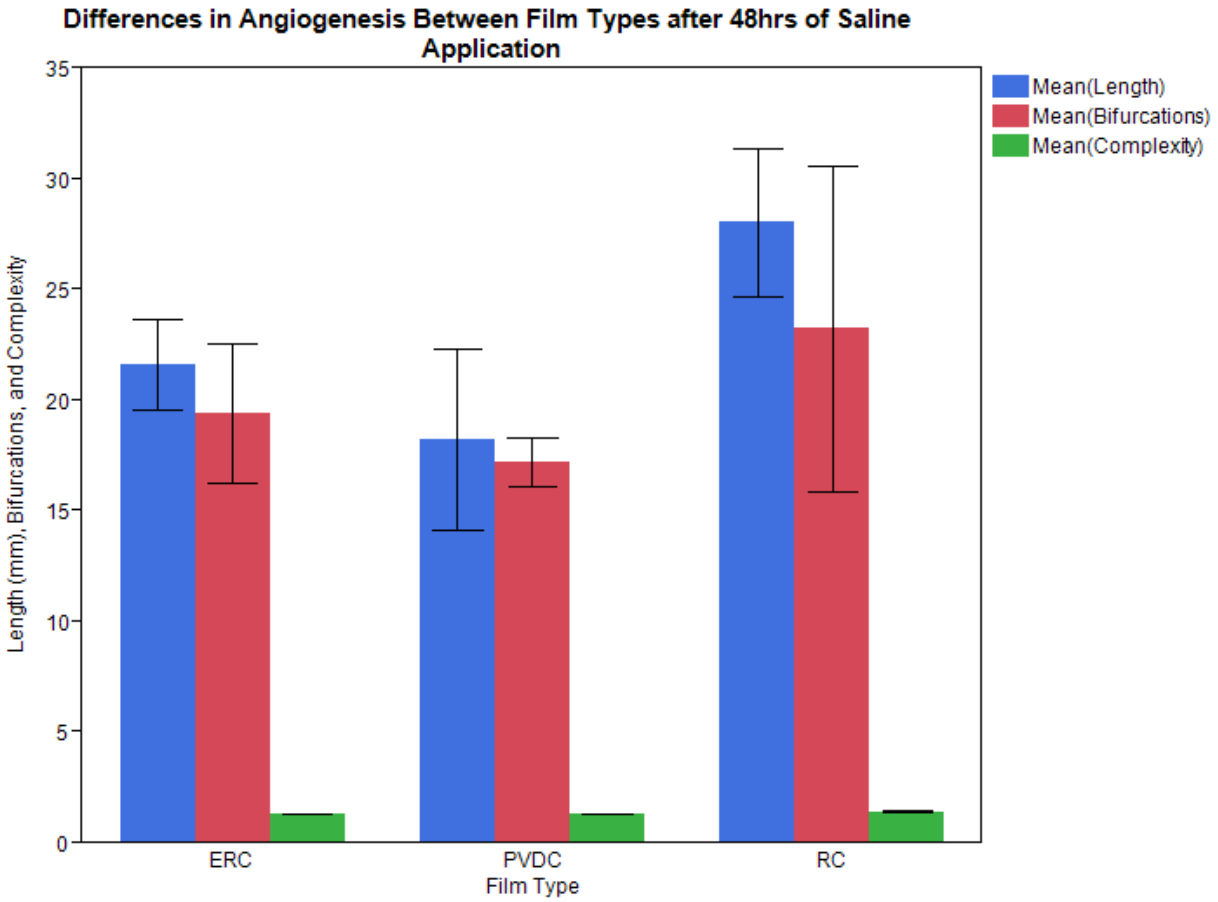

Figure 27
AV Angiogenesis: Comparison among Films for Saline Application
There were found no significant differences in angiogenesis among the three film groups when placed on the AV and application of saline for 48 hours.

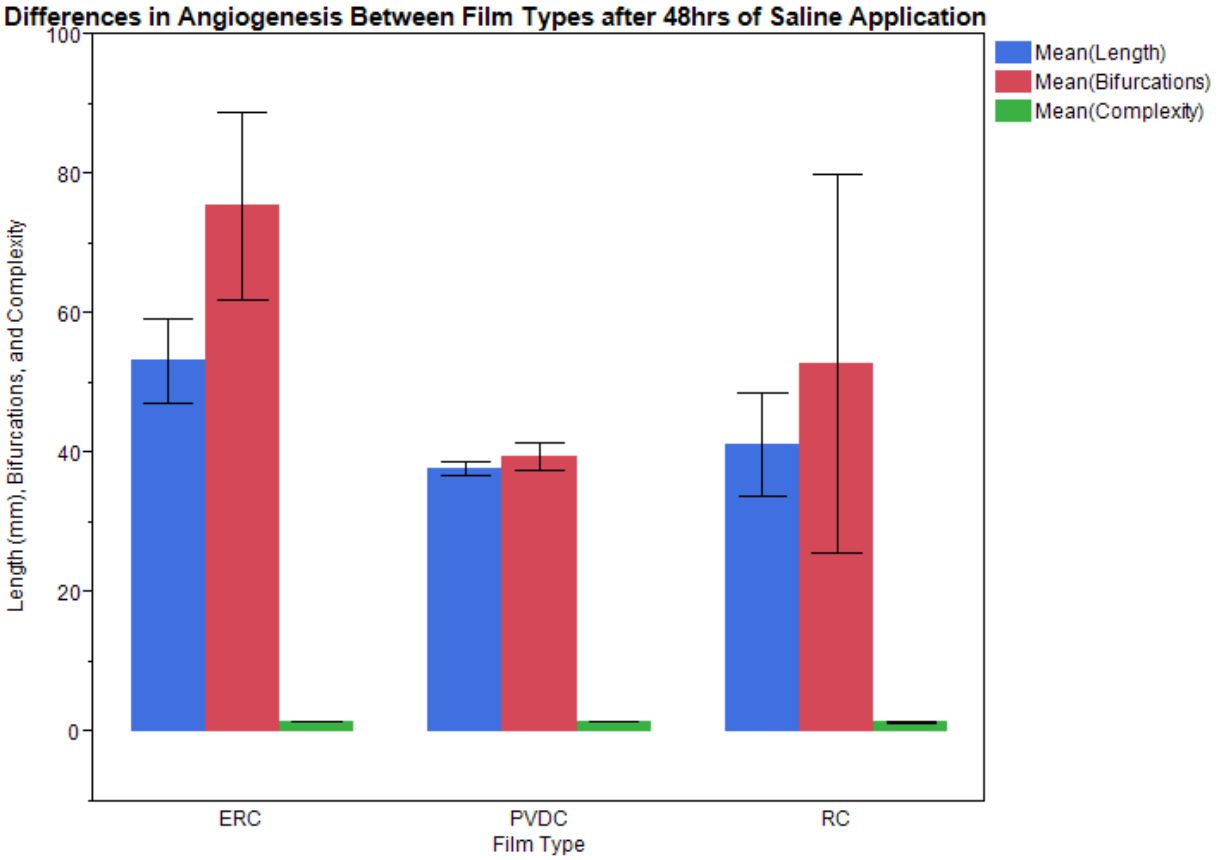

Figure 28
CAM Angiogenesis: Comparison among Films for Saline Application
No significant differences were found in angiogenesis among the three film groups when placed on the CAM and application of saline for 48 hours.

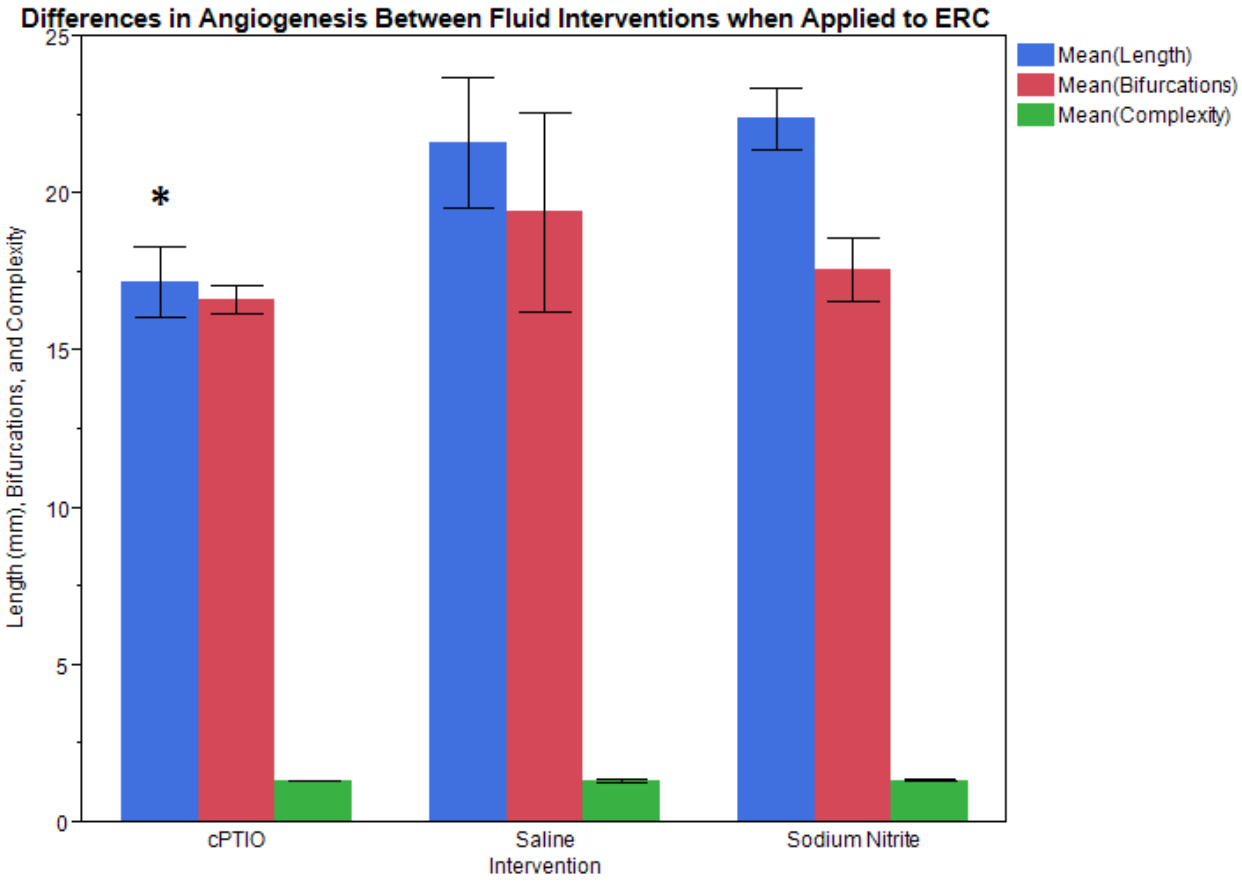

Figure 29
AV Angiogenesis (in ERC) by Intervention
There was a significant reduction in length when cPTIO was applied to the central hole of an ERC film patch on the AV (*, $p<0.05$). The other angiogenic endpoints had no significant differences.

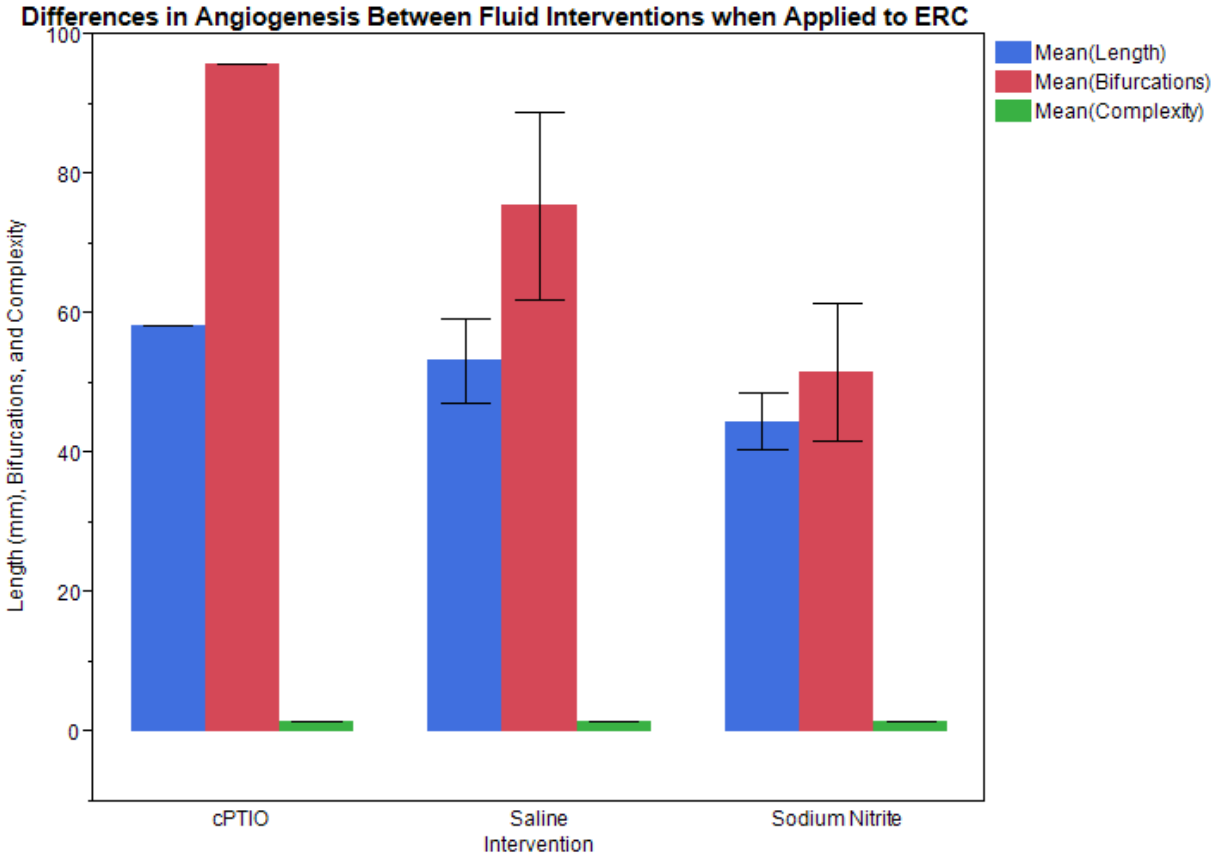

Figure 30
CAM Angiogenesis (in ERC) by Intervention
There was no significant difference between the angiogenesis observed in ERC attributable to the fluid intervention applied.

Effect of Local Hypoxia on Angiogenesis with Nitrite Application

The angiogenic effects of different levels of local oxygen were examined in embryos treated with 48 hours of sodium nitrite application. In the AV, after 48 hours of nitrite application, there was a trend of increased angiogenesis under the PVDC film compared to the RC and ERC films in all three quantification methods, although it was not significant (Figure 31). When looking for confounding factors, control for the different rates of natural angiogenic development was tried. The experimental (under the film) data were normalized by dividing by the control (away from the film) data on the same embryo. This normalization accentuated the effect of the local hypoxic areas under the PVDC film when compared to the normoxic areas of the same AV (Figure 32). Film type was found to produce a significant difference by nonparametric ANOVA in this angiogenic ratio whether measured by length, bifurcations, or complexity ($p<0.04$).

In the CAM, after 48 hours of nitrite application, there was no significant difference between the angiogenesis observed at different oxygen availabilities (Figure 33). There were some variations that may suggest trends, but they did not extend between the different angiogenic endpoints, reducing their credibility.

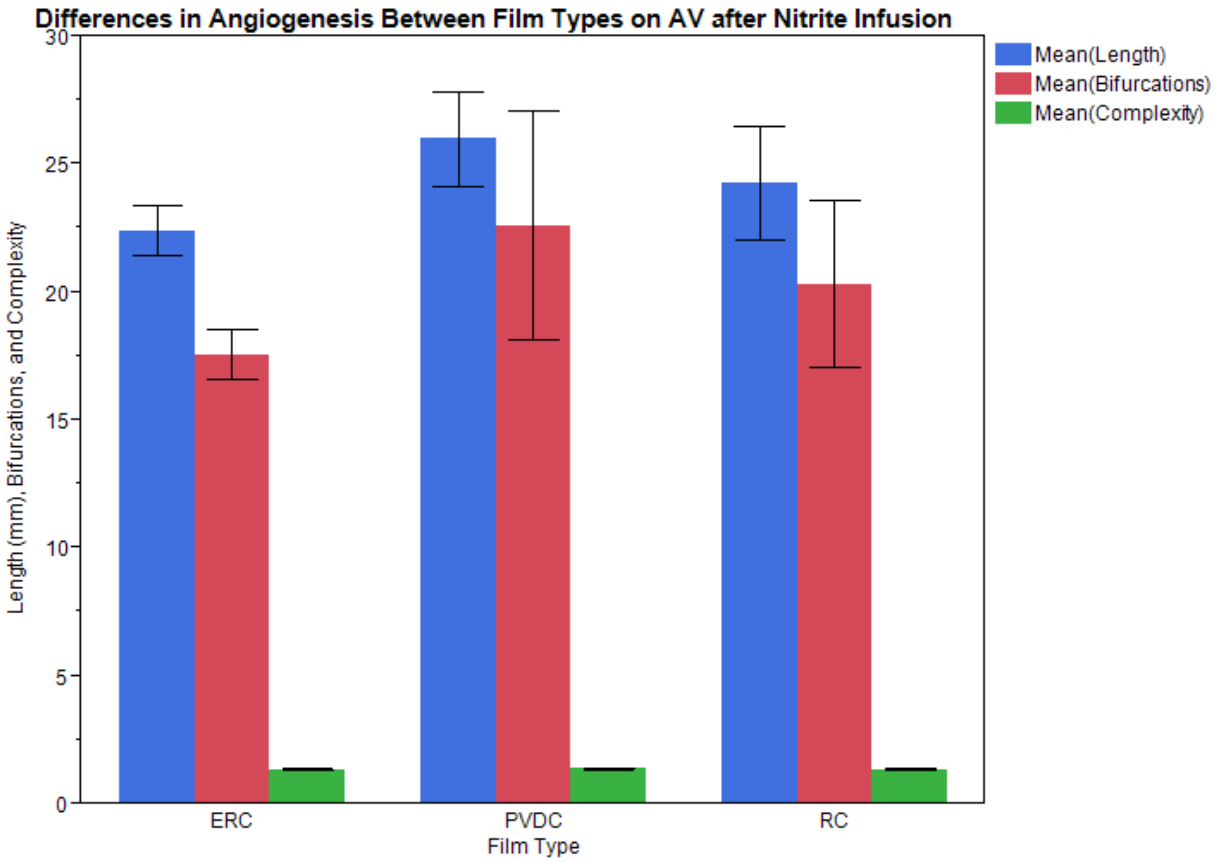

Figure 31

Angiogenesis in AV by Film Type after 48 hours of Nitrite Application

While there were no significant differences among the film groups, it was noted that the PVDC group tended to show increased angiogenesis.

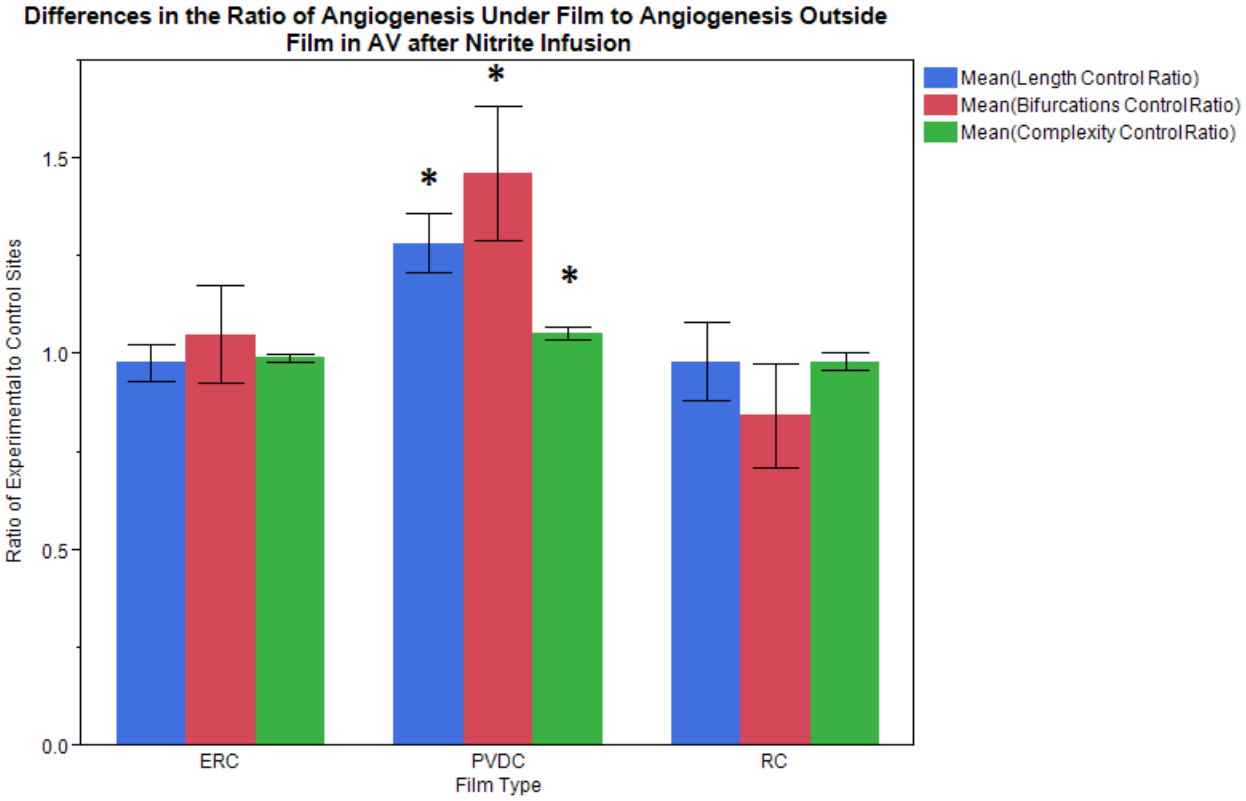

Figure 32
Angiogenesis Control Ratio in AV by Film Type after 48 hours of Nitrite Application
Angiogenesis data were normalized by dividing the observed angiogenesis measures at experimental sites (under the film and directly exposed to the fluid intervention) by those observed in control sites (away from the film). When applying nitrite, angiogenesis increased in the local hypoxic environment under the PVDC film compared to normoxic film and non-film controls (* $p < 0.03$).

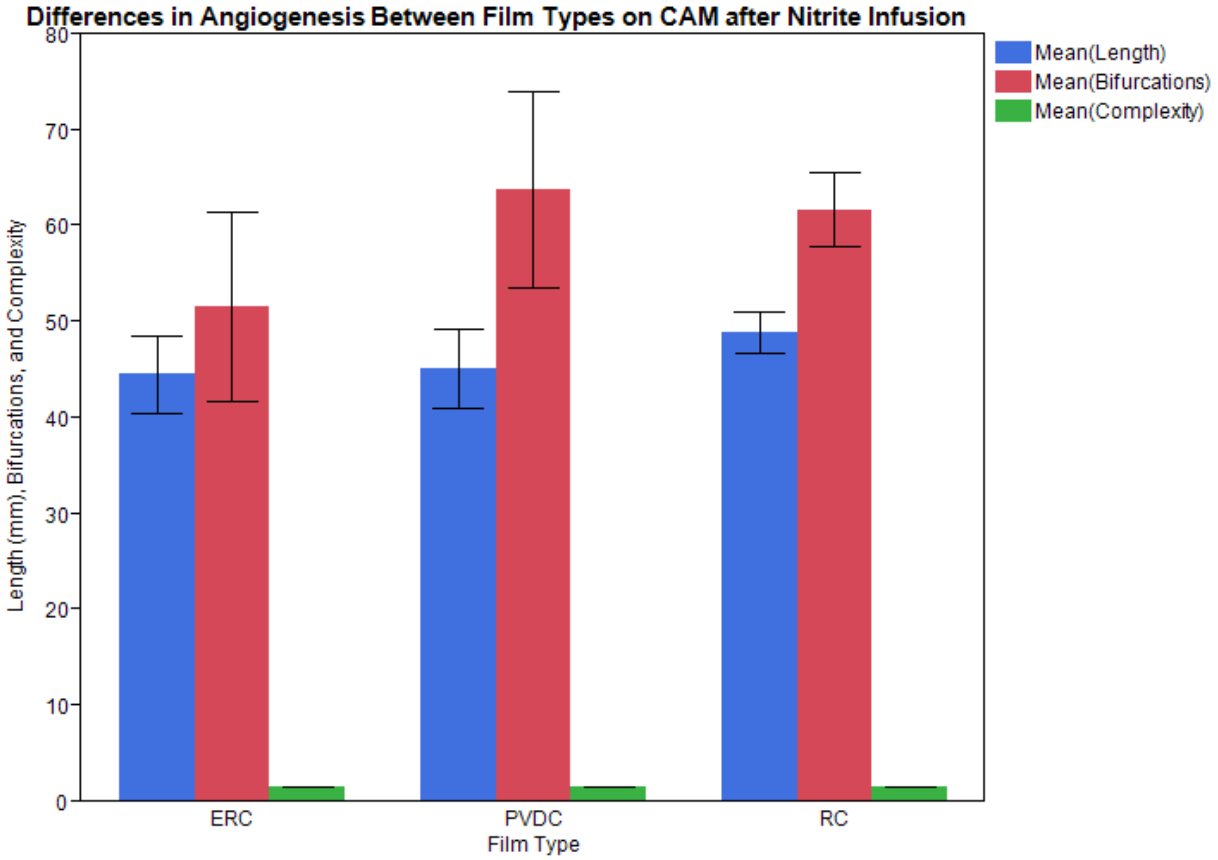

Figure 33

Angiogenesis in CAM by Film Type after 48 hours of Nitrite Application

Changes in local oxygenation did not produce a significant change in angiogenesis in the CAM with nitrite application.

Effect of Different Solutions in a Hypoxic Environment

The angiogenic effects of different chemical interventions were compared after 48 hours of application to a locally hypoxic vascular area. In the AV, there was a clear trend in all three angiogenic parameters that nitrite increased angiogenesis, while the addition of cPTIO to the nitrite reversed this effect (Figure 34).

Identical testing in the CAM gave slightly different results. cPTIO results are currently inconclusive due to a small number of trials. The data show an increase in the number of bifurcations observed after nitrite application, but this change was not statistically significant (Figure 35).

cPTIO was added to nitrite applied to embryonic vascular beds as a NO scavenger. Reversal of the effects of nitrite would indicate nitrite was producing the observed biological effects using a NO-mediated pathway. Unexpectedly, when applying nitrite and cPTIO to the AV, a novel effect was observed (Figure 36). In areas under film (both PVDC and RC films) the vasculature appeared to have a much more ordered, hierarchical structure. Areas of uncovered yolk sac, however, displayed vessels that appeared to be organized in a capillary plexus with poorly defined feed arterioles and venules.

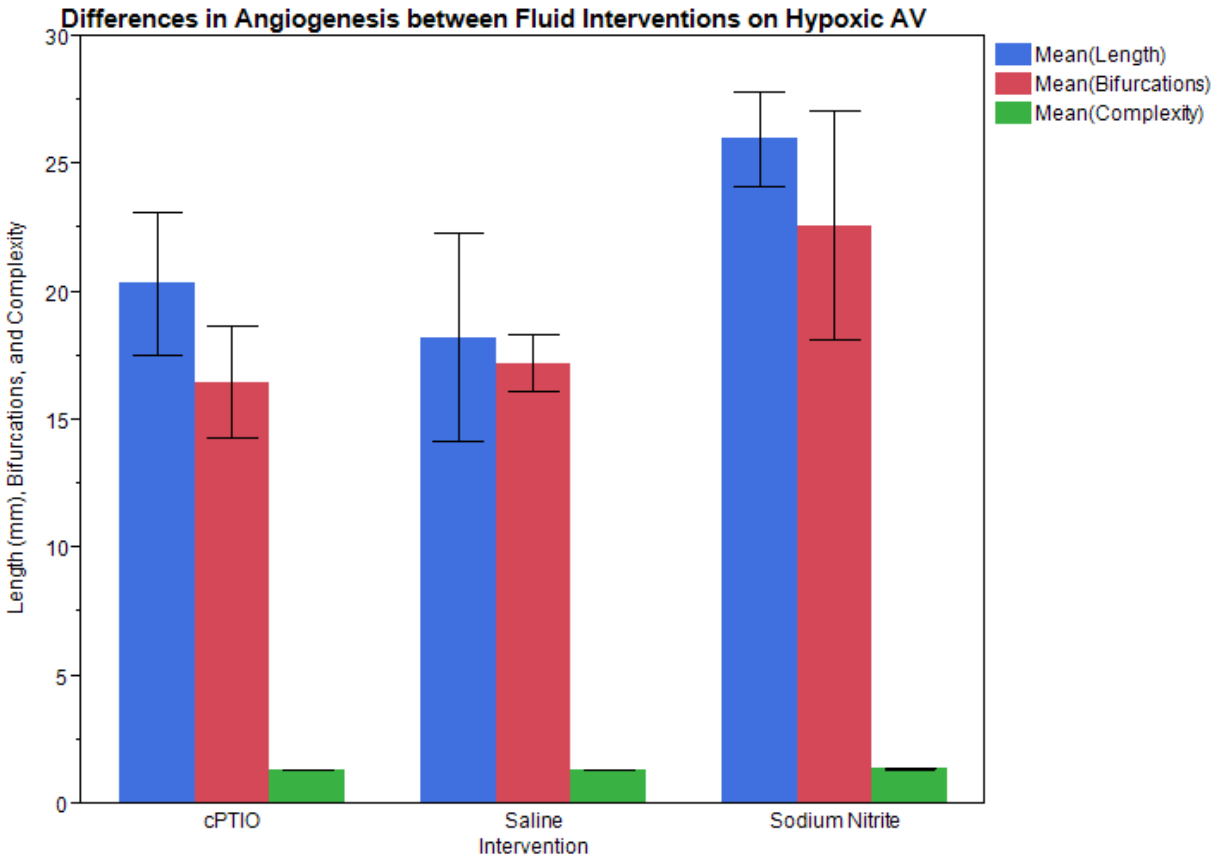

Figure 34

Angiogenesis in hypoxic AV by Intervention

While not statistically significant, there was a trend of increased angiogenesis produced by nitrite in hypoxic AV above saline control. This increase returned back to saline levels when cPTIO was added to the nitrite.

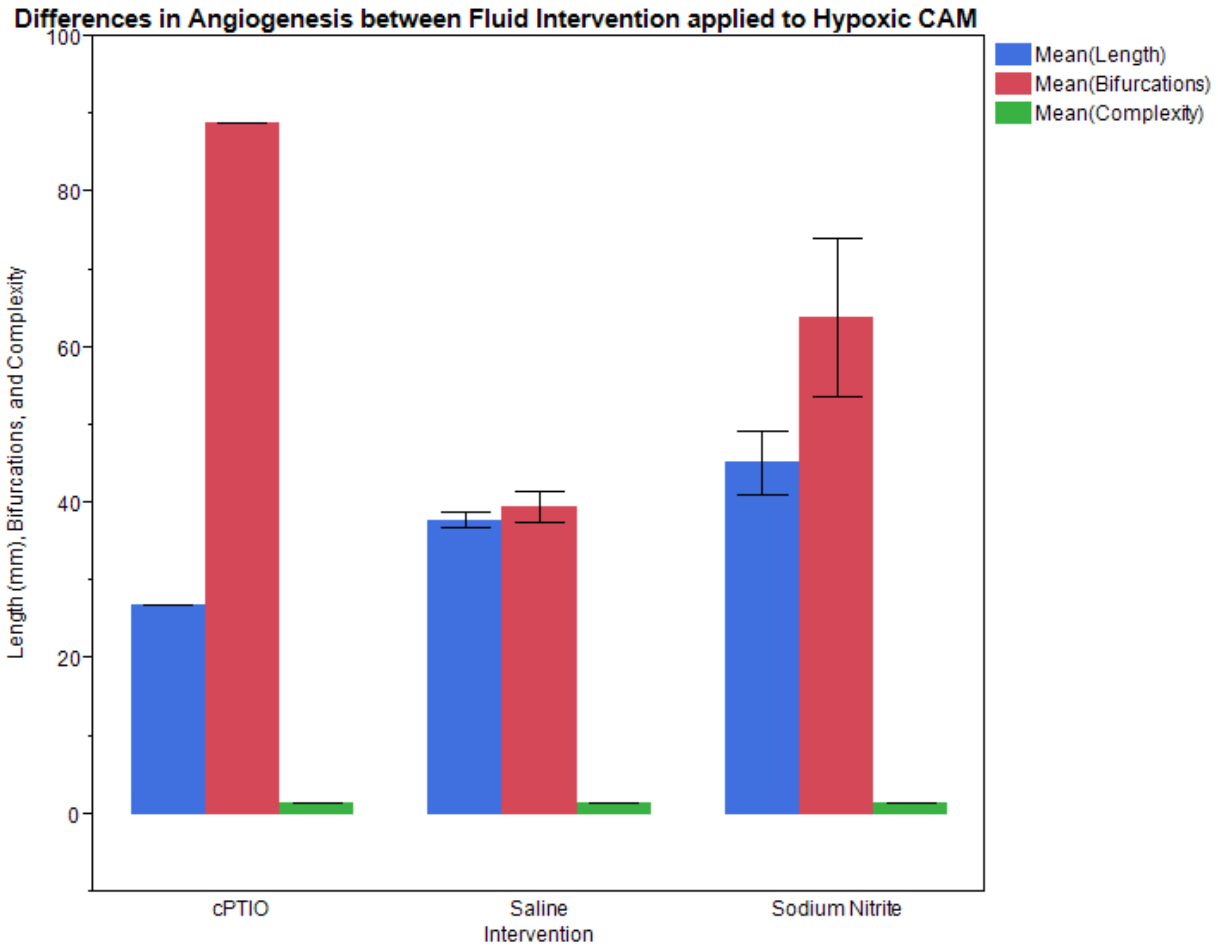

Figure 35

Angiogenesis in hypoxic CAM by Intervention

There were no significant differences in angiogenesis produced by applying nitrite or nitrite and cPTIO over saline in the hypoxic CAM.

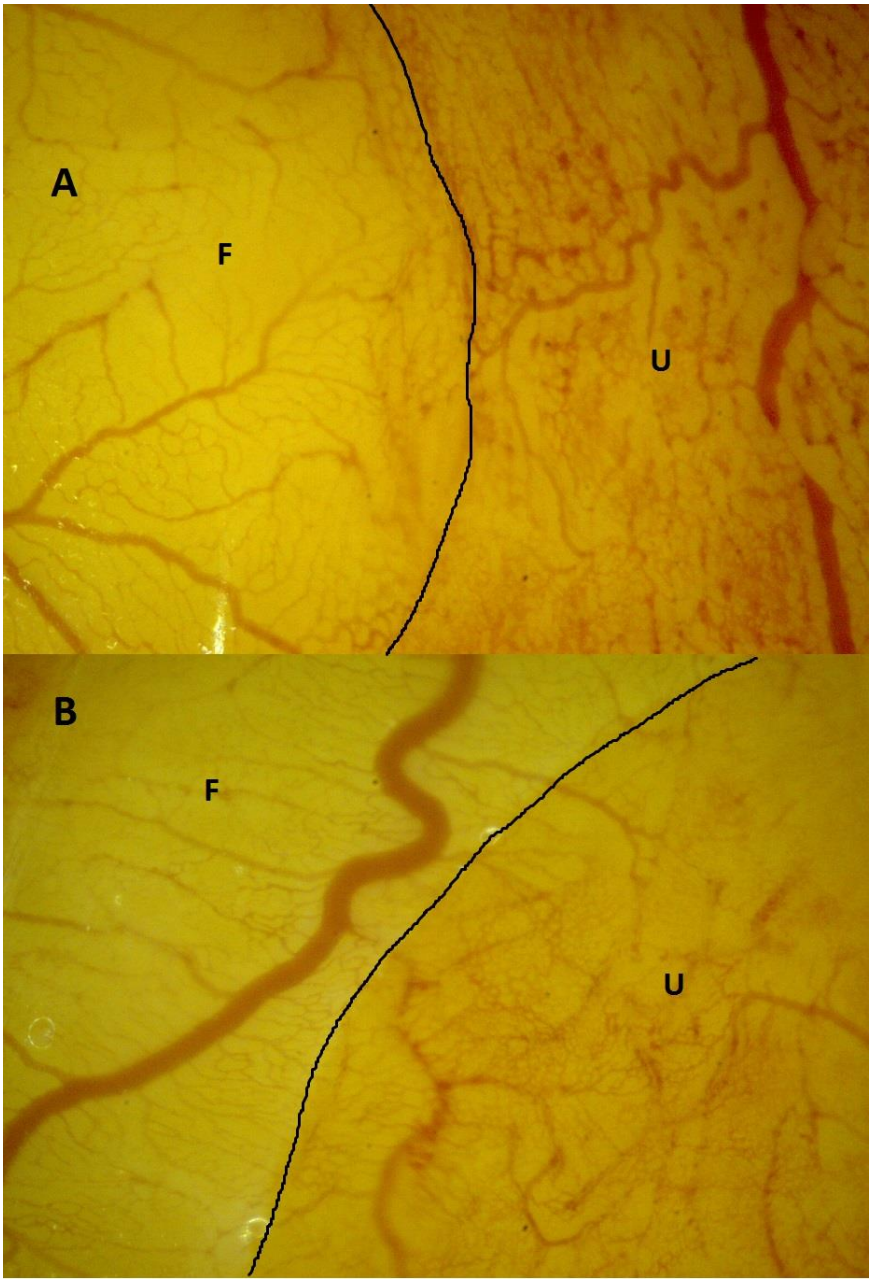

Figure 36
Gross AV Vascular Changes Induced by cPTIO
When cPTIO was applied to AV, a marked difference between the vascular morphology was observed between the areas under the film (F) and those that were uncovered (U). This applied both to PVDC film groups (A) and RC film groups (B) (ERC pictured, but uses the same type of high-permeability film). The drawn black line represents the edge of the film and interface point between vasculature in contact and not in contact with film.

CAM Overgrowth

An observation was made that in some cases of film (primarily PVDC) placed on the CAM, the growth of the CAM (referring to the organ, not the vessels within, as has usually been referred to previously in this dissertation) was so robust as to come up out of the plane and begin to overlap the edges of film piece. At times this interfered with observation of the vasculature under the film and impeded the number and size of sites of angiogenesis quantification. This occurred more frequently in RC than ERC films, potentially because the process is accelerated or more apparent around a smaller structure.

DISCUSSION

Novel Materials and Methods

The materials and techniques used to cultivate and observe chicken embryos represent several novel advancements. The Poultry Dish has advantages over both established embryo containment devices – the LDPE hammock and the simple petri dish. Dunn, et al (2005) showed that a hanging sack improves embryo survival and that the moderate permeability of the material suspending the yolk appears to be a positive factor. The Poultry Dish incorporates a hanging sack which promotes increased embryonic survival but also, because of the off-center placement of the ingress, there exists ample space for the CAM to expand. The quantification of vascular networks was impaired when the CAM overlapped the yolk because of a reduction in contrast, as well as the presence of AV vessels within the same frame. The Poultry Dish proved to be critical in ensuring embryonic survival until D12 for a full course of solution application and subsequent CAM growth.

While an automated microscope platform that moves at a constant rate is not novel, this represents the first time it has been used in conjunction with PQM measurements. The regular acquisition rate of PO_2 measurements, combined with the consistent stage motion, allowed the collection of an accurate scan of the PO_2 profile across the tissue covered by the gas barrier films. Sequential scans with adjusted starting locations could be used in future work to produce 2-D PO_2 profiles in asymmetric tissues. Also, as long as the diameter of the excitation region is smaller than the step size, there will be no overlap of successive excitations (i.e., no multiple

excitations of the same tissue) and therefore oxygen consumption by the method will not require compensation for the PO_2 values obtained.

Barrier films represent a novel method of producing localized regions of hypoxia with unaltered blood flow for in vivo optical analysis of vascular beds which are supplied by oxygen through diffusion from the atmosphere. PVDC film is often used in PQM to prevent atmospheric oxygen from interfering with measurements of PO_2 in vivo for the purposes of observing tissues not normally in contact with room air. In the case of vascular networks of the chick embryo, the AV acquires oxygen primarily by diffusion through the egg shell, until the CAM grows over it and replaces that function, and the primary function of the CAM is transport of oxygen to the embryo.

Induction of Local Hypoxia using Gas Barrier Film

It was shown that topical application of small pieces of gas barrier film could impede oxygen diffusion into the covered tissue. Tissue PO_2 is a function of oxygen flow and, even if oxygen inflow is inhibited, oxygen outflow (primarily for the cellular respiration fuelling angiogenesis) continues and the availability of oxygen becomes scarcer. Ar, et al (1987) showed that the CAM is responsible for an oxygen consumption rate of 0.071 mmol/hr at D12, representing 18% of the oxygen use of the entire egg contents. The observation of low PO_2 under the PVDC film was confirmed to be an effect of the barrier properties of the film and not the presence of the film itself by use of a negative control film. RC film has similar mechanical and optical properties to PVDC, but possesses a much higher permeability to oxygen. This was confirmed by PQM measurements in which the PO_2 under the PVDC film was found to be less than 20 mmHg while

the PO_2 under the RC film was found to be more than 110 mmHg (atmospheric PO_2 is about 160 mmHg), which represents a hyperoxic environment compared to the natural in ovo state.

PO_2 Gradient around Film Boundary Interface Region

In the CAM the time required for blood to equilibrate from 10% O_2 saturation to 90% O_2 saturation is 0.87s at D10 (Tazawa, 1976). This time corresponds closely with the time necessary for a full circuit of blood through the CAM vasculature. However, the full blood transit length of the CAM is not necessary for equilibration because arterial (embryonic venous) blood is not fully depleted of oxygen, but has a PO_2 of 30.9 mmHg at D10 in ovo (Tazawa, 1973), or 30% saturation of chicken embryonic Hb. Based on these previous findings that Hb oxygen binding is the limiting factor for blood PO_2 equilibration time, it might be predicted that the distance required for equalization from a low PO_2 to a high PO_2 would be long. However, our data showed a very rapid shift between high and low PO_2 which is evidence that, for a tissue exposed to atmospheric PO_2, the tissue PO_2 is not dependent on blood PO_2. Visschedijk et al (1988) showed that oxygen diffuses much more quickly through the shell than it does laterally through the CAM. This helps explain the close proximity of high and low PO_2 regions at the PVDC film boundary. This ability of the CAM to maintain PO_2 gradients within strict confines makes it an attractive model for future studies examining the size of the insult necessary to transition from local to global physiological responses.

Vascular Bed Comparisons

The CAM and AV vasculatures, despite originating from the same embryo and having some gross visual similarities, are quite distinct and allow for the examination of different responses to

experimental interventions. Data derived from the two vascular beds cannot be directly compared, however, due to differences in vascular network morphology. The CAM arteriolar and venular vascular patterns have bifurcations much more frequently, resulting in a lower length/bifurcation ratio (average segment length) and more complexity. Therefore, when comparing quantitative data derived from the two vascular beds, the data must first be normalized either using a baseline measure of vascularity or a control group.

The CAM is the much more studied of the two vascular networks, but there is some precedent for the use of the AV as a model for angiogenesis. Nico et al (2001) used immunohistochemistry to detect VEGF produced by AV endothelial cells and VEGFR-2 receptors in adjacent endodermal cells at D6, D10 and D14. They concluded that VEGF is necessary for the observed angiogenesis and for maintaining endothelial cell health.

Baseline Comparisons

To directly make comparisons between data collected after 48 hours of application of test solution, it was helpful to ensure there were no sources of bias due to a significant difference in the populations independent of the intervention. No significant difference was observed between the baseline vascularity among the chemical interventions and among the film types. The one significant difference noted was a reduction in the number of bifurcations between observations under the film when compared to same-embryo controls outside and away from the film. The other angiogenic measures (total network length and complexity) were not significantly different, which alleviates concern about a systematic source of error. To aid in comparisons of the angiogenic data between experimental and control groups for the different films data were

normalized by dividing the vascularity after 48 hours by the corresponding measurement at baseline.

Angiogenesis at Control Sites

It is common for local disturbances in homeostasis to produce far-reaching changes in complex physiological systems. Observations of angiogenic changes away from the site of intervention would imply diffusion of the applied chemical beyond the site of application at efficacious concentrations or the transmission of a chemical signal. In both the AV and CAM, no significant differences were found among the film types or interventions. The lack of observable differences between the film types is consistent with their biological inertness. The unresponsiveness of distant sites to react to localized interventions opens them up for use as reliable controls of angiogenic rates in the same embryo without the local influences of film, hypoxia, or fluid intervention.

Comparisons of vascularity at baseline and after 48 hours can offer a sense of the amount of naturally occurring angiogenesis not attributable to experimental intervention. In the AV this basal level of angiogenesis appears very small, if present at all, over the period examined (D6-D8). This suggests that any inducement of angiogenesis can be solely attributed to the observed intervention. However, it is not an attractive model to test anti-angiogenic compounds. In the CAM, there was a statistically significant increase in vascularity attributable to endogenous angiogenesis between D10 and D12. Interventions producing more angiogenesis over that time period can be labeled pro-angiogenic while those resulting in less vascularity can be labeled anti-angiogenic.

Effect of Local Hypoxia on Angiogenesis

As mentioned in the Introduction, it is established that hypoxic environments have been shown to increase angiogenesis in the CAM. Dusseau et al (1988) incubated whole eggs under conditions of reduced atmospheric oxygen from D7 to D10 and D14 and detected an increase of angiogenesis in the CAM when compared to a normal oxygen environment. Strick et al (1991) continued this work and subjected eggs to a range of atmospheric conditions from 12% to 20% oxygen from D7 to D14. Angiogenesis in the CAM was shown to have a dose-response relationship with global atmospheric oxygen levels with the most angiogenesis at 12% O_2 and the least at 70% O_2. The angiogenic response to hypoxia was seen as an appropriate homeostatic adaptation aimed at restoring oxygen flow to the developing embryo. An increase in CAM vascularity increased the surface area available for gas diffusion to restore oxygen flow.

The angiogenic response to localized hypoxia appears to be more nuanced, however. A study by Wagner-Amos et al (2003) showed that local changes in oxygen transport have a different effect. They coated half an egg with wax from D10 to D15 to prevent any gas exchange under the covered portion, while increasing the atmospheric oxygen to compensate and return oxygen transport to normal levels through only the uncovered half. While the hyperoxic half did not show any changes in angiogenesis from control, the hypoxic half had reduced vascularity. Reizis et al (2005) examined various parameters of the CAM after in ovo incubation. They found increased angiogenesis and reduced CAM thickness isolated to that portion of the CAM adjacent to the air sac. Since the shell over the air sac has a greater density of pores, that region of the CAM should be exposed to a higher local oxygen environment than the CAM directly adjacent

to the shell. This is a reversal of the results of global hypoxia but makes sense physiologically. The purpose of the CAM is to transport oxygen and increasing the vascularity of a hypoxic region would be counterproductive to this purpose. Blood would be shunted towards areas of lower oxygen and reduce the PO_2 of returned blood. The reduction in angiogenesis observed accomplishes the opposite, maintaining high PO_2. This does, however, raise a puzzling question of how the same trigger (hypoxia) can have different responses (Corona, 2000).

This finding of localized hypoxia reducing angiogenesis in the CAM was reflected in a trend of the data that was not statistically significant. The size of the region under hypoxia appears to be a key factor in the angiogenic response and the size of the regions of hypoxia produced by the films were typically <10% of the total CAM area (compared to 100% in the Dusseau (1988) study and 50% in the Strick (1991) study). An increase in the size of the film pieces used or an increase in experimental trials may improve significance.

Höper et al (1996) showed that incubation of eggs until D4 in both hypoxic and hyperoxic atmospheric environments led to increased AV angiogenesis when compared to normoxic conditions. Based on these findings, it would be expected that the areas under the PVDC film should display more angiogenesis. However, these findings are based on normoxic global conditions. We found no difference in angiogenesis, but this may be because our comparisons were primarily between hypoxic (PVDC) and hyperoxic (RC and ERC) conditions. At face value, however, this is an indication that simply changing the local oxygen environment is not sufficient to produce a significant change in angiogenesis.

Until the CAM physically associates with the eggshell near D7, the vitelline vasculature is a major source of oxygen transport to the embryo. Meuer et al (1987) used microelectrodes to determine that blood PO_2 increased from 50 mmHg in the vitelline arteries to 80 mmHg in the lateral vitelline veins after transit through the AV. After D7, the growing CAM assumes primary oxygen transport function and it is not clear how specialized the vitelline vasculature is for gas transport. While the AV has gas exchange capabilities, for most of its existence its sole purpose is nutrient and waste transport. More work is necessary to determine whether its responses to hypoxia are consistent with a pulmonary vasculature or a non-pulmonary vasculature.

Effect of Nitrite on Angiogenesis

While NO is generally considered to promote angiogenesis and acts in the VEGF angiogenic pathway (Ziche, 1994), this does not seem to be the case in the CAM model. NO has been shown by Pipili et al (1994) to produce a dose-dependent reduction in angiogenesis when applied via the NO donor sodium nitroprusside. This NO-mediated action was supported by an observed increase in release of cGMP. NOS inhibitors L-NMMA and L-NAME stimulated angiogenesis in a way that was abolished with the addition of L-arginine, an NO precursor. These anti-angiogenic effects of NO donors were replicated by Powell et al (2001) using SNAP and SNAG to inhibit FGF-initiated angiogenesis in the CAM. Furthermore, Pipili also found that endogenous iNOS expression by the CAM corresponded with the time period of maximal angiogenesis (D8-D11). This was also the period with highest endogenous NO production (determined by nitrite compound composition in the CAM). Data showed a trend of reduced angiogenesis in the CAM, while not statistically significant, is supported by a consensus among the three quantification measures of vascularity and a reversal of angiogenesis with the addition

of cPTIO to the nitrite. These data support the model of nitrite-mediated NO release due to the similarities of the nitrite effects to those of NO applied through a direct NO donor, as well as its inhibition by a NO scavenger.

The effects of NO have not been examined in the AV and this dissertation represents novel data about its angiogenic effects in this model. The data show that nitrite, under conditions of high PO_2, did not significantly influence AV angiogenesis compared to a saline control. However, there was a significant reduction in total network vascular length when cPTIO was added to the nitrite. Gievn that nitrite needs an external reducing agent, perhaps Hb, to be converted into NO and this would explain why there is no observable change attributable to nitrite at high PO_2. The cPTIO, however, will act as a scavenger of endogenously produced NO regardless of the reduction status of nitrite and may therefore implicate endogenous NO acting as a pro-angiogenic agent in the AV.

Nitrite and Hypoxia

A model has been proposed in which nitrite is converted into NO by a reducing agent in a reducing (low oxygen) environment. There is evidence that NO helps mediate the hypoxic response through HIF-1α activation (Sandau, 2001), and many investigations into the role of NO on tumor angiogenesis are performed under hypoxic conditions. Previous studies testing nitrite on the chick embryo for direct comparison proved elusive, however. The only nitrite testing in the chick embryo model (Mohamadi, 2013) did not examine angiogenic endpoints and concluded that nitrite injection reduced body weight and serum protein content.

Nitrite, when applied to AV for 48 hours, only stimulated angiogenesis under hypoxic conditions. By three measures of vascularity, the group of embryos receiving nitrite and experiencing local hypoxia had significantly more vascularity (normalized to control sites on the same embryo away from the site of film and liquid intervention) than embryos with high-permeability film or no film allowing for high tissue PO_2. Furthermore, given a hypoxic local AV environment, there was a clear trend that the application of nitrite increased angiogenesis across the three angiogenic parameters and that this pro-angiogenic effect could be inhibited with the addition of a NO scavenger. Other findings show that neither hypoxia nor nitrite alone was sufficient to significantly impact AV angiogenesis. Observations that vascularity was lower under both RC film and no film support the hypothesis that the vascular changes are attributable to local hypoxia and not simply physical contact with the film. The results comparing different interventions in a hypoxic environment show that the increased angiogenesis appears to be linked specifically to nitrite and its capacity to produce NO. The reduction in vascularity associated with saline contradicts any possibility that the angiogenesis is linked to the method of fluid application or a solubility change due to the addition of fluid volume. The reduction in angiogenesis back to baseline (and not below it as seen in normoxic conditions) supports the hypothesis that nitrite acts through an NO intermediate which can be quenched by cPTIO.

In the CAM, nitrite under hypoxic conditions did not produce a reduction of angiogenesis as was predicted**.** However, cPTIO application with the nitrite did show some signs of vascular remodeling and angiogenesis which indicates the potential presence of endogenous anti-angiogenic NO action in the CAM between D10 and D12.

cPTIO qualitatively altered the vascular morphology of the AV, producing a relatively undifferentiated vascular sinus in exposed areas in contrast to microvessels in a highly hierarchical branching capillary plexus under the film. This phenomenon is particularly interesting because the effect occurred under both the PVDC and RC films, suggesting it is independent of oxygen. The response is, however, dependent on the presence of film and not just concentration of the cPTIO because the morphological change was observed to be maintained between the large, central exposed area of the ERC and the vasculature underneath the film. It is difficult to make any predictions about the interaction of physical contact or pressure and NO on vascular development, but it does appear to indicate that NO plays a major role in the development and arrangement of microvessels in the AV.

The two vascular networks of the chicken embryo appear to have different reactions to local changes in oxygen availability. The ability of Hb to produce NO from endogenous nitrite may be an important factor in local blood flow regulation and remodeling in response to local hypoxia. The data have shown that the angiogenic response to nitrite under hypoxic conditions in each vascular bed reflects its function in regard to oxygen transport and promotes angiogenic changes to alleviate the mismatch between oxygen supply and demand. In the AV, angiogenesis increases the flow of oxygenated blood to the hypoxic region, while in the CAM, angiogenesis decreases to reduce shunting blood to a poorly perfused area and thereby prevents a reduction in blood PO_2 returning to the growing embryo.

Conclusions

Barrier films were found to be an effective method for inducing local hypoxia in the *ex ovo* chick embryo model and potentially any model where oxygen is primarily delivered by diffusion

instead of blood flow. Low-permeability PVDC film was able to create areas of consistently low PO_2 which could re-equilibrate to normal PO_2 within a short distance.

A trend in the data supports previous findings by others that local hypoxia reduces angiogenesis in the CAM. The AV, however, did not show any angiogenic response to changes in local hypoxia alone. Likewise, the application of nitrite outside of a hypoxic environment did not appear to have any significant angiogenic effect. However the combination of nitrite and hypoxia produced a significant increase in angiogenesis in the AV and appears to reduce angiogenesis in the CAM. This finding in the AV is supported by a consensus across the three vascular endpoints measured and a reversal in both film controls and chemical controls.

The two vascular networks of the chicken embryo appear to have different reactions to local changes in oxygen availability. The ability of Hb to produce NO from endogenous nitrite may be an important factor in local blood flow regulation and remodeling in response to local hypoxia. The data have shown that the angiogenic response to nitrite under hypoxic conditions in each vascular bed reflects its function in regard to oxygen transport and promotes angiogenic changes to alleviate the mismatch between oxygen supply and demand. In the AV, angiogenesis increases the flow of oxygenated blood to the hypoxic region, while in the CAM, angiogenesis decreases to reduce shunting of blood to a poorly perfused region and thereby prevents a reduction in blood PO_2 returning to the growing embryo. Hypoxia-induced NO mobilization represents a potential initiator of a long-term vascular adaptation to hypoxia similar in effect to the immediate vascular tone changes to increase blood flow in areas away from poorly-ventilated regions and to improve ventilation/perfusion mismatch in the lung.

Future Aims

A comparison between a direct NO donor and nitrite would clarify the role of an NO intermediate in the angiogenic changes observed with nitrite application. Similar results between the effects of nitrite and an NO donor under hypoxic conditions would support the hypothesis that nitrite's physiological effects are as a result of NO production. Maintenance of the angiogenic effects at normoxic conditions would support the hypothesis that nitrite conversion to NO is hypoxia-dependent.

Injection of the PQM probe into the embryonic vasculature would be helpful for determining PO_2 profiles within the vascular network, similar to those data collected for tissue PO_2 in this dissertation. The relatively slow rate of oxygen binding may result in a more flattened curve appearance with a much longer distance necessary to transition between high and low PO_2. This would be significant because Hb is thought to be a major reducing agent in the production of NO from nitrite and this activity is PO_2-dependent. If the blood PO_2 does not drop sufficiently over the distance traversed under the film, we could hypothesize that another reducing agent residing within the low PO_2 region of the interstitial tissue is primarily responsible for the nitrite-initiated NO effects observed in the present study.

There is evidence that responses to hypoxia by the chick embryo are time and development dependent (Chan, 2005). The experimental conditions of this study can be performed at a range of times during chick embryo development. In order to maintain unobstructed observation of the AV after significant CAM growth, the CAM may have to be impeded to clear a testable area for the AV.

In the presence of cPTIO and nitrite that part of the AV covered by the gas barrier film appears to have a vascular pattern reminiscent of a more mature embryo with a more developed vasculature. This phenomenon can be studied through examination of the genetic expression of the endothelial cells under and outside the film and comparing those results with control endothelial cells over the spectrum of vascular development in the AV.

References

Ahn, E., Jeon, H., Lim, E., Jung, H., & Park, E. (2007). Anti-inflammatory and anti-angiogenic activities of *gastrodia elata* blume. *Journal of Ethnopharmacology, 110*(3), 476-482.

Akaike, T., Yoshida, M., Miyamoto, Y., Sato, K., Kohno, M., Sasamoto, K., . . . Maeda, H. (1993). Antagonistic action of imidazolineoxyl N-oxides against endothelium-derived relaxing factor/. bul. NO (nitric oxide) through a radical reaction. *Biochemistry, 32*(3), 827-832.

Allen, W., & Wilson, D. (1993). Early embryonic angiogenesis in the chick area vasculosa. *Journal of Anatomy, 183*(Pt 3), 579.

American Cancer Society. (2013). *Cancer facts & figures 2013.* (). Atlanta: American Cancer Society.

Ar, A., Girard, H., & Rodeau, J. (1991). Oxygen uptake and chorioallantoic blood flow changes during acute hypoxia and hyperoxia in the 16 day chicken embryo. *Respiration Physiology, 83*(3), 295-312.

Ar, A., Girard, H., & Dejours, P. (1987). Oxygen consumption of the chick embryo's respiratory organ, the chorioallantoic membrane. *Respiration Physiology, 68*(3), 377-388.

Auerbach, R., Kubai, L., Knighton, D., & Folkman, J. (1974). A simple procedure for the long-term cultivation of chicken embryos. *Developmental Biology, 41*(2), 391-394.

Barnes, A. E., & Jensen, W. N. (1959). Blood volume and red cell concentration in the normal chick embryo. *American Journal of Physiology--Legacy Content, 197*(2), 403-405.

Bauer, K. S., Cude, K. J., Dixon, S. C., Kruger, E. A., & Figg, W. D. (2000). Carboxyamido-triazole inhibits angiogenesis by blocking the calcium-mediated nitric-oxide synthase-vascular endothelial growth factor pathway. *Journal of Pharmacology and Experimental Therapeutics, 292*(1), 31-37.

Baumann, R., Padeken, S., Haller, E., & Brilmayer, T. (1983). Effects of hypoxia on oxygen affinity, hemoglobin pattern, and blood volume of early chicken embryos. *American Journal of Physiology-Regulatory, Integrative and Comparative Physiology, 244*(5), R733-R741.

Baumann, R., & Meuer, H. (1992). Blood oxygen transport in the early avian embryo. *Physiological Reviews, 72*(4), 941-965.

Burke, A. J., Sullivan, F. J., Giles, F. J., & Glynn, S. A. (2013). The yin and yang of nitric oxide in cancer progression. *Carcinogenesis, 34*(3), 503-512.

Carmeliet, P. (2005). Angiogenesis in life, disease and medicine. *Nature, 438*(7070), 932-936.

Carmeliet, P., & Jain, R. K. (2000). Angiogenesis in cancer and other diseases. *Nature, 407*(6801), 249-257.

Celebra-Thomas, J. (2005). Solutions for chick embryology. Retrieved, 2011, from http://www.swarthmore.edu/NatSci/sgilber1/DB_lab/Chick/Chick_solutions.html

Chan, T., & Burggren, W. (2005). Hypoxic incubation creates differential morphological effects during specific developmental critical windows in the embryo of the chicken (< i> gallus gallus</i>). *Respiratory Physiology & Neurobiology, 145*(2), 251-263.

Chandra M., R., S. (1987). Characteristics of polymers. *Plastics technology handboook* (pp. 80-83). NY: M. Dekker.

Cooke, J. P. (2003). NO and angiogenesis. *Atherosclerosis Supplements, 4*(4), 53-60.

Corona, T. B., & Warburton, S. J. (2000). Regional hypoxia elicits regional changes in chorioallantoic membrane vascular density in alligator but not chicken embryos. *Comparative Biochemistry and Physiology Part A: Molecular & Integrative Physiology, 125*(1), 57-61.

Demir, S., Mirshahi, N., Tiba, M. H., Draucker, G., Ward, K., Hobson, R., & Najarian, K. (2009). Image processing and machine learning for diagnostic analysis of microcirculation. *Complex Medical Engineering, 2009. CME. ICME International Conference on,* 1-5.

Deryugina, E. I., & Quigley, J. P. (2008). Chick embryo chorioallantoic membrane models to quantify angiogenesis induced by inflammatory and tumor cells or purified effector molecules. *Methods in Enzymology, 444*, 21-41.

Dohle, D. S., Pasa, S. D., Gustmann, S., Laub, M., Wissler, J. H., Jennissen, H. P., & Dünker, N. (2009). Chick ex ovo culture and ex ovo CAM assay: How it really works. *Journal of Visualized Experiments: JoVE,* (33)

Doukas, C. N., Maglogiannis, I., & Chatziioannou, A. A. (2008). Computer-supported angiogenesis quantification using image analysis and statistical averaging. *Information Technology in Biomedicine, IEEE Transactions on, 12*(5), 650-657.

Dragon, S., & Baumann, R. (2003). Hypoxia, hormones, and red blood cell function in chick embryos. *Physiology, 18*(2), 77-82.

Dunn, B. E., Fitzharris, T. P., & Barnett, B. D. (2005). Effects of varying chamber construction and embryo pre-incubation age on survival and growth of chick embryos in shell-less culture. *The Anatomical Record, 199*(1), 33-43.

Dusseau, J. W., & Hutchins, P. M. (1988). Hypoxia-induced angiogenesis in chick chorioallantoic membranes: A role for adenosine. *Respiration Physiology, 71*(1), 33-44.

Elias, H., & Hyde, D. (1983). Stereological measurements of isotropic structures. *A Guide to Practical Stereology*, , 25-44.

Erasmus, B. D., & Rahn, H. (1976). Effects of ambient pressures, he and SF6 on O2 and CO2, transport en the avian egg. *Respiration Physiology, 27*(1), 53-64. doi:http://dx.doi.org.proxy.library.vcu.edu/10.1016/0034-5687(76)90017-7

Folkman, J., Merler, E., Abernathy, C., & Williams, G. (1971). Isolation of a tumor factor responsible for angiogenesis. *The Journal of Experimental Medicine, 133*(2), 275-288.

Furchgott, R. F., & Bhadrakom, S. (1953). Reactions of strips of rabbit aorta to epinephrine, isopropylarterenol, sodium nitrite and other drugs. *Journal of Pharmacology and Experimental Therapeutics, 108*(2), 129-143.

Furchgott, R. F., & Zawadzki, J. V. (1980). The obligatory role of endothelial cells in the relaxation of arterial smooth muscle by acetylcholine.

Golub, A. S., Barker, M. C., & Pittman, R. N. (2007). PO2 profiles near arterioles and tissue oxygen consumption in rat mesentery. *American Journal of Physiology-Heart and Circulatory Physiology, 293*(2), H1097-H1106.

Hamburger, V., & Hamilton, H. L. (1951). A series of normal stages in the development of the chick embryo. *Journal of Morphology, 88*(1), 49-92.

Hiroshi, T., & Tsukasa, O. (1974). Microscopic observation of the chorioallantoic capillary bed of chicken embryos. *Respiration Physiology, 20*(1), 81-89.

Høiby, M., Aulie, A., & Reite, O. B. (1983). Oxygen uptake in fowl eggs incubated in air and pure oxygen. *Comparative Biochemistry and Physiology Part A: Physiology, 74*(2), 315-318.

Höper, J., Jahn, H., Demir, R., & Höper, K. (1996). Influence of environmental oxygen concentration on enlargement and vascular density of the area vasculosa in chick embryos. *Advances in Experimental Medicine and Biology, 428*, 169-172.

Horn, P., Cortese-Krott, M. M., Keymel, S., Kumara, I., Burghoff, S., Schrader, J., . . . Kleinbongard, P. (2011). Nitric oxide influences red blood cell velocity independently of changes in the vascular tone. *Free Radical Research, 45*(6), 653-661.

Jakobson, Å. M., Hahnenberger, R., & Magnusson, A. (2009). A simple method for Shell-less cultivation of chick embryos. *Pharmacology & Toxicology, 64*(2), 193-195.

Jia, L., Wu, C., Guo, W., & Young, X. (2000). Antiangiogenic effects of< i> S</i>-nitrosocaptopril crystals as a nitric oxide donor. *European Journal of Pharmacology, 391*(1), 137-144.

Knighton, D., Ausprunk, D., Tapper, D., & Folkman, J. (1977). Avascular and vascular phases of tumour growth in the chick embryo. *British Journal of Cancer, 35*(3), 347.

Kumar, D., Branch, B. G., Pattillo, C. B., Hood, J., Thoma, S., Simpson, S., . . . Langston, W. (2008). Chronic sodium nitrite therapy augments ischemia-induced angiogenesis and arteriogenesis. *Proceedings of the National Academy of Sciences, 105*(21), 7540-7545.

Kurz, H., Ambrosy, S., Wilting, J., Marmé, D., & Christ, B. (1995). Proliferation pattern of capillary endothelial cells in chorioallantoic membrane development indicates local growth control, which is counteracted by vascular endothelial growth factor application. *Developmental Dynamics, 203*(2), 174-186.

Lapennas, G. N., & Reeves, R. B. (1983). Oxygen affinity and equilibrium curve shape in blood of chicken embryos. *Respiration Physiology, 52*(1), 13-26.

Lee, P. C., Salyapongse, A. N., Bragdon, G. A., Shears, L. L., Watkins, S. C., Edington, H. D., & Billiar, T. R. (1999). Impaired wound healing and angiogenesis in eNOS-deficient mice. *American Journal of Physiology-Heart and Circulatory Physiology, 277*(4), H1600-H1608.

León-Velarde, F., & Monge-C, C. (2004). Avian embryos in hypoxic environments. *Respiratory Physiology & Neurobiology, 141*(3), 331-343.

Lomholt, J. P. (2005). The development of the oxygen permeability of the avian egg shell and its membranes during incubation. *Journal of Experimental Zoology, 198*(2), 177-184.

Lundberg, J. O., & Weitzberg, E. (2010). NO-synthase independent NO generation in mammals. *Biochemical and Biophysical Research Communications, 396*(1), 39-45.

Mayer, B. W., & Packard, D. S. (1978). A study of the expansion of the chick area vasculosa. *Developmental Biology, 63*(2), 335-351.

Meuer, H. (1992). Erythrocyte velocity and total blood flow in the extraembryonic circulation of early chick embryos determined by digital video technique. *Microvascular Research, 44*(3), 286-294.

Meuer, H., & Baumann, R. (1987). Oxygen supply of early chick embryo in normoxia and hypoxia. *The Journal of Experimental Zoology.Supplement: Published Under Auspices of the American Society of Zoologists and the Division of Comparative Physiology and Biochemistry/the Wistar Institute of Anatomy and Biology, 1*, 203.

Meuer, H., & Bertram, C. (1993). Capillary transit times and kinetics of oxygenation in the primary respiratory organ of early chick embryo. *Microvascular Research, 45*(3), 302-313.

Meuer, H., & Egbers, C. (1990). Changes in density and viscosity of chicken egg albumen and yolk during incubation. *Journal of Experimental Zoology, 255*(1), 16-21.

Meuer, H., & Baumann, R. (1988). Oxygen pressure in intra-and extraembryonic blood vessels of early chick embryo. *Respiration Physiology, 71*(3), 331-341.

MOHAMADI, E., DANESHYAR, M., FARROKHI, A. F., & ALIZADEH, E. (2013). Evaluation of different sodium nitrite levels in ovo injection on embryo growth and development, and some blood metabolites on newly hatched chicks. *Animal Sciences Journal, 25*(4), 52-59.

Murray, H. A. (1925). Physiological ontogeny a. chicken embryos. ii. catabolism. chemical changes in fertile eggs during incubation. selection of standard conditions. *The Journal of General Physiology, 9*(1), 1-37.

Murray, H. A. (1926). Physiological ontogeny a. chicken embryos. xii. the metabolism as a function of age. *The Journal of General Physiology, 10*(2), 337-343.

Nico, B., Vacca, A., De Giorgis, M., Roncali, L., & Ribatti, D. (2001). Vascular endothelial growth factor and vascular endothelial growth factor receptor-2 expression in the chick embryo area vasculosa. *The Histochemical Journal, 33*(5), 283-286.

Nilsen, N. Ø. (1981). Microangiography in explanted chick embryos. *Microvascular Research, 22*(2), 156-170.

Noiri, E., Lee, E., Testa, J., Quigley, J., Colflesh, D., Keese, C. R., . . . Goligorsky, M. S. (1998). Podokinesis in endothelial cell migration: Role of nitric oxide. *American Journal of Physiology-Cell Physiology, 274*(1), C236-C244.

Palmer, R. M., Ferrige, A., & Moncada, S. (1987). Nitric oxide release accounts for the biological activity of endothelium-derived relaxing factor.

Papapetropoulos, A., García-Cardeña, G., Madri, J. A., & Sessa, W. C. (1997). Nitric oxide production contributes to the angiogenic properties of vascular endothelial growth factor in human endothelial cells. *Journal of Clinical Investigation, 100*(12), 3131.

Patan, S. (2004). Vasculogenesis and angiogenesis. *Angiogenesis in brain tumors* (pp. 3-32) Springer.

Patel, R. P., Hogg, N., & Kim-Shapiro, D. B. (2011). The potential role of the red blood cell in nitrite-dependent regulation of blood flow. *Cardiovascular Research, 89*(3), 507-515.

Piiper, J., Tazawa, H., Ar, A., & Rahn, H. (1980). Analysis of chorioallantoic gas exchange in the chick embryo. *Respiration Physiology, 39*(3), 273-284.

Pinsky, M. (1995). Regional blood flow distribution. *The splanchnic circulation* (pp. 1-13) Springer.

Pipili-Synetos, E., Kritikou, S., Papadimitriou, E., Athanassiadou, A., Flordellis, C., & Maragoudakis, M. (2000). Nitric oxide synthase expression, enzyme activity and NO production during angiogenesis in the chick chorioallantoic membrane. *British Journal of Pharmacology, 129*(1), 207-213.

Pipili-Synetos, E., Papageorgiou, A., Sakkoula, E., Sotiropoulou, G., Fotsis, T., Karakiulakis, G., & Maragoudakis, M. (1995). Inhibition of angiogenesis, tumour growth and metastasis by the NO-releasing vasodilators, isosorbide mononitrate and dinitrate. *British Journal of Pharmacology, 116*(2), 1829-1834.

Pipili-Synetos, E., Sakkoula, E., Haralabopoulos, G., Andriopoulou, P., Peristeris, P., & Maragoudakis, M. (1994). Evidence that nitric oxide is an endogenous antiangiogenic mediator. *British Journal of Pharmacology, 111*(3), 894-902.

Polytarchou, C., & Papadimitriou, E. (2004). Antioxidants inhibit angiogenesis in vivo through down-regulation of nitric oxide synthase expression and activity. *Free Radical Research, 38*(5), 501-508.

Powell, J., Mohamed, S., Kerr, J., & Mousa, S. A. (2001). Antiangiogenesis efficacy of nitric oxide donors. *Journal of Cellular Biochemistry, 80*(1), 104-114.

Reizis, A., Hammel, I., & Ar, A. (2005). Regional and developmental variations of blood vessel morphometry in the chick embryo chorioallantoic membrane. *Journal of Experimental Biology, 208*(13), 2483-2488.

Ribatti, D. (1995). A morphometric study of the expansion of the chick area vasculosa in shell-less culture. *Journal of Anatomy, 186*(Pt 3), 639.

Ribatti, D. (2008). Chick embryo chorioallantoic membrane as a useful toolto study angiogenesis. *International Review of Cell and Molecular Biology, 270,* 181.

Risau, W., & Flamme, I. (1995). Vasculogenesis. *Annual Review of Cell and Developmental Biology, 11*(1), 73-91.

Rizzo, V., Kim, D., Durán, W. N., & DeFouw, D. O. (1995). Differentiation of the microvascular endothelium during early angiogenesis and respiratory onset in the chick chorioallantoic membrane. *Tissue and Cell, 27*(2), 159-166.

Romijn, C., & Roos, J. (1938). The air space of the hen's egg and its changes during the period of incubation. *The Journal of Physiology, 94*(3), 365-379.

Sandau, K. B., Fandrey, J., & Brüne, B. (2001). Accumulation of HIF-1α under the influence of nitric oxide. *Blood, 97*(4), 1009-1015.

Sasayama, S., & Fujita, M. (1992). Recent insights into coronary collateral circulation. *Circulation, 85*(3), 1197-1204.

Schmitz, P., & Janocha, S. (2000). Films. *Ullmann's Encyclopedia of Industrial Chemistry,*

Simão, F., Pagnussat, A. S., Seo, J. H., Navaratna, D., Leung, W., Lok, J., . . . Lo, E. H. (2012). Pro-angiogenic effects of resveratrol in brain endothelial cells: Nitric oxide-mediated regulation of vascular endothelial growth factor and metalloproteinases. *Journal of Cerebral Blood Flow & Metabolism, 32*(5), 884-895.

Splawinski, J., Michna, M., Palczak, R., Konturek, S., & Splawinska, B. (1988). Angiogenesis: Quantitative assessment by the chick chorioallantoic membrane assay. *Methods and Findings in Experimental and Clinical Pharmacology, 10*(4), 221.

Strick, D. M., Waycaster, R. L., Montani, J., Gay, W. J., & Adair, T. H. (1991). Morphometric measurements of chorioallantoic membrane vascularity: Effects of hypoxia and hyperoxia. *American Journal of Physiology-Heart and Circulatory Physiology, 260*(4), H1385-H1389.

Tazawa, H. (1971). Measurement of respiratory parameters in blood of chicken embryo. *Journal of Applied Physiology, 30*(1), 17-20.

Tazawa, H. (1973). Hypothermal effect on the gas exchange in chicken embryo. *Respiration Physiology, 17*(1), 21-31.

Tazawa, H., & Mochizuki, M. (1976). Estimation of contact time and diffusing capacity for oxygen in the chorioallantoic vascular plexus. *Respiration Physiology, 28*(1), 119-128.

Toda, N., & Ayajiki, K. (2007). Phylogenesis of constitutively formed nitric oxide in non-mammals. *Reviews of physiology biochemistry and pharmacology* (pp. 31-80) Springer.

Vargas, A., Zeisser-Labouèbe, M., Lange, N., Gurny, R., & Delie, F. (2007). The chick embryo and its chorioallantoic membrane (CAM) for the< i> in vivo</i> evaluation of drug delivery systems. *Advanced Drug Delivery Reviews, 59*(11), 1162-1176.

Visschedijk, A., Girard, H., & Ar, A. (1988). Gas diffusion in the shell membranes of the hen's egg: Lateral diffusion in situ. *Journal of Comparative Physiology B, 158*(5), 567-574.

Vitturi, D. A., & Patel, R. P. (2011). Current perspectives and challenges in understanding the role of nitrite as an integral player in nitric oxide biology and therapy. *Free Radical Biology and Medicine, 51*(4), 805-812.

Wagner-Amos, K., & Seymour, R. S. (2003). Effect of local shell conductance on the vascularisation of the chicken chorioallantoic membrane. *Respiratory Physiology & Neurobiology, 134*(2), 155-167.

Ware, J. A., & Simons, M. (1997). Angiogenesis in ischemic heart disease. *Nature Medicine, 3*(2), 158-164.

Webb, A., Bond, R., McLean, P., Uppal, R., Benjamin, N., & Ahluwalia, A. (2004). Reduction of nitrite to nitric oxide during ischemia protects against myocardial ischemia–reperfusion damage. *Proceedings of the National Academy of Sciences of the United States of America, 101*(37), 13683-13688.

White, H. D., & Chew, D. P. (2008). Acute myocardial infarction. *The Lancet, 372*(9638), 570-584.

Zacharakis, N., Tone, P., Flordellis, C., Maragoudakis, M., & Tsopanoglou, N. (2006). Methylene blue inhibits angiogenesis in chick chorioallontic membrane through a nitric oxide-independent mechanism. *Journal of Cellular and Molecular Medicine, 10*(2), 493-498.

Zhang, R., Wang, L., Zhang, L., Chen, J., Zhu, Z., Zhang, Z., & Chopp, M. (2003). Nitric oxide enhances angiogenesis via the synthesis of vascular endothelial growth factor and cGMP after stroke in the rat. *Circulation Research, 92*(3), 308-313.

Zheng, L., Golub, A. S., & Pittman, R. N. (1996). Determination of PO2 and its heterogeneity in single capillaries. *American Journal of Physiology-Heart and Circulatory Physiology, 271*(1), H365-H372.

Zhou, Y., Yan, H., Guo, M., Zhu, J., Xiao, Q., & Zhang, L. (2013). Reactive oxygen species in vascular formation and development. *Oxidative Medicine and Cellular Longevity, 2013*

Ziche, M., Morbidelli, L., Masini, E., Amerini, S., Granger, H., Maggi, C. e. a., . . . Ledda, F. (1994). Nitric oxide mediates angiogenesis in vivo and endothelial cell growth and migration in vitro promoted by substance P. *Journal of Clinical Investigation, 94*(5), 2036.

Appendix 1

Egg Tracking Protocol
Batch Received:
of
eggs:
Notes:

	Plate Type	Date Measured	Date Discarded	Details
A				
B				
C				
D				
E				
F				
G				
H				
I				
J				
K				
L				

Day:	1	2	3	4	5	6	7
Temp:							
Cond:							
Day:	8	9	10	11	12	13	14
Temp:							
Cond:							

Appendix 2

The ImageJ commands used are as follows:

CAM image processing

Open in ImageJ

Analyze -> Set Scale -> Set “distance in pixels” to 770, Set “known distance” to 1mm

Click global, OK

Select Square selection box

Highlight a 3mmx3mm section of the image

Right click inside the selected box and duplicate, then close the original

Image -> Color -> Split channels

Close red and blue windows (leave green for manipulation)

Maximize the remaining image

Image -> Adjust -> Brightness/Contrast

Lower max to right end of histogram

Increase min until edges start to darken

Double click brush tool, set width to 10 pixels

Trace vasculature with brush tool (color – 0,0,0)

Increase min and trace and revealed vessels (if necessary)

In contrast, Reduce Max to 0

Apply brightness/contrast changes

Process -> Binary -> Make binary

File -> Save (will save as tif file)

Length – Analyze -> Histogram, record Mode (should be # of white pixels)

Subtract from total# of pixels to find black pixels, divide by brush width, then convert units

Bifurcations – count acute angles (mark with brush spots to keep track), intersections (or inevitable close intersections) and sharp bends count

Open FracLac through plugins menu

Standard Box Count

Select Files -> open folder -> *.tif -> select all binary images

This may need to be done more than once, there seems to be a limit of files that can be processed at one time.

Michael Connery

MATRICULATION DATE: Summer, 2008
MENTOR: Roland Pittman, PhD
DATE ENTERED LAB: Summer, 2008

EDUCATION:

B.S. – Biomedical Engineering, University of Virginia (2005)

TEACHING EXPERIENCE:

Undergraduate Physiology Lab Teaching Assistant, Virginia Commonwealth University (2012)
Physiology Curriculum Collaborator, Virginia Commonwealth University (2010)
Medical Physiology Lab Teaching Assistant, Virginia Commonwealth University (2010)
MCAT Instructor, Kaplan (2005-2006)
Biomedical Engineering Grader, University of Virginia (2005)

PREVIOUS RESEARCH EXPERIENCE:

Undergraduate Research Assistant - Klaus Ley lab, Department of Physiology, University of Virginia (2003-2004)
Summary of work: Transfected cells with an altered ion channel.

Undergraduate Research Assistant – Bill Walker lab, Department of Biomedical Engineering, University of Virginia (2004-2005)
Summary of work: Computer simulations calculating depth of field for proposed ultrasound device.

DISSERTATION TITLE:

Effects of nitrite and oxygen on angiogenesis in vascular networks of the chicken embryo.

SCIENTIFIC MEETINGS/ABSTRACTS:

Song, B.K., **Connery, M.D**., Moon-Massat, P., and Pittman, R.N. Tissue oxygenation and oxygen consumption following hemorrhage and resuscitation using a hemoglobin-based oxygen carrier and human serum albumin. FASEB J. 23:948.6, 2009.

Connery, M.D., Kameneva, M.V., and Pittman, R.N. Determining the dose-dependent effects of long-chain soluble polymers in rat spinotrapezius muscle. FASEB J. 24: 2010.